SAFETY ANALYSIS REPORT

for the

WASHINGTON STATE UNIVERSITY
MODIFIED TRIGA NUCLEAR REACTOR

Submitted To

U.S. NUCLEAR REGULATORY COMMISSION

FOR RENEWAL OF FACILITY LICENSE R-76

Prepared by W. E. Wilson

WASHINGTON STATE UNIVERSITY
NUCLEAR RADIATION CENTER
Pullman, Washington 99164

May 1979

TABLE OF CONTENTS

6.0 SAFETY ANALYSIS

- 6.1 General Considerations
- 6.2 Design Bases
- 6.3 Design Limits
- 6.4 Accident Analysis

7.0 REFERENCES

8.0 APPENDICES

- A. Safety Analysis for Conversion to FLIP Fuel
- B. Environmental Impact Appraisal
- C. Emergency Plan
- D. Facility License
- E. Technical Specifications

LIST OF TABLES

LIST OF FIGURES

Chapter 2

Figure

Chapter 3

Figure

Chapter 4

Figure

Chapter 4 (Cont.)

Chapter 5

Figure

Chapter 6

Figure

1.0 INTRODUCTION AND GENERAL INFORMATION

1.1 Introduction and Summary

This report describes the Washington State University modified TRIGA reactor and the operation of the reactor with a core of mixed Standard and FLIP* fuel. This report supersedes and replaces all previous SAFETY ANALYSIS REPORTS and descriptions of the Washington State University reactor.

The Washington State University reactor has been in operation since March 1961. From 1961 to 1967 the reactor was fueled with MTR type fuel elements and operated at a maximum power level of 100 kilowatts. In 1967 the reactor was shut down and the core and control systems were modified so that the reactor could operate with TRIGA type fuel. The orginal core grid box was retained and the MTR fuel elements were replaced with a special 4-rod cluster of TRIGA fuel rods designed to replace a MTR fuel element. From July 1967 to date the reactor has operated as a modified TRIGA reactor with a maximum steady state power level of 1 MW. In February of 1976 the core was loaded with a mixture of Standard and FLIP fuel.

1.2 Principal Design Criteria

The existing reactor system operates with a mixture of Standard and and FLIP types of TRIGA fuel in the steady-state or pulsed modes. The maximum continuous steady state power level is 1 MW and the average maximum pulsed power level is 2000 MW. Standard TRIGA fuel contains uranium-zirconium hydride enriched in U-235 to 20%. FLIP TRIGA fuel contains uranium-zirconium hydride enriched in U-235 to 70% and 1.5 wt% erbium as a burnable poison to offset the added U-235. The reactivity worths of

---

*FLIP (Fuel Life Improvement Program) is a new type long-lifed fuel developed by Gulf Energy and Environmental Systems for TRIGA reactors.

both types of fuel are about equal. The increased U-235 content of FLIP fuel along with the burnable poison yields a fuel that has a significantly larger core lifetime potential than standard TRIGA fuel.

The safety of the modified system, as with all TRIGA reactors, comes from the large prompt negative temperature coefficient that is inherent in a water-moderated, U-ZrH fueled reactor. The overall operating characteristics for the Washington State University Modified TRIGA reactor fueled with various combinations of fuels is discussed in the report attached to Appendix A. The data in this report were calculated using the EXTERMINATOR-2(1) code and multigroup cross-section data (2) obtained from Gulf Energy and Environmental Systems.

1.3 Design Highlights

The Washington State University Modified TRIGA reactor is located in the Nuclear Radiation Center which is situated in the northeast corner of the campus at Pullman, Washington. The core is located in a 242,000 liter above-ground pool which is, in turn, cooled and purified by external cooling and purification systems. Reactor experimental facilities include incore irradiation positions, a thermal column, and numerous beam tubes.

1.4 Conclusions

Past experience with the Washington State University TRIGA reactor and other TRIGA reactors clearly indicates that a properly designed reactor system fueled with TRIGA type fuel can be safely operated at steady-state power levels of 1 MW and pulsed to a power level of 2000 MW. This history of safe and conservative reactor design has permitted TRIGA type reactors to be sited in urban areas without the need for specially designed containment structures. Furthermore, the W.S.U. reactor fueled with a mixture of

Standard and FLIP fuels has operated for over three years without a single fuel related problem.

The information presented in this safety analysis report indicates that the continued operation of the Washington State University Modified TRIGA reactor will pose no health or safety hazards to the public. Furthermore, the system is safe when operated in a normal manner or even if a highly abnormal condition occurs. The three major accidents considered are: (1) accidental fuel addition, (2) pulsing of the reactor (transient rod ejection) while operating at full power, and (3) loss of coolant accident. In all of these postulated accidents, no loss of fuel cladding integrity would occur. Also the Design Base Accident, which is the loss of the integrity of the cladding on one TRIGA rod in air, is shown to not present a significant hazard to the general public.

2.0 SITE CHARACTERISTICS

2.1 Location

Washington State University is located in the southeastern corner of the State of Washington in the town of Pullman as shown in Figure 2.1-1. The town of Pullman, Washington has a population of 23,500 and is located in Whitman County about eleven kilometers from the Washington-Idaho border as shown in Figure 2.1-2. In addition to the town of Pullman, the town of Moscow, Idaho is located approximately 13 kilometers east of the site just across the Washington-Idaho border. Moscow has a population of 17,700 and is the location of the University of Idaho. The Palouse region surrounding the towns of Pullman and Moscow is a rural agricultural area devoted to dry land farming.

The actual reactor site is 3.2 kilometers east of the center of the town of Pullman and 1.6 kilometers east of the main portion of campus as shown on Figure 2.1-3. The site is surrounded by university-owned property for at least .4 kilometers in all directions used for the grazing of livestock as shown in the site photograph of Figure 2.1-6. The Moscow-Pullman airport is located 3 kilometers east of the site and the closest occupied dwelling is 411 meters west of the site.

2.2 Population Density

The population distribution about the site in 500 meter increments out to 3 kilometers in eight directional segments is shown in Figure 2.2-1 and tabulated in Table 2.2-1. The population distribution was calculated for a typical day with the university students, faculty, and staff present on the campus. A circle with a radius of 400 meters about the site has no permanently occupied dwellings.

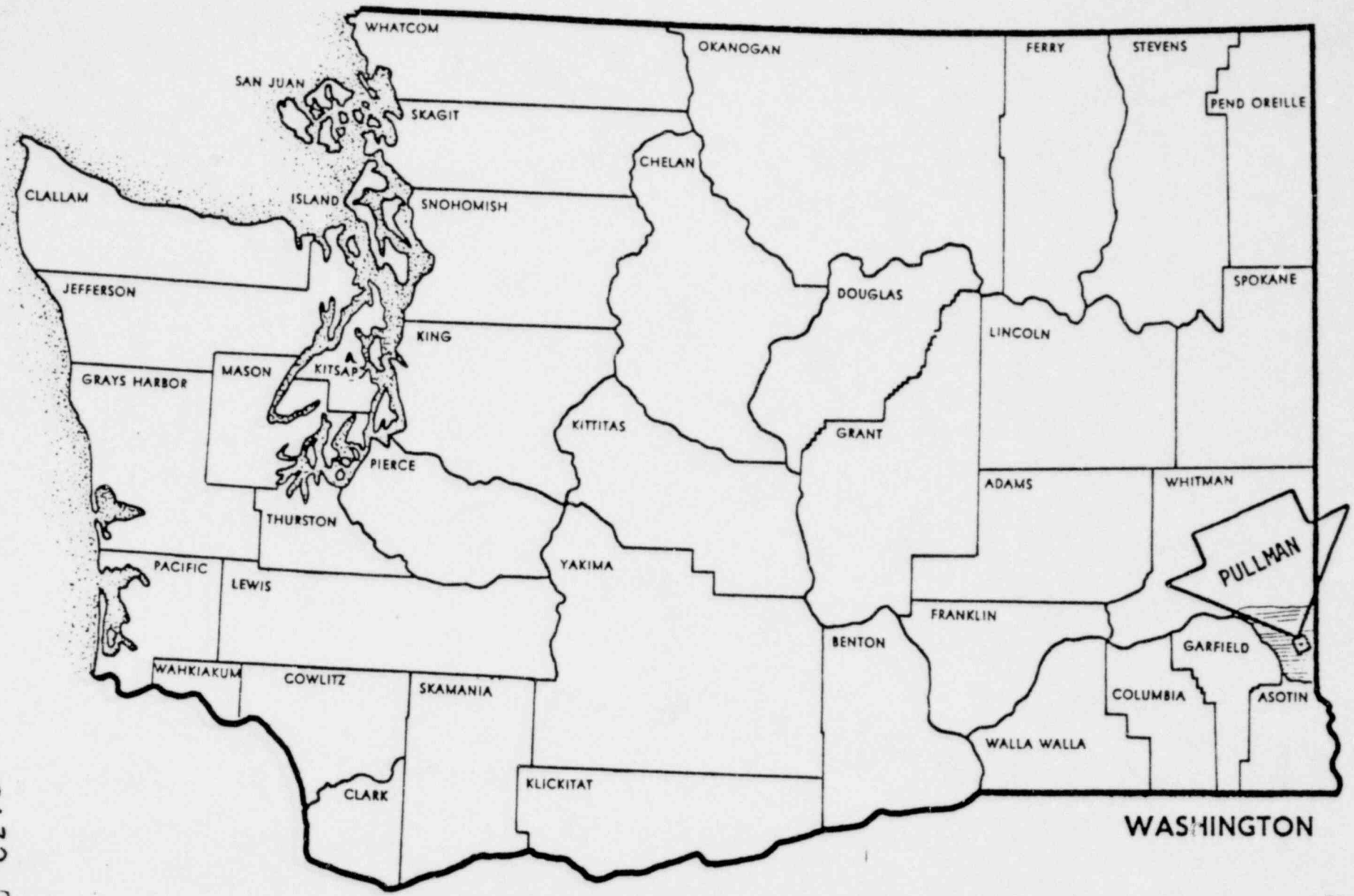

FIGURE 2.1-1

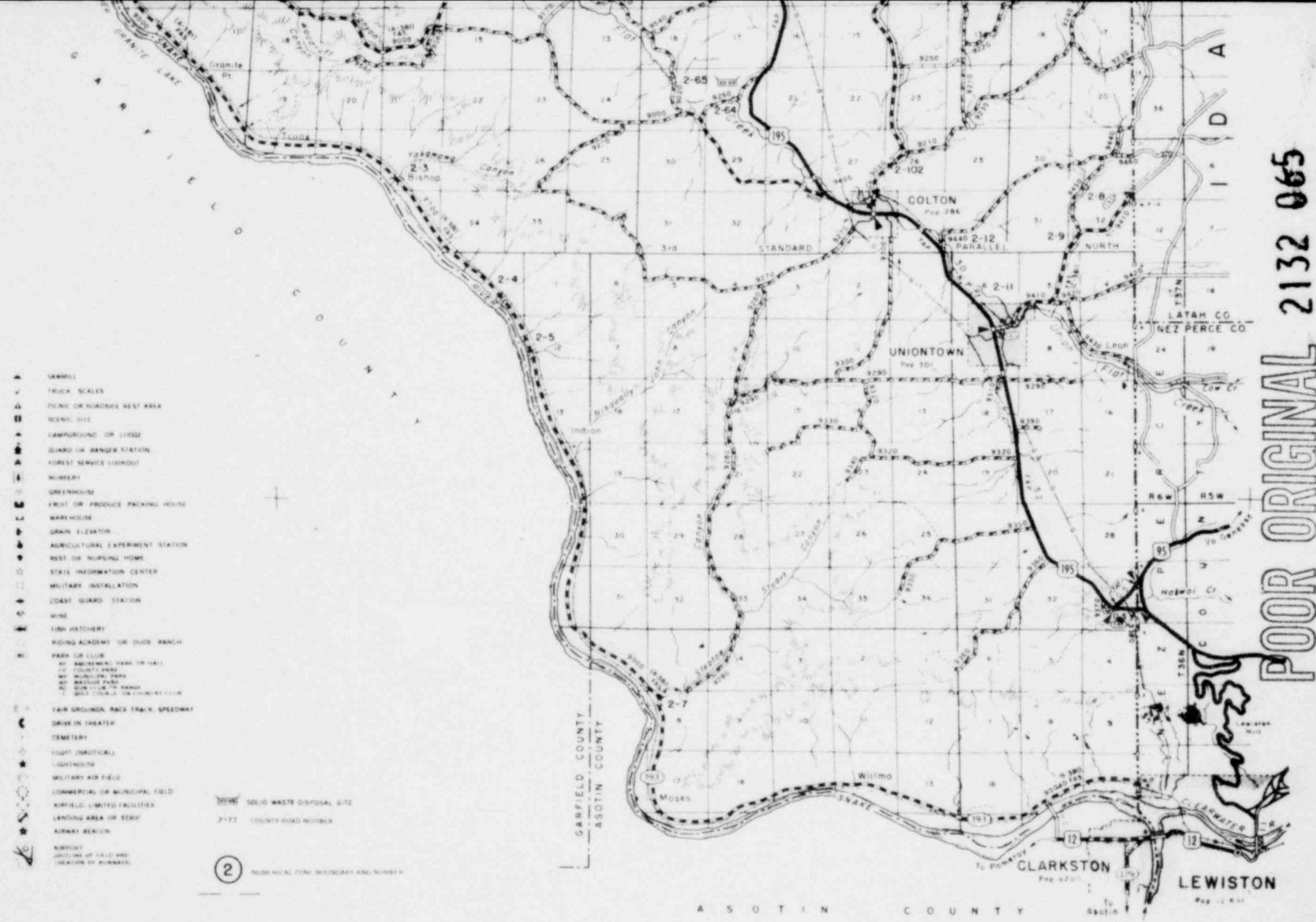

Whitman County Map in Pullman Area
Figure 2.1-2

Figure 2.1-3

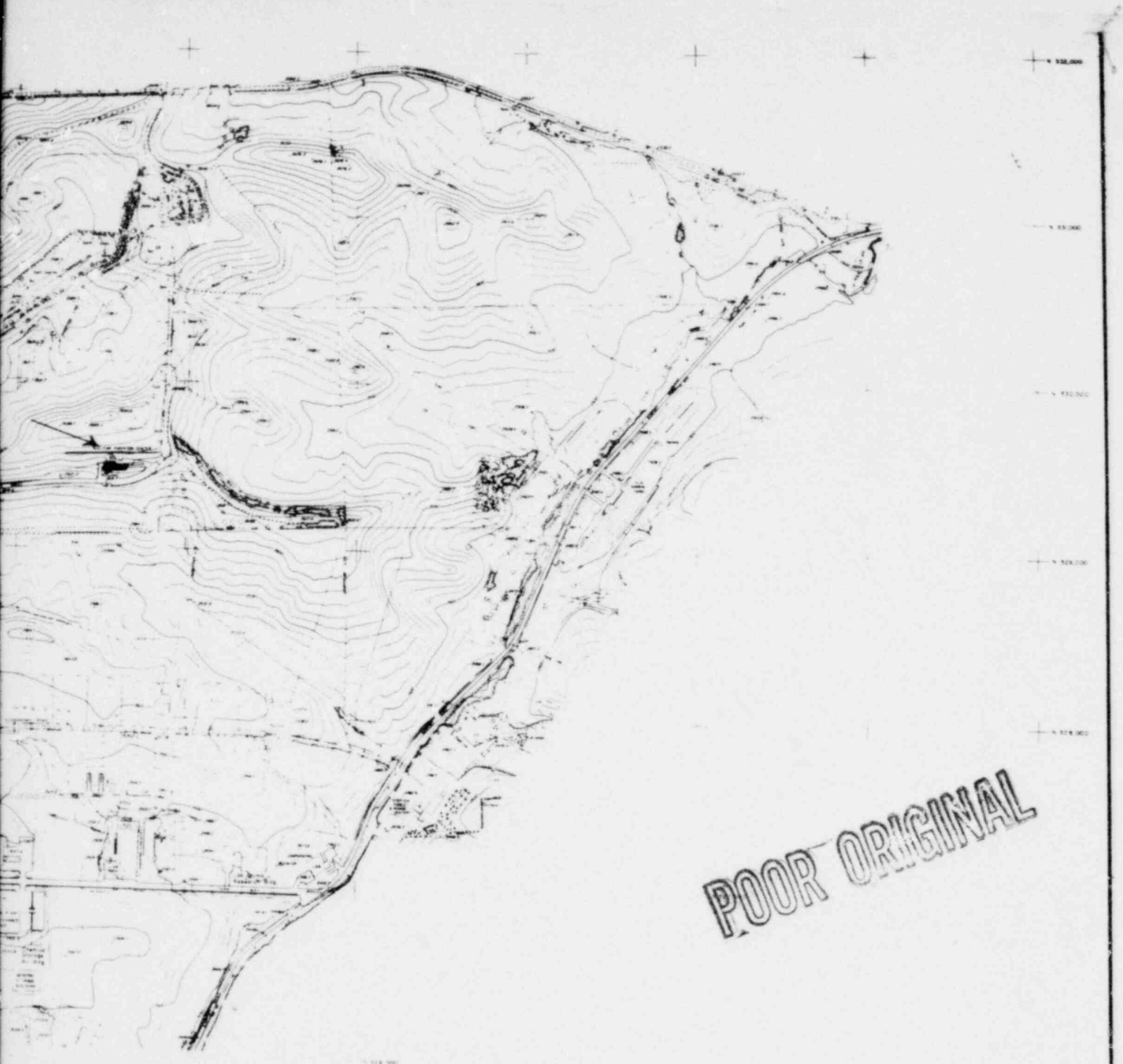

N

Revised September, 1977 DJW
Revised January, 1977 DJW
REVISED NOVEMBER 1970

DATE OF PHOTO 7-9-1970

TOPOGRAPHIC MAP

CONTOUR INTERVAL 10'

SERIES 4

Mapped by WALKER & ASSOCIATES, INC.
Seattle - Spokane
JOB NO. 69-2009

CKD
TRD
APPD
DATE MAY 1969
SCALE 1" = 400'

WASHINGTON STATE UNIVERSITY
PULLMAN, WASHINGTON
DEPT OF PHYSICAL PLANT

SHEET 1 OF 1
DWG NO.
FILE NO.

2132 008

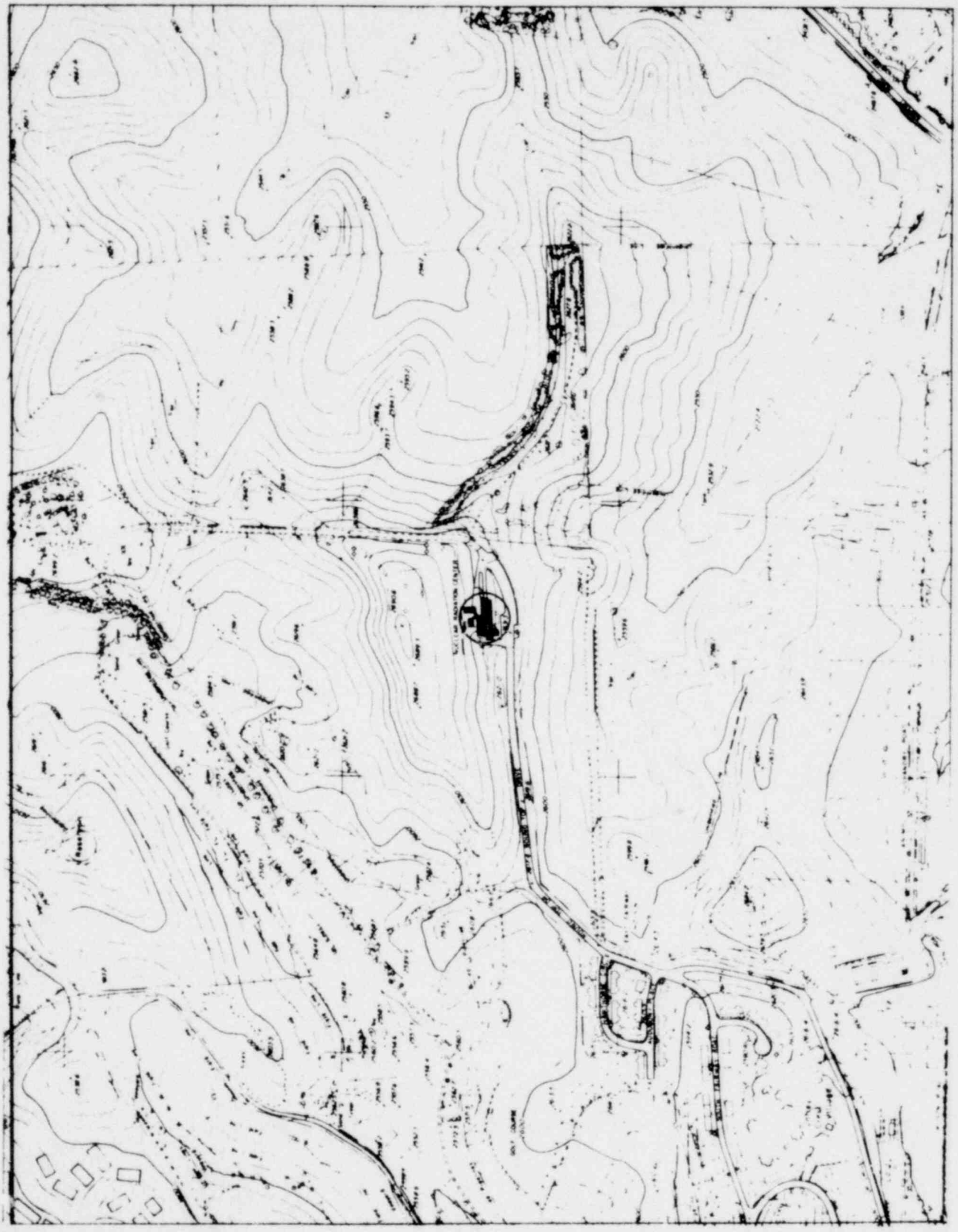

Site Area Topography Map

FIGURE 2.1-4

FIGURE 2.1-5

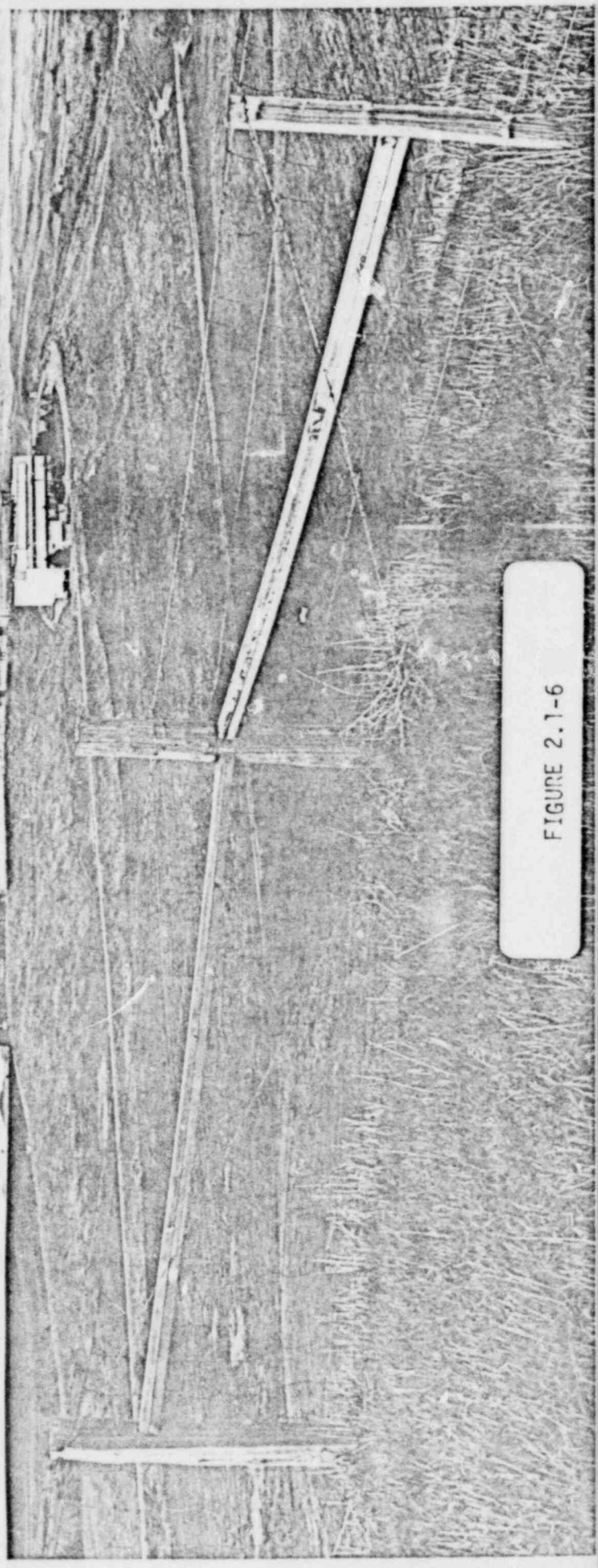

FIGURE 2.1-6

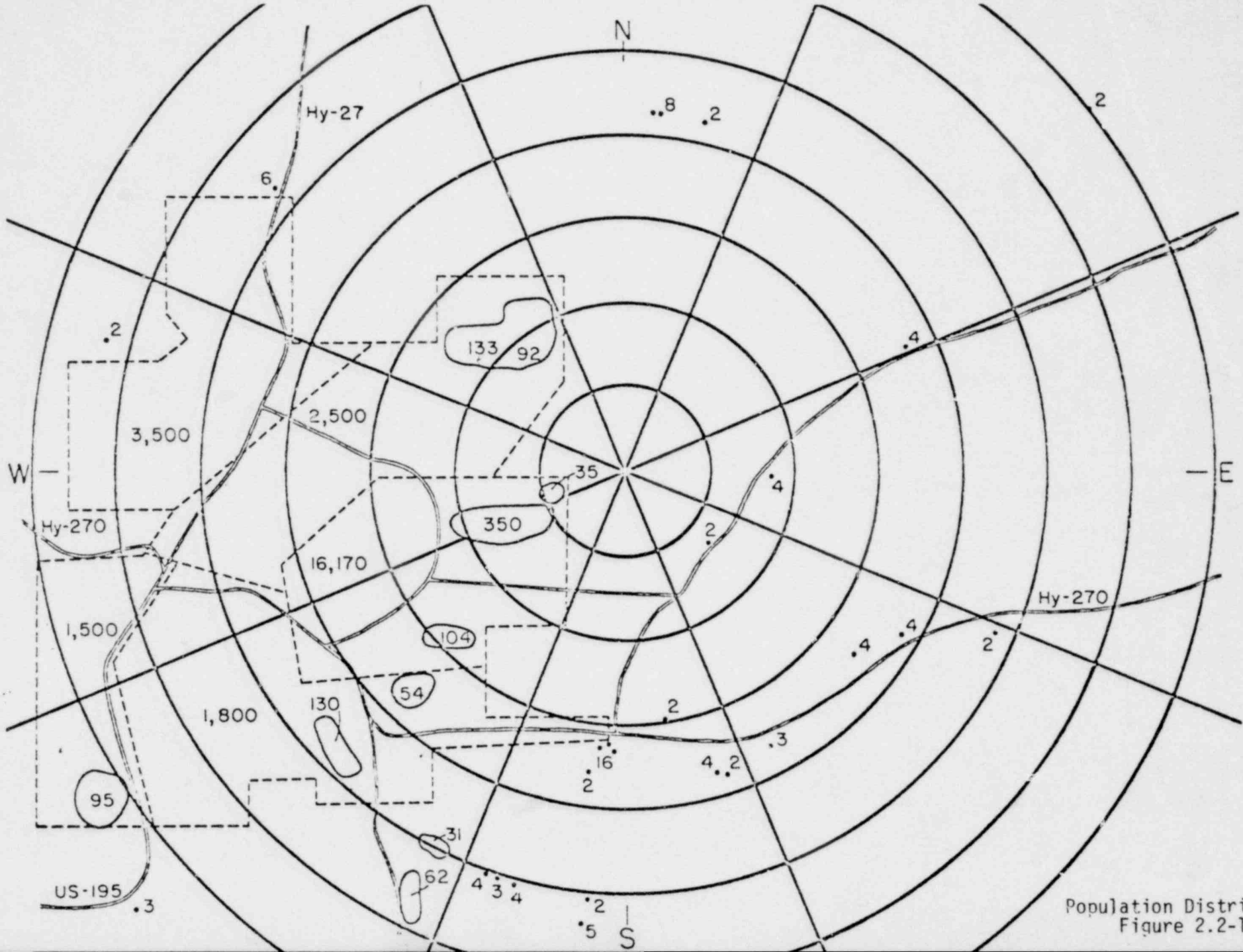

2132 072

Population Distribution
Figure 2.2-1

TABLE 2.2-1

POPULATION DISTRIBUTION AROUND REACTOR SITE

Number of Residents per Octant

Distance Meters	N	NE	E	SE	S	SW	W	NW
0 - 500							35	
500 - 1000	0	0	4	2	800	1,032	66	92
1000 - 1500	0	0	0	0	27	1,574	3,393	233
1500 - 2000	0	0	0	15	18	5,454	5.280	0
2000 - 2500	0	0	0	0	0	700	2,800	76
2500-3000	10	2	4	2	30	588	3,200	280
3500	4	0	4	9	4	340	233	8
TOTALS	14	2	12	28	879	9,688	15,007	689

2.3 Climatology

Pullman is situated at latitude 47° north of the equator and consequently is about midway between the equator and the North Pole. From May to August, when the sun remains above the horizon from 14 to 16 hours a day, Pullman receives more solar radiation than does the equator. In December, the sun rises only about 20° above the southern horizon at noon and is in the sky only about 8 hours. Therefore, the daily accumulation of solar radiation in winter is less for two reasons: 1) the days are shorter, and 2) the sun's rays, striking the earth at an angle, are spread over a larger area. Because of this great variation in energy intake, Pullman experiences pronounced differences in temperature and other weather conditions from summer to winter.

The latitude of Pullman is only one factor influencing the climate pattern at the site. Other factors are its location with respect to land and water areas, mountain barriers, and prevailing winds. Pullman is approximately 480 kilometers inland from the Pacific Ocean; and the Cascade Mountains, which average more than 2 kilometers in height, separate Pullman from the coast. The combined effect of the distance from the ocean and the existence of the mountain barrier creates a climate with a continental characteristic. However, because the prevailing winds blow inland from the Pacific Ocean, winters are considerably warmer than otherwise might be expected 480 kilometers inland at a latitude of 47° north. Winters in Pullman are characterized by cloudy skies and frequent snowstorms. On the average, the sun shines in Pullman only about 30% of the time during the winter months.

During the summer months, the westerly winds weaken, and continental climatic conditions prevail. Rainfall, cloud cover, and relative

humidity are thus at their minimum; the daily mean temperature and daily temperature variation are at their maximum. Summers in Pullman are characterized by warm clear days and cool nights. On the average, the sun shines in Pullman about 80% of the time during the summer months.

2.4 Meteorology

2.4.1 General

Washington State University is located in eastern Washington in a dry-land agricultural area, known as the Palouse region. The climate of this region is moderate, being a transitional region between the Columbia Basin and the mountains of Idaho. Precipitation and temperature data at the Washington State University campus have been accumulated since 1893 by the Department of Agronomy at the school. This extensive backlog of data was utilized to prepare the temperature and precipitation tables given in this section. The wind data were obtained from a detailed analysis of wind velocity and direction data for the year 1953.

2.4.2 Wind Velocity and Direction

In order to obtain wind data that are relevant to the site, charts taken from a wind recorder located on top of Wilson Hall during 1953 were analyzed in detail. Wilson Hall is approximately 1.6 kilometers WSW of the site. The monitoring station was at an elevation of 824 meters and the reactor site at 808 kilometers. All more recent wind data are taken at the Moscow-Pullman airport which is about 3.2 kilometers ENE, at an elevation considerably below the site, and thus not valid.

A wind rose indicating the frequency of occurrence of winds at the site is given in Figure 2.4-1. It is to be noted that the prevailing winds are from a westerly direction and blow over Pullman

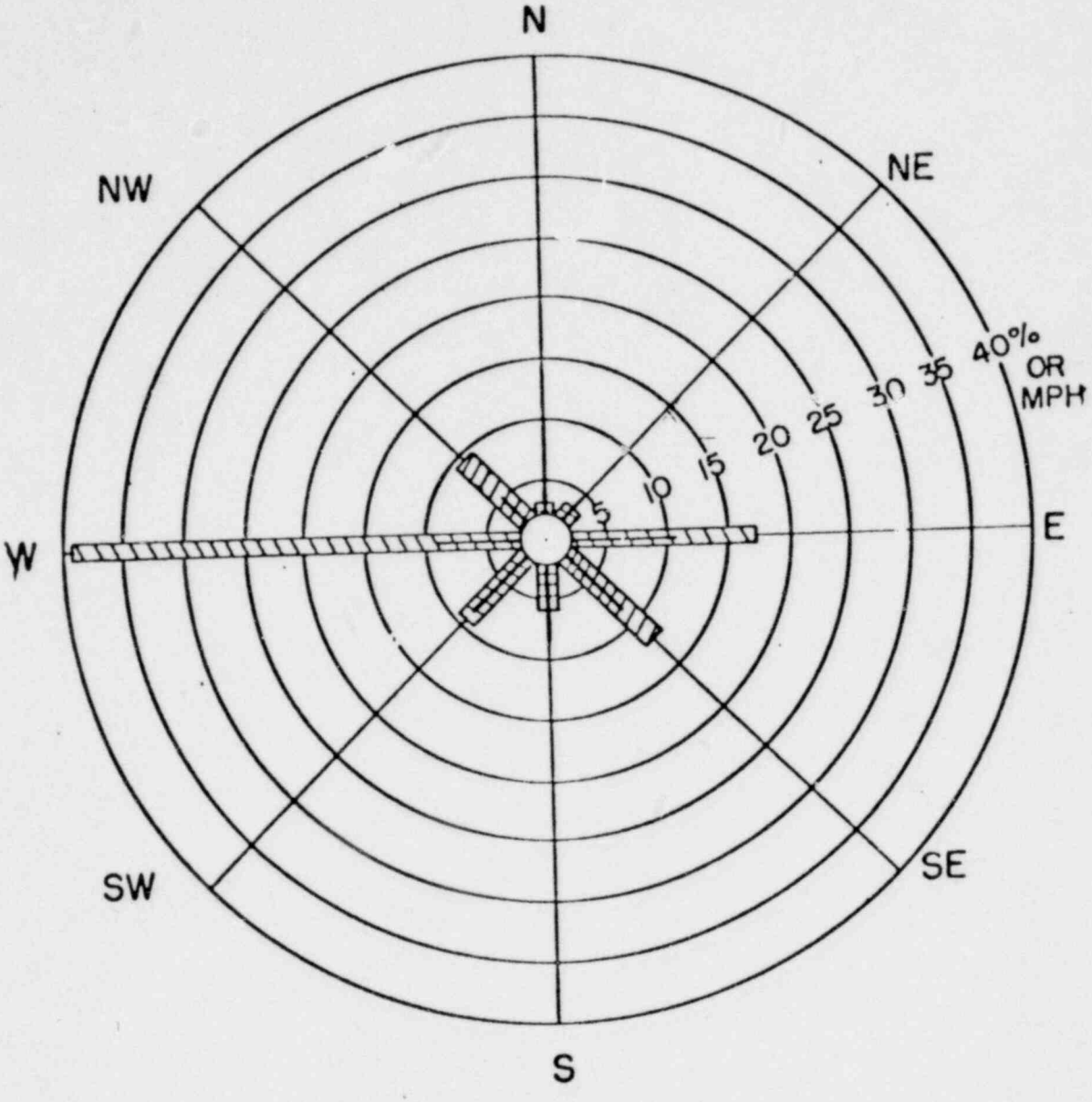

Frequency Distribution and Mean Wind Speed at Site
from Direction Shown

(Hatched Area is Percent Occurrence -
Solid Line is Mean Speed in MPH)
- 1 M.P.H. = 1.61 Kilometer/Hr -

FIGURE 2.4-1

and the campus toward the site. The major population density is upwind from the site about 57% of the time and downwind only about 21% of the time. Furthermore, about 79% of the time the wind blows in a direction in which there are no inhabitants for about .8 kilometers around the site.

The total number of hours of wind by direction and velocity is given in Table 2.4 and total time for winds of all velocities for each month is given in Table 2.4. These tables indicate that the average annual wind velocity is 16 kilometers/hr. Winds in January, the high month, average 21 kilometers/hr. Furthermore, the wind velocity was greater that 5 kilometers/hr 94% of the time and greater than 8 kilometers/hr 76% of the time. In general, one may conclude that there is almost always a light breeze blowing over the site.

2.4.3 Precipitation and Temperature

The monthly average precipitation, monthly mean temperature, and monthly mean daily variation from minimum to maximum temperature at the site are tabulated in Table 2.4. The seasonal variations depicted in this table are a graphic representation of the climatic conditions that prevail at the site as previously described.

2.4.4 Temperature Inversions

Quantitative data on temperature inversions in the vicinity of the site are nonexistent. The closest points for which inversion data are available are at Spokane and Richland. However, the meteorological conditions at these two cities are significantly different from those at Pullman, making these data not applicable. The frequency distribution of winds of less than 3 kilometers/hr is depicted in Figure 2.4-2. These low velocity winds blow only about 6% of the

TABLE 2.4-1

Total Number of Hours of Wind by Direction and Velocity, 1953

Velocity Kilometers Per Hour	DIRECTION							
	N	NE	E	SE	S	SW	W	NW
0-3	31.6	33.2	84.4	63.8	25.8	57.2	134.4	112.5
4-6	135.3	109.0	131.9	141.7	90.8	123.5	514.5	273.5
7-10	34.6	71.6	185.8	191.0	97.0	118.8	612.1	229.2
11-13	15.5	39.9	201.3	260.7	114.6	136.9	548.0	104.2
14-16	13.6	17.7	227.4	161.6	63.6	76.6	490.1	46.3
17-21	0.2	0.5	296.3	130.5	75.8	109.5	454.0	8.6
22-24			103.7	76.8	25.5	72.6	164.0	0.5
25-32		1.1	230.1	78.6	19.6	72.2	256.9	2.0
33			19.2	6.8	8.5	17.2	49.4	

TABLE 2.4-2

Total Time for Winds of all Velocities

Month 1953	N hours	NE hours	E hours	SE hours	S hours	SW hours	W hours	NW hours
January	2.3	3.4	43.3	123.7	93.7	135.3	243.4	16.0
February	18.0	5.7	52.4	87.0	63.2	56.9	278.7	90.0
March	14.2	10.0	146.5	123.5	31.5	81.8	308.3	19.4
April	13.9	24.0	152.2	45.5	31.6	73.2	310.4	69.0
May	23.9	29.3	157.4	51.1	32.2	56.8	296.6	88.2
June	27.0	38.1	64.5	25.5	18.1	68.8	347.0	106.5
July	58.0	57.3	81.3	63.8	17.3	31.0	257.5	124.1
August	24.4	39.3	96.3	92.2	54.1	48.3	267.1	110.6
September	28.5	34.4	141.0	81.5	46.7	75.1	265.5	38.4
October	15.0	37.0	208.5	106.0	34.6	54.8	225.0	62.2
November	5.5	3.9	257.2	134.9	33.5	36.3	158.7	37.5
December	1.5	0.1	112.4	157.6	71.1	78.4	284.9	36.3
Total	232.2	282.51	1,513.0	1,092.3	527.6	796.7	3243.1	798.2
Percent	2.7	3.3	17.8	12.9	6.2	9.4	38.2	9.4
Av. Duration (hrs.)	.94	1.26	1.46	.85	.75	.66	1.47	.73

TABLE 2.4-3

Monthly Average Precipitation,

Daily Mean Temperature,

And Mean Daily Minimum To Maximum Temperature Difference,

1893-1970

Month	Precipitation in Centimeters	Daily Mean Temperature in Degrees C.	Mean Daily Minimum to Maximum
January	6.78	-2.6	5.7
February	5.33	0.2	6.7
March	5.38	3.8	8.4
April	3.78	8.5	10.8
May	3.71	12.7	11.8
June	3.91	15.4	12.7
July	0.99	19.9	15.7
August	1.32	19.1	15.3
September	2.74	14.3	13.0
October	4.85	10.0	10.4
November	6.27	3.2	6.7
December	6.96	0.1	5.7

Annual Total Precipitation - 49.50 centimeters

Annual Average Temperature - 8.7°C

Annual Average Difference between Minimum and Maximum Temperatures - 10.2

time whereas winds in the 5 to 7 kilometer/hr range blow about 18% of the time.

If the assumption is made that a temperature inversion can only be maintained with winds of below 3 kilometers/hr, then inversions could occur only about 6% of the time. The distribution of the low velocity winds further indicates that the population center west of the site would be downwind only about 22% of the time during which inversions could possibly occur.

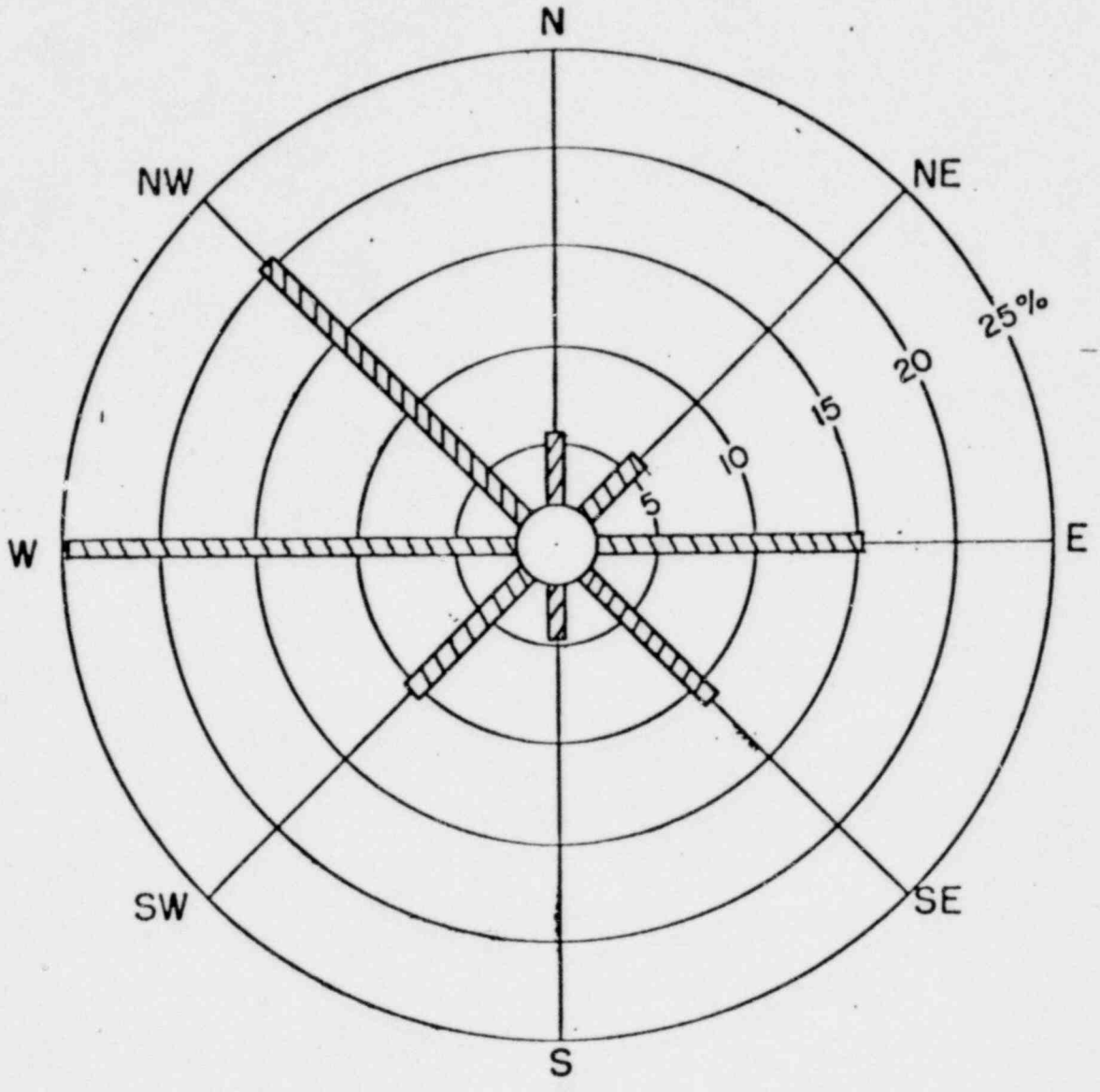

Frequency of Occurrence of Winds
of Less Than 3 Kilometers/Hr
from Direction Shown

FIGURE 2.4-2

2.5 Geology

2.5.1 Regional Geologic History

Pullman is situated in Eastern Washington near the eastern margin of the Columbia River Plateau. In early Miocene times the area was mountainous with a relief of over 1400 meters. These mountains, composed mostly of pre-Cambrian sedimentary and metamorphic rocks and Cretaceous granite, formed the basement rock across which the Columbia River Basalts would flow during the Miocene epoch. These basalt flows were numerous as well as extensive and advanced from the west and the south into the region.

The basalts of the Columbia plateau are somewhat unique in that a large thickness of volcanic material accumulated in a relatively short period on the geologic time scale. The lava flows extended over a 160,000 square kilometer area in the short span of about 3 million years about 16 to 13 million years ago. The total thickness of the basalt varies from 1000 meters in the Pullman area to a maximum of over 3 kilometers in the Pasco Basin. Individual flows were enormous and involved of the order of 300 cubic kilometers of lava. The source of the immense amount of heat needed to create the lava flows is postulated to be a "Hot Spot" in the magma below the region. Some geologists believe that the "Hot Spot" remained stationary as the Pacific Plate moved west. This theory accounts for the young basalts in southern Idaho and the geothermal activity in Yellowstone National Park. The "Hot Spot" is thus postulated to presently reside under the Yellowstone Park region.

The basalt that flowed into the pre-flow terrain of the region progressively submerged the basement features and dammed up the well-established drainage systems. Numerous lakes were created along the margin of the growing basalt plateau. Weathering of the exposed basement uplands produced

detritus materials which rapidly filled in the temporary Miocene lakes established by the advancing basalt. Such lacustrine deposits were subsequently buried by flows from renewed basaltic eruptions triggering a repetition of the accumulation cycle. The solidified lava flows were nearly horizontal, however, the lava evidently erupting from many different locations at different times so that individual flows are not continuous across the plateau. The orginal upper surface of the basalts were probably quite rough but very low in relief.

At the end of the outpourings of the lavas of the Columbia River Basalt in early Pliocene times, mild folding of the basalt began. The folding continued through middle and late Pliocene and into Pleistocene time. Deformations in this age include the Cascadian orogeny which greatly affected the climatic conditions of the region. The main tetonic events during this period include; the uplift of the Cascade Range, Oregon Coast Range, Olympic Mountains, and Blue Mountains; the downwarping of the Lewiston Grade, the Snake River Region, and the Walla Walla Plateau; a slightly westerly increasing subsidence of the Columbia Plateau; the isostatic depression of the Pasco Basin; and block faulting of the Great Basin and Payette section. Volcanic eruptions accompanied the deformations particularly in the Middle Cascades giving rise to the volcanic peaks of the Cascade Range.

Following the cessation of the major igneous activity in early Pliocene times, the basalts and lacustrine deposits became subjected to moderate erosion as the drainage patterns began to develop. This initiated the dissection of the plateau surface. During the Pleistocene epoch the modified surface was capped with the loess of the Palouse formation and produced the rolling-hill topography of the region. The most significant geological event during the past million years is the Spokane flood at the end of the

Ice Age. The advancing ice sheet dammed the Columbia, Spokane, and Clark Fork Rivers. The water that was impounded behind the dams filled the tributary valleys for many miles.

The lake created by the damming of the Clark Fork contained an estimated 1000 cubic kilometers of water or about half the volume of present day Lake Michigan. When the ice dam at the mouth of the Clark Fork failed, the lake drained at an estimated flow rate of 15 cubic kilometers per hour. The incredible force of the massive flood scoured the Rathdrum Prairie and Spokane Valley creating the "Channeled Scablands" in the Sprague-Cheney area. Similar events during the ice age created the present features of the Columbia Plateau including Grand Coulee.

The region has seen a very unique sequence of geological events beginning with a vast series of lava flows. The lava flows were followed by a regional tilting of the land and by the deposition of a 30-60 meter layer of wind blown silt. The great glacial lake formed by the damming of the Clark Fork and the destructive flood created by the sudden release was the final event that brought this area to its present character.

2.5.2 Site Geology

The Columbia River formation in the Pullman area is approximately 1000 meters thick and consists of alternating layers of basalt and the silts and clays of the Latah formation. A geologic cross section of the Pullman area is shown in figure 2.5-1. The Palouse Formation Soil at the site is 35 to 55 meters thick. Structurally the layers of basalt in the Pullman area have not been disturbed since their deposition. The major movements in this section of the Columbia Plateau have been the Lewiston downwarp and the westerly subsidence.

2.5.2 Geologic Hazards

No known geologic hazards such as Karst terrain, cavernous conditions, tectonic depressions, surface or subsurface subsidence or uplifts, or active volcanoes, are present at the site or in the immediate vicinity of Pullman. Also, there are no conditions present which could produce rock-falls, avalanches, floods, tsumani, mudflows, or permafrost at the site.

2.5.4 Site Groundwater Conditions

The main aquifers in the Pullman area are associated with the Latah Formation interbeds between basalt flows as shown in Figure 2.5-1. Horizontal migration within an aquifer may also occur in the vesticular or porous top of the basalt layers. The cities of both Pullman and Moscow obtain their water from deep aquifers over 200 meters below the surface. Carbon-14 dating of the water from the deep aquifers indicate that no measurable recharge has occurred in recent times. Accordingly it is believed that a layer of impervious basalt of about 100 meters below the surface prevents the downward migration of surface waters.

Recharge of the shallow aquifers is believed to occur at the eastern end of the Moscow-Pullman basin where the basalts contact the Pre-Tertiary Moscow Mountain Formation (see Figure 2.5-1). Additional recharge also occurs by infiltration from streams and precipitation waters. However, surface waters percolate slowly downward due to the high water retention capacity of the Palouse Formation as well as the thickness of such soils. Accordingly liquids discharged at the reactor site in the event of an accident will not enter the local aquifer. In addition, there are no rivers or streams within one kilometer of the site.

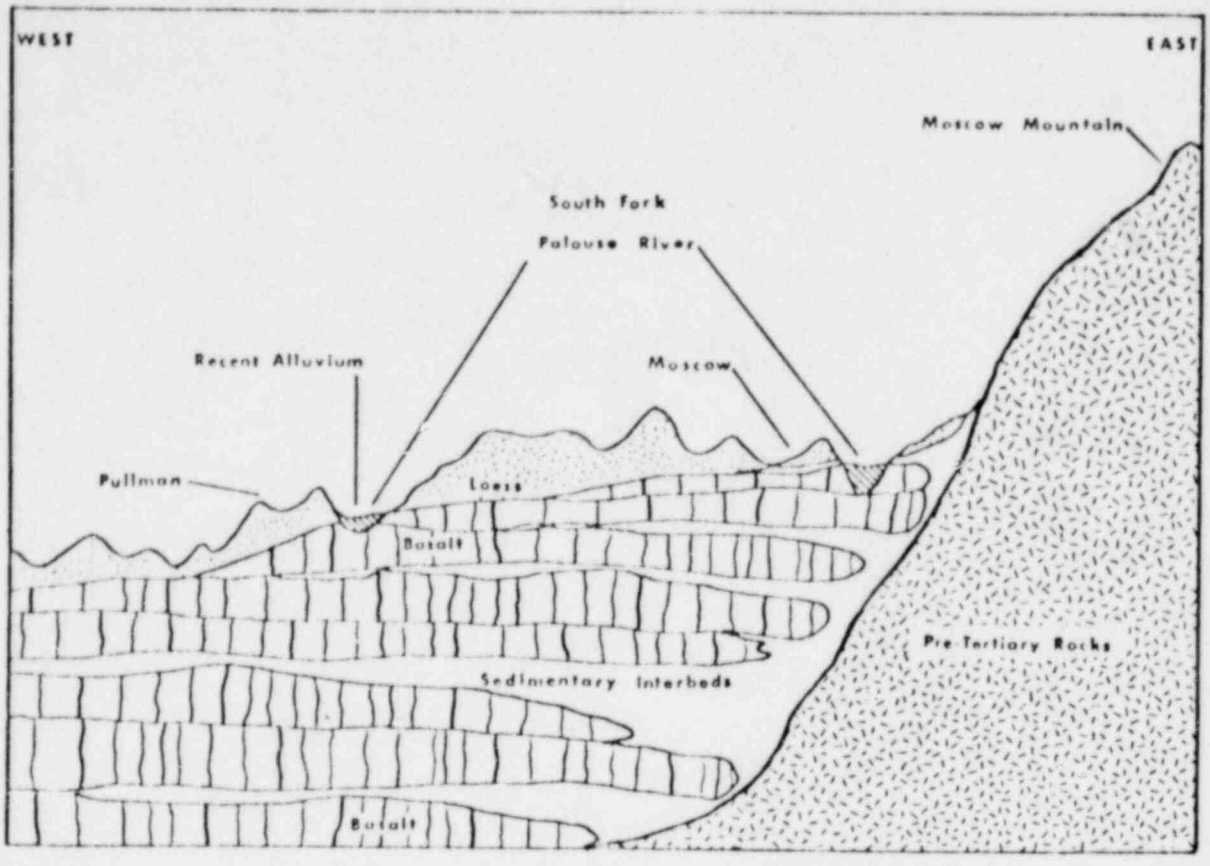

Figure 2.5-1

Schematic geologic section through the Pullman-Moscow basin (from Ichimura, 1978).

2.6 Seismology

Realistic predictions regarding earthquakes, or earth shocks, as well as their frequency and severity, can only be based upon seismic history of the area. Significant geological features, such as known slip-planes or faults, play an important role in the seismic history of any region. Thus these features as well as past shocks must be taken into consideration in depicting the seismology of the site.

The overall geological features of the Pullman area are described in the section on geology and will not be repeated here. In this section we are concerned with the geological features of this area that could possibly produce earthquakes. The significant faults within a circle of a 100 mile radius of the site are shown in Figure 2.6-1. From this drawing it is evident that there are no known significant faults in the immediate vicinity of Pullman. The closest active fault is the Walla Walls fault, some 70 miles from Pullman. The closest inactive faults are the Vista and Wilma faults associated with the Lewiston Downwarp.

Historically, the seismic activity within 200 miles of the site is low, with infrequent earthquakes of low intensity and magnitude. The occurrences of earthquakes within 200 miles of Pullman are listed in Table 2.6-1. It is noteworthy that only two shocks have occurred at Pullman in recorded history, both of them of low intensity.

Based on the geology of the Pullman area and the past seismic activity, the probability of the occurrence of significant earthquakes in the future can be said to be very small.

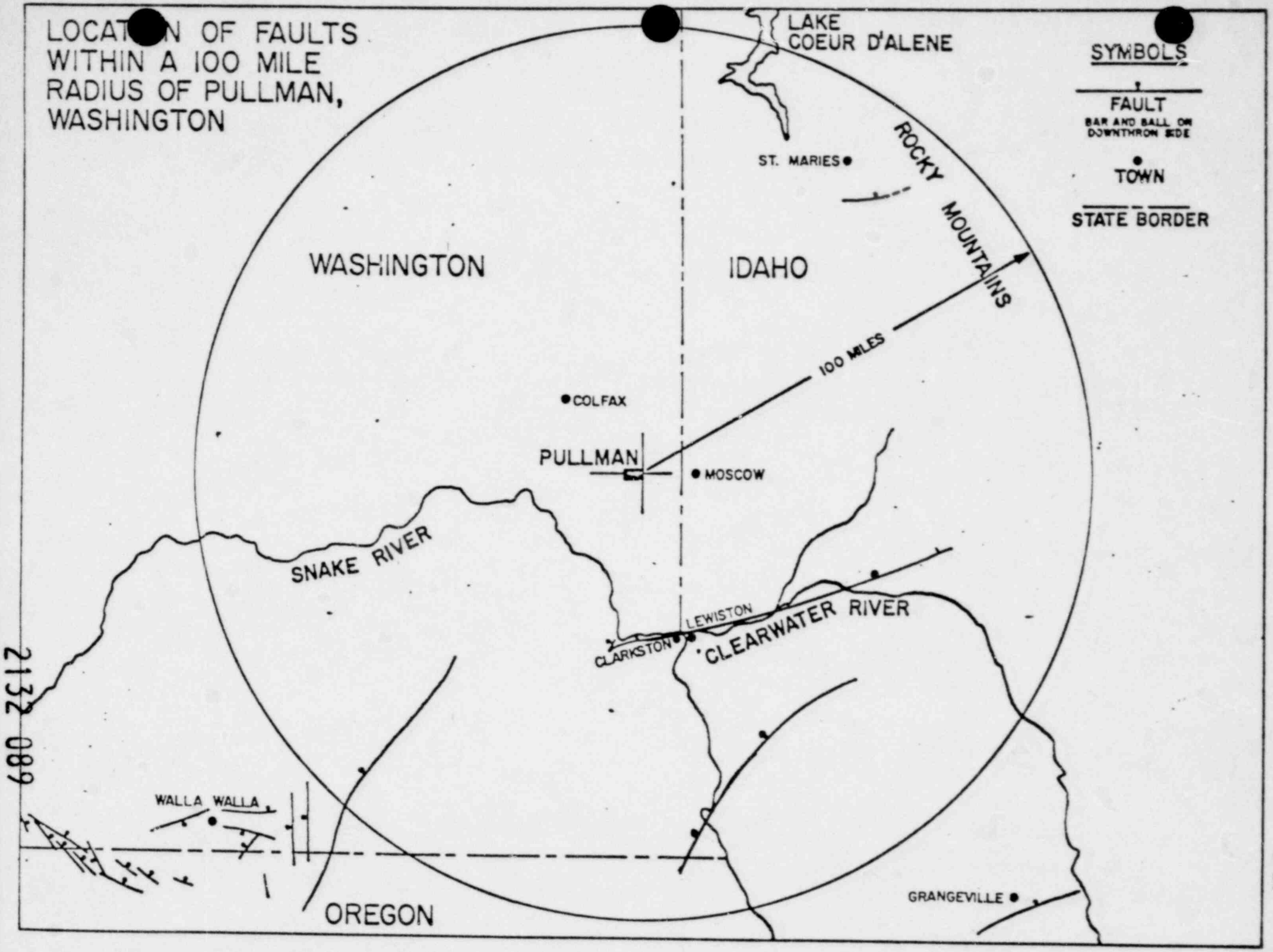

2132 089

2-25

FIGURE 2.6-1

TABLE 2.6-1

HISTORIC EARTHQUAKES 1872-1979
WITHIN 200 MILES OF SITE*

Year	Date	Location of Epicenter	Approximate Distance from Pullman	Intensity at Epicenter**
1872-73	Dec. 16-Jan. 1	Walla Walla	70 miles	Unknown
1874	Unknown	Yakima	155	Unknown
1875	May 6	Yakima	155	Unknown
1875	May 7	Yakima	155	Severe
1887	April 29	Walla Walla	70	Felt
1898	Feb. 22	Ellensburg	160	Felt
1906	Jan. 2	NE Washington	---	Felt Over 200 Square Miles
1906	Nov. 2	Colville	130	V
1909	May 24	47.6N, 120.0W	140	Felt
1911	July 5	Ellensburg	160	V
1915	Dec. 10	Spokane	65	III-IV
1918	Nov. 1	46.7N, 119.5W	105	V-VI
1920	Nov. 28-29	Spokane	65	Felt
1921	Sept. 14	Walla Walla	70	V-VI
1922	Jan. 31	Republic	150	Felt

* Data abstracted from "Washington State Earthquakes 1840 through 1965", "Seismic Trends in Washington State", and "Washington State Earthquakes Jan. 1969 - June 1979", all by N. H. Rasmussen, Seismologist, Geology Department, University of Washington, Seattle, Washington.

**Modified Mercalli Intensity Scale of 1931.

Year	Date	Location of Epicenter	Approximate Distance from Pullman	Intensity at Epicenter**
1922	June 1	Spokane	65	IV
1922	Oct. 16	Hermiston, Ore.	120	III
1924	Jan. 6	Walla Walla	70	IV
1924	May 27	Walla Walla	70	IV
1926	April 11	Walla Walla	70	III
1926	April 23	Walla Walla	70	IV
1930	Sept. 3	47.3N, 117.8W	70	V
1935	Oct. 24	Ellensburg	160	Felt
1936	July 16	46.0N, 118.3W	70	VII
1936	July 18-20	Walla Walla	70	Felt
1936	July 30	Freewater, Ore.	80	VI
1936	July 30	Walla Walla	70	III-VI
1936	Aug. 4	45.8N, 118.6W	115	V
1936	Aug. 28	Walla Walla	70	IV
1936	Nov. 17	Walla Walla	70	II'
1937	Feb. 8	Walla Walla	70	III
1937	Feb. 9	Walla Walla	70	IV
1937	June 4	Walla Walla	70	IV
1937	June 17	Walla Walla	70	Felt
1937	Aug. 11	Spokane	65	Felt
1937	Sept. 20	Walla Walla	70	Felt
1938	May 9	Walla Walla	70	Felt
1938	May 24	Walla Walla	70	Felt
1938	Aug. 11	Milton, Ore.	80	VI
1938	Oct. 27	Milton, Ore.	80	VI

Year	Date	Location of Epicenter	Approximate Distance from Pullman	Intensity at Epicenter**
1939	Feb. 6	Ellensburg	160	Felt
1940	Jan. 6	Ephrata	120	Felt
1940	Nov. 14	47.7N, 121.5W	165	III
1941	Jan. 3	Pullman	0	Felt
1941	April 7	Republic	150	VI
1941	July 29	Spokane	65	Felt
1942	Nov. 1	48.0N, 116.7W	85	VI
1943	April 24	47.3N, 120.6W	110	VI
1944	Sept. 2	Walla Walla	70	IV
1945	April 29	47.4N, 121.7W	150	VII
1945	April 30	47.4N, 121.7W	150	VI
1945	May 1	47.4N, 121.7W	150	V
1945	Sept. 23	Walla Walla	70	IV
1949	Feb. 6	Wapato	155	III
1949	April 14	Pullman	0	Felt
1950	June 25	Cheney	55	IV
1952	Mar. 4	Spokane	65	V
1952	July 27	47.8N, 121.9W	155	IV
1952	July 29	47.8N, 121.9W	155	Felt
1952	Nov. 10	47.6N, 121.5W	165	Felt
1955	Feb. 6	Grand Coulee Dam	120	IV
1955	July 15	Soap Lake	120	IV
1955	Nov. 3	48.1N, 121.7W	170	V
1956	Feb. 24	Electric City	120	V
1956	Nov. 18	48.1N, 121.8W	165	Felt

Year	Date	Location of Epicenter	Approximate Distance from Pullman	Intensity at Epicenter**
1957	Feb. 11	47.5N, 121.7W	150	VI
1957	Nov. 1	47.0N, 121W	185	V
1958	Apr. 12	48N, 120W	150	VI
1958	Apr. 12	Electric City	120	IV
1959	Jan. 21	Walla Walla	70	IV
1959	Aug. 6	47.8N, 120.0W	145	VI
1959	Nov. 23	46.7N, 121.7W	140	V
1961	May 22	47.6N, 120.2W	145	IV
1961	June 28	Rocky Reach Dam	145	IV
1961	Oct. 31	48.4N, 120W	170	V
1961	Nov. 7	Spokane	65	Felt
1962	Jan. 15	47.8N, 120.2W	155	VI
1963	Jan. 25	La Grande, Ore.	105	III
1963	Dec. 22	48.3N, 119.3W	130	V
1964	Oct. 18	47.9N, 121.9W	155	IV
1966	Dec. 24	47.9N, 121.3W	155	III
1967	June 6	48.2N, 119.1W	125	IV
1969	Oct. 9	46.8N, 121.7W	140	VI
1969	Nov. 1	47.9N, 121.9W	165	V
1969	Nov. 10	48.5N, 121.4W	190	V
1971	Oct. 25	46.7N, 119.6W	105	IV

Year	Date	Location of Epicenter	Approximate Distance from Pullman	Intensity at Epicenter**
1974	July 14	47.6N, 120.7W	177	IV
1975	June 28	46.2N, 119.7W	125	III
1975	Sept. 18	47.8N, 118.2W	89	III
1975	Dec. 3	45.6N, 118.9W	113	III
1976	Apr. 13	45.24N, 120.2W	174	IV
1976	May 15	47.71N, 120.03W	151	III
1976	June 15	46.45N, 117.68W	31	III
1976	June 15	47.63N, 120.3W	160	III
1976	July 23	46.08N, 118.75W	87	III
1976	Aug. 30	47.62N, 120.18W	154	III
1976	Dec. 13	47.64N, 120.13W	153	III
1977	Jan. 27	46.94N, 119.59W	115	III
1977	Mar. 10	45.89N, 119.68W	132	III
1977	Apr. 21	49.12N, 117.67W	168	IV
1977	July 13	47.06N, 120.95W	179	IV
1978	June 27	46.94N, 121.14W	188	III
1979	Jan. 19	47.92N, 119.69W	144	IV
1979	April 8	46.0N, 118.42W	78	IV

3.0 FACILITY STRUCTURE

3.1 General Description

The W.S.U. TRIGA reactor is located within the Nuclear Radiation Center which is pictured in Figure 3.1-1. The Center is a 1200 square meter laboratory devoted to nuclear related research and educational activities. The laboratory building is a concrete structure located east of the main portion of campus. All the utilities for the laboratory including heating, cooling, ventilation, and power distribution are contained within the structure. A set of floor plans for the Center is shown in Figures 3.1-2(a) to 3.1-2(d).

The reactor core is located in the reactor pool, the top of which is accessible via Pool Room 201 depicted in Figure 3.1-2(c). The pool room, control room, and reactor shop have a combined volume of 1×10^9 cm^3 and only two external exits on the east side. The reactor console is situated adjacent to the pool room in Room 201B and the reactor shop is located in Room 201A. A radiochemistry laboratory is located in Room 101 just below the control room and the beam room is located in Room 2 on the ground level below the radiochemistry laboratory. A list of rooms in the Center is given in Table 3.1-1.

3.2 Heating and Air Conditioning System

The Center contains two independent heating and ventilation systems. One system serves the laboratory areas exclusive of the reactor and the other serves the reactor. A third air handling system serves the fume hoods in the various laboratories. The hoods in all radiochemistry laboratories have absolute filters.

The reactor ventilation system as shown in Figure 3.2-1 has provisions for operation in the normal, isolation, and dilution modes. In the normal mode 7.08×10^5 cm^3/sec of externally treated air is discharged into the pool room. This loop is shut off in the isolation and dilution modes.

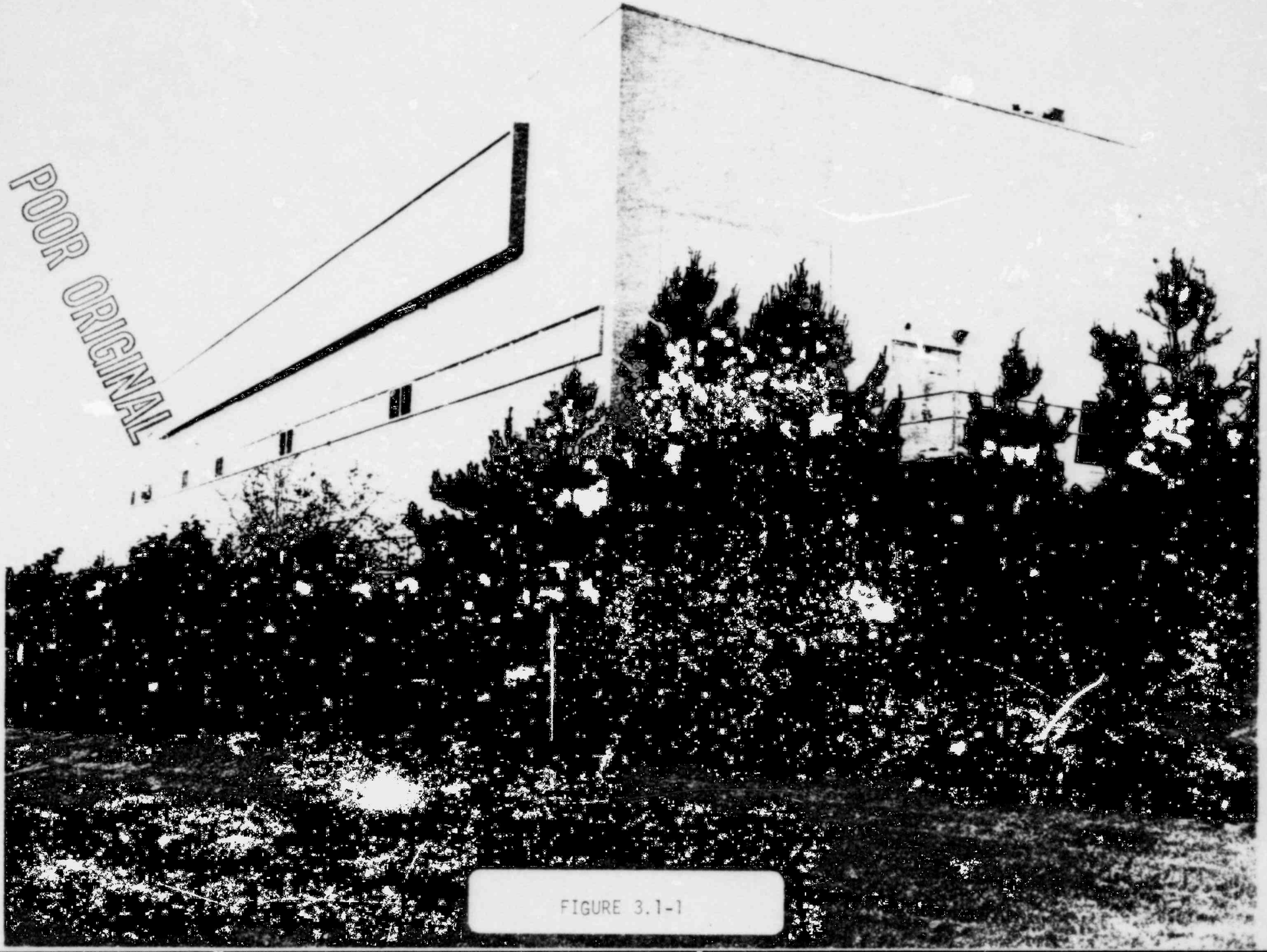

POOR ORIGINAL

2132 097

FIGURE 3.1-1

TABLE 3.1-1

Nuclear Radiation Center Room Listing

Room	Description
002	Neutron Beam Room
002A	Source and Material Storage
003	Rest Room - Women
004	Lounge - Women
005	Rest Room - Men
006	Electrical Panel, Utilities
010	Boiler Room
B10	Transformer Vault
B10A	Transformer Vault
020	Storage
021	Radioactive Waste Storage
B21	Neutron Generator
050	Secretary, Receptionist
050A	Director
050B	Associate Director
050V	Entryway
101	Radiochemistry Laboratory
101A	Pool Treatment Pump
105	Janitor Storage
106	Pool Water Treatment
110	Radiochemistry Laboratory
112	Faculty Office
112A	Passageway
112B	Photo Darkroom
112C	Decontamination Room
114	Chemistry Laboratory
115	Graduate Student Offices
115A	Faculty Office
116	Computer-Analyzer Room
116A	Faculty Office
117	Counting Room
117A	Faculty Office
119	Standards Laboratory
121	Sample Preparation Laboratory
122	Storage - Building Maintenance
123	Bay
123A	Gas Cylinder Storage
124	Rest Room - Men
150	Counting Room
151	Conference Room
201	Reactor Pool Room
201AA	Reactor Supervisor
201A	Reactor Shop
201B	Reactor Control Console
201C	Heat Exchanger Pump Room
210	Sample Preparation Laboratory
210A	Effluent Sampler
212	Geologic Materials Laboratory
214	Organic Chemistry Laboratory
215	Atomic Absorption Laboratory
217	Faculty Office
217A	Faculty Office
218	Electronics Shop
218A	Electronics Office
220	Storage
221	Chemistry Laboratory
222	Machine Shop
223	Bay
250	Secretary
250A	Faculty Office
250B	Library
250C	Faculty Office
300 & 301	Ventilation, Air Control Equipment

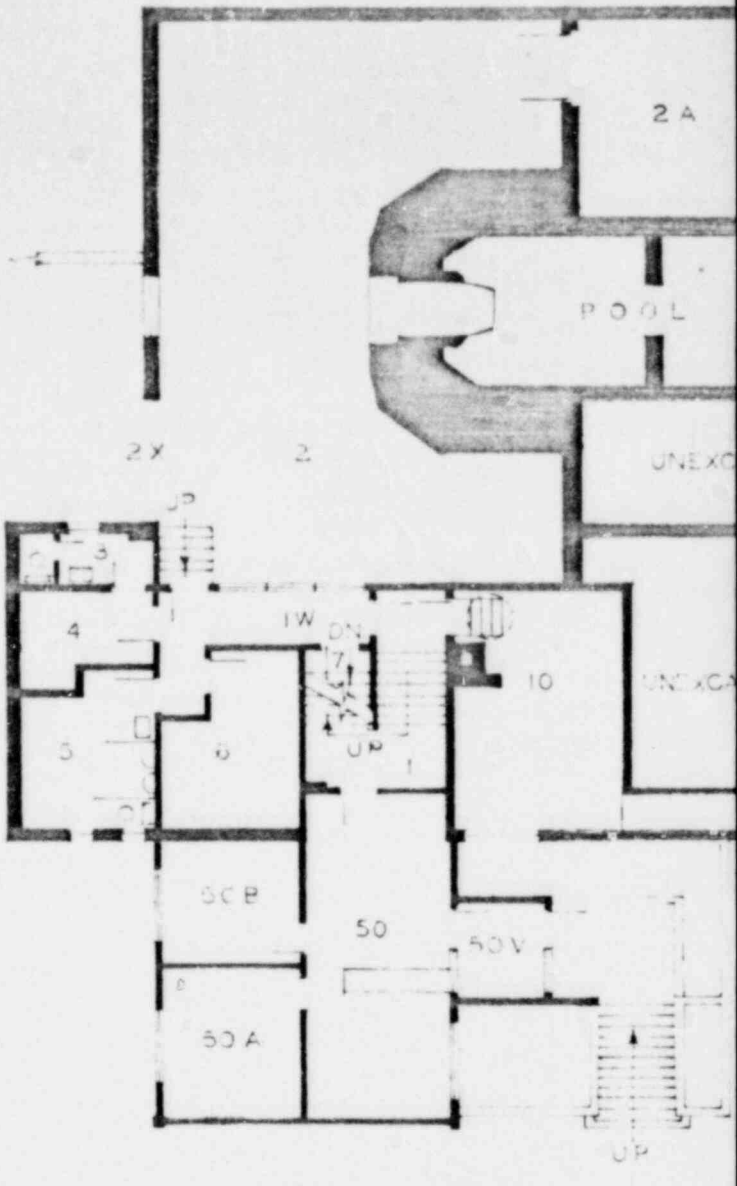

GROUND FLOOR PLAN
SCALE: 1/16"=1'-0"

TRANSFORMER VAULT- 533 SQ. FT.
BASEMENT — 284 SQ. FT.
GROUND — 5702
FIRST — 6381
SECOND — 7182
PENTHOUSE- 5948

TOTAL — 24,132 SQ. FT.

BASEMENT — 5,683 SQ. FT.
GROUND — 5,702
TRANSFORMER VAULT — 533

REVISION DATES

2-14-69	6-16-72
3-25-70	5-31-78
9 24 71	

WASHINGT
PULL

2132 099

FIGUR

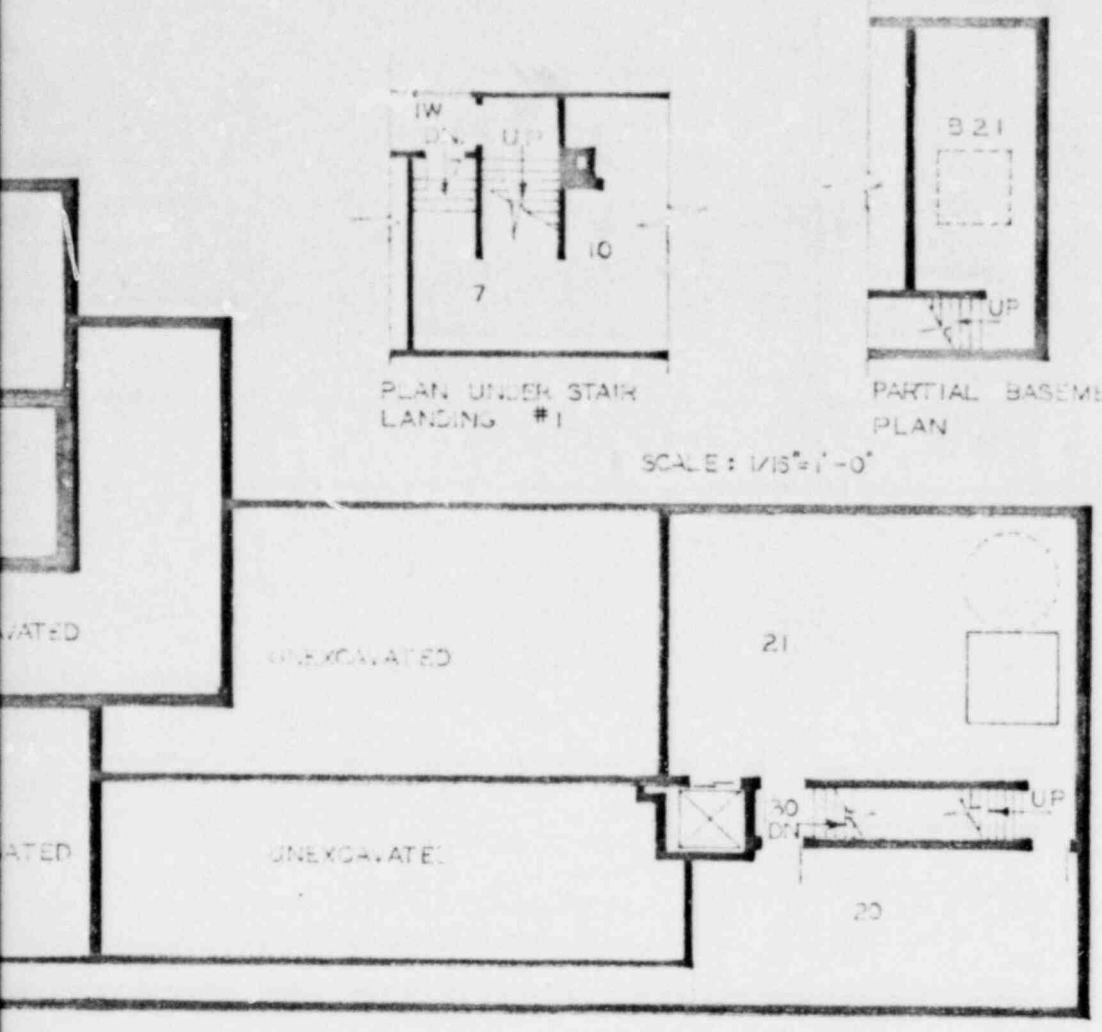

PLAN UNDER STAIR LANDING #1

PARTIAL BASEMENT PLAN

SCALE: 1/15"=1'-0"

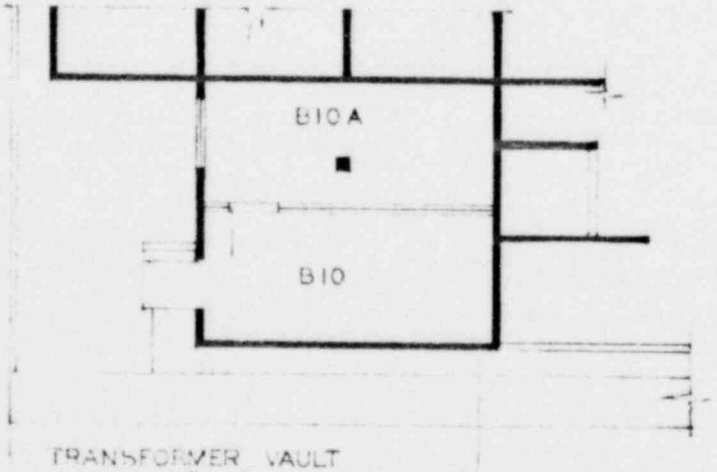

TRANSFORMER VAULT
SCALE: 1/16"=1'-0"

R-1

ON STATE UNIVERSITY MAN, WASHINGTON	NUCLEAR, RADIATION CENTER	BLDG. NO. 74

E 3.1-2

2132 100

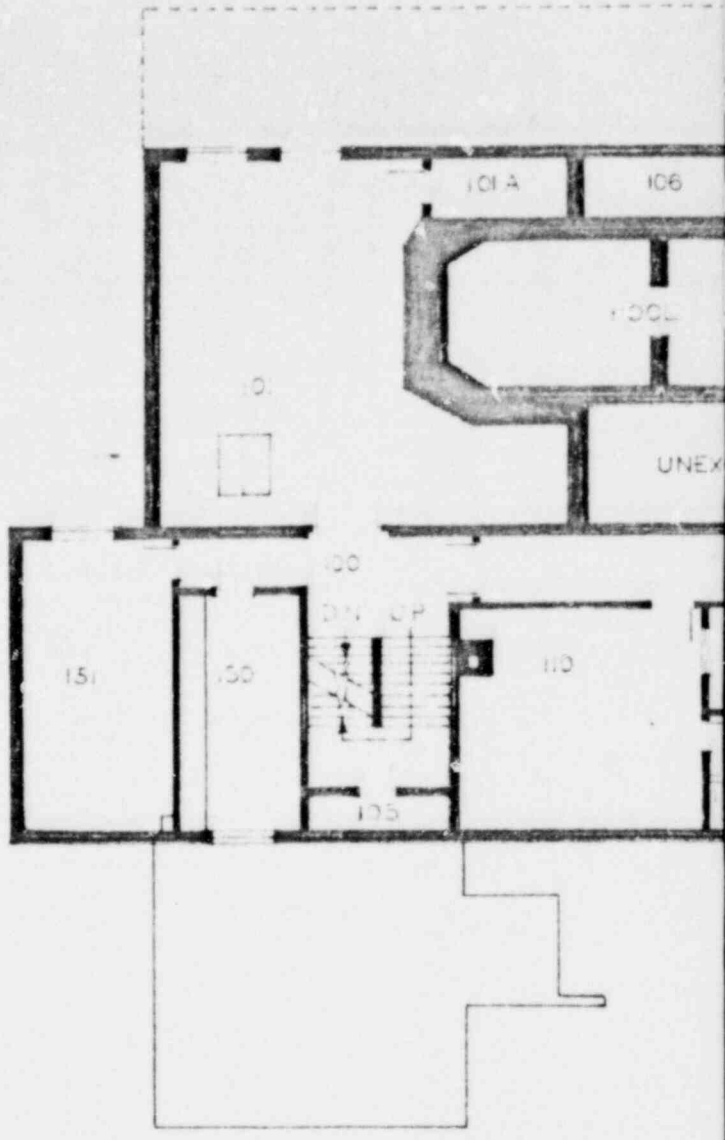

FIRST FLOOR PLAN
SCALE: 1/16"=1'-0"

6,381 SQ. FT.	REVISION DATES 2-4-69 3-25-70 6-16-72	WASHING PUL

2132 101

FIG

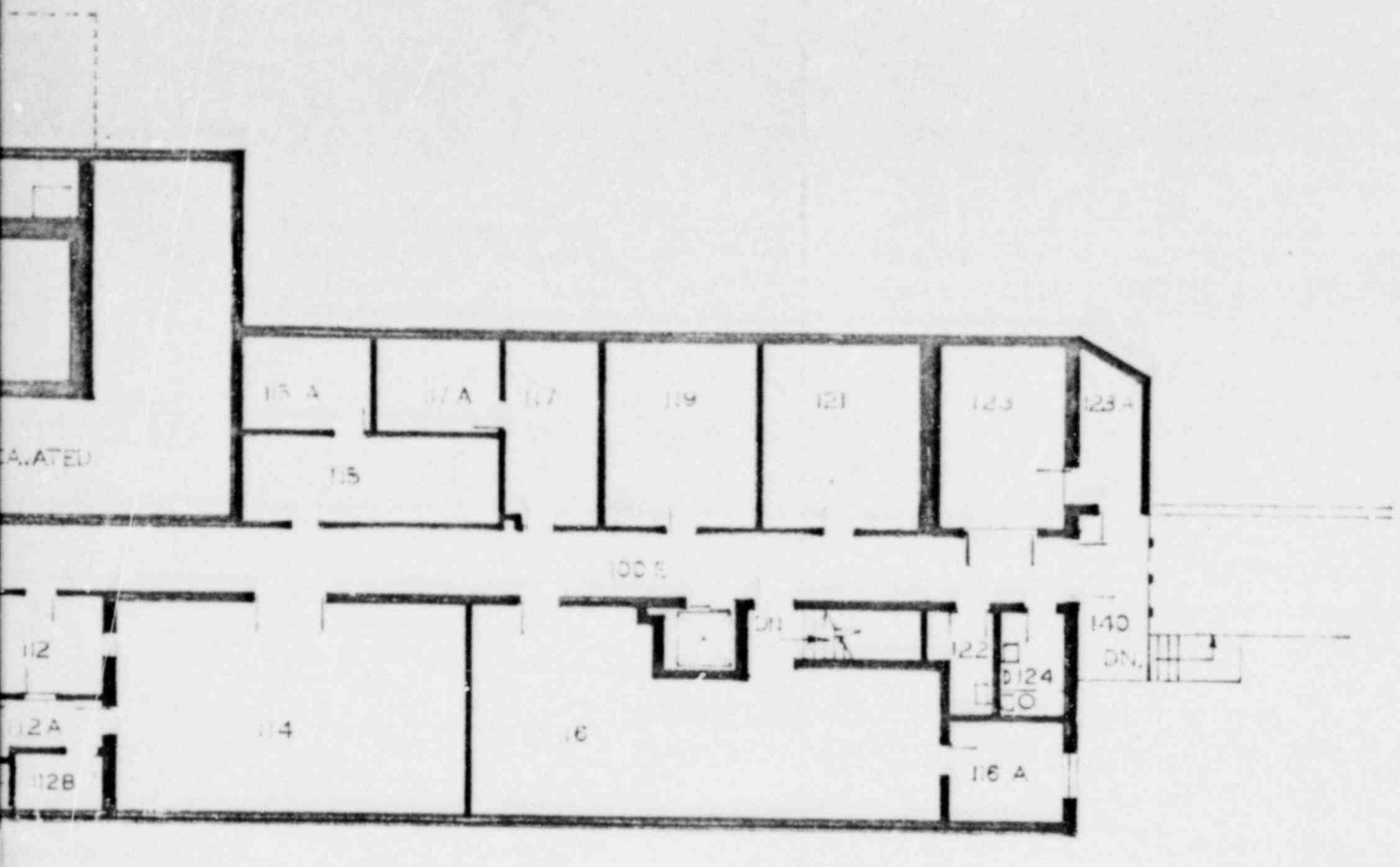

NORTH

R-2

TON STATE UNIVERSITY LMAN, WASHINGTON	NUCLEAR RADIATION CENTER	BLDG. NO. 74

RE 3.1-26

2132 102

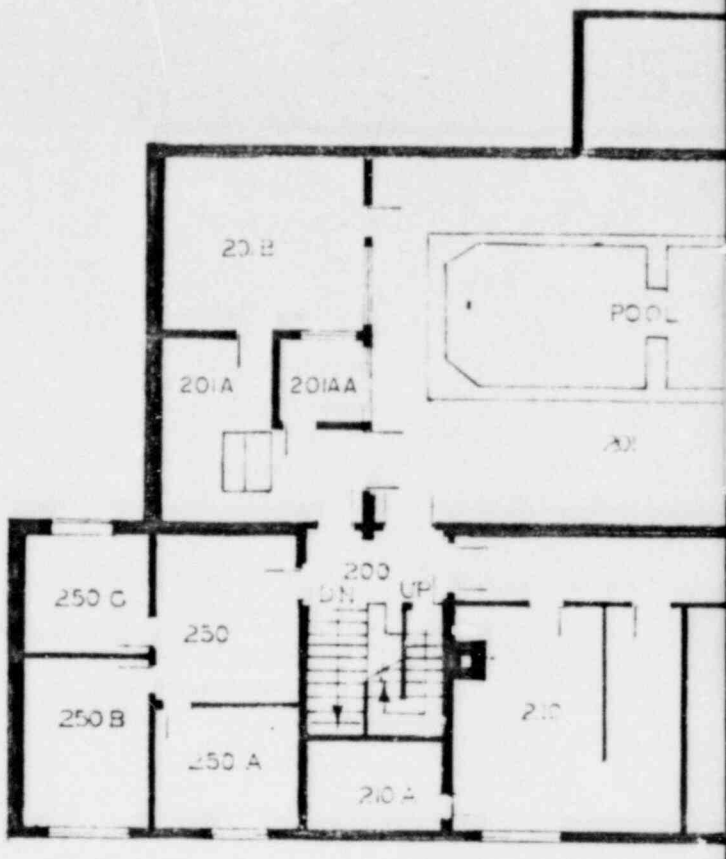

SECOND FLOOR PLAN
SCALE: 1/8"=1'-0"

7,282 SQ. FT.	REVISION DATES		WASHINGT
	2-14-69	4-26-78	PUL
	3-25-70		
	6-16-72		

FIGU

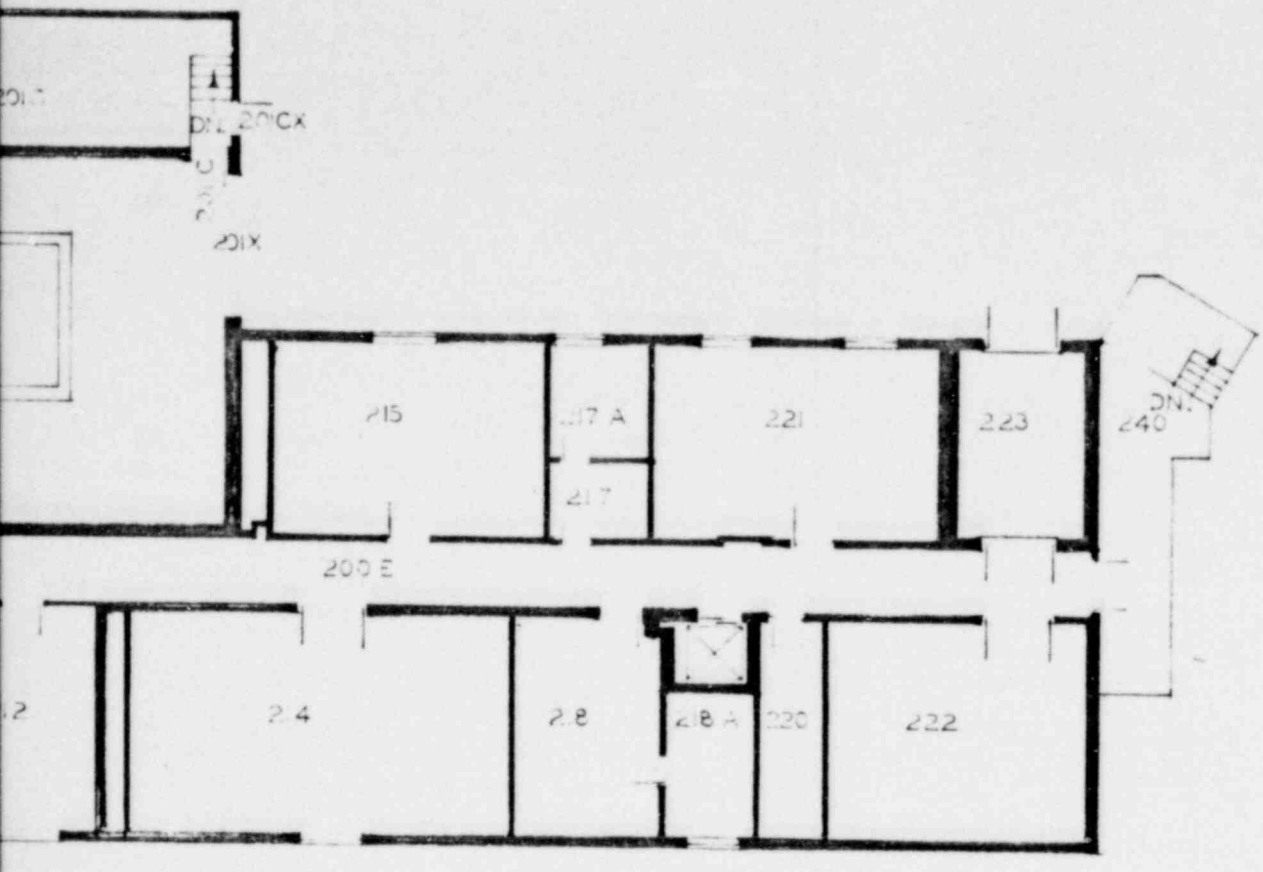

R-3

ON STATE UNIVERSITY MAN, WASHINGTON	NUCLEAR RADIATION CENTER	BLDG. NO. 74

RE T1-2c

2132 104

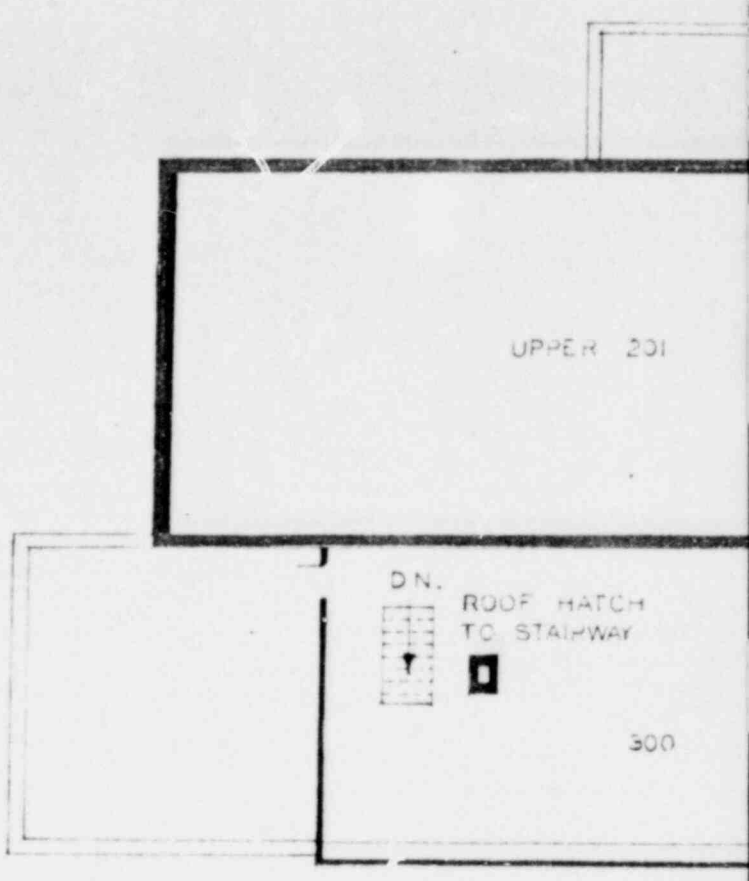

PENTHOUSE FLOOR PLAN
SCALE: 1/16"=1'-0"

3,946 SQ. FT.	REVISION DATES 2-14-69 3-25-70 6-16-72	WASHINGT PULL

FIG

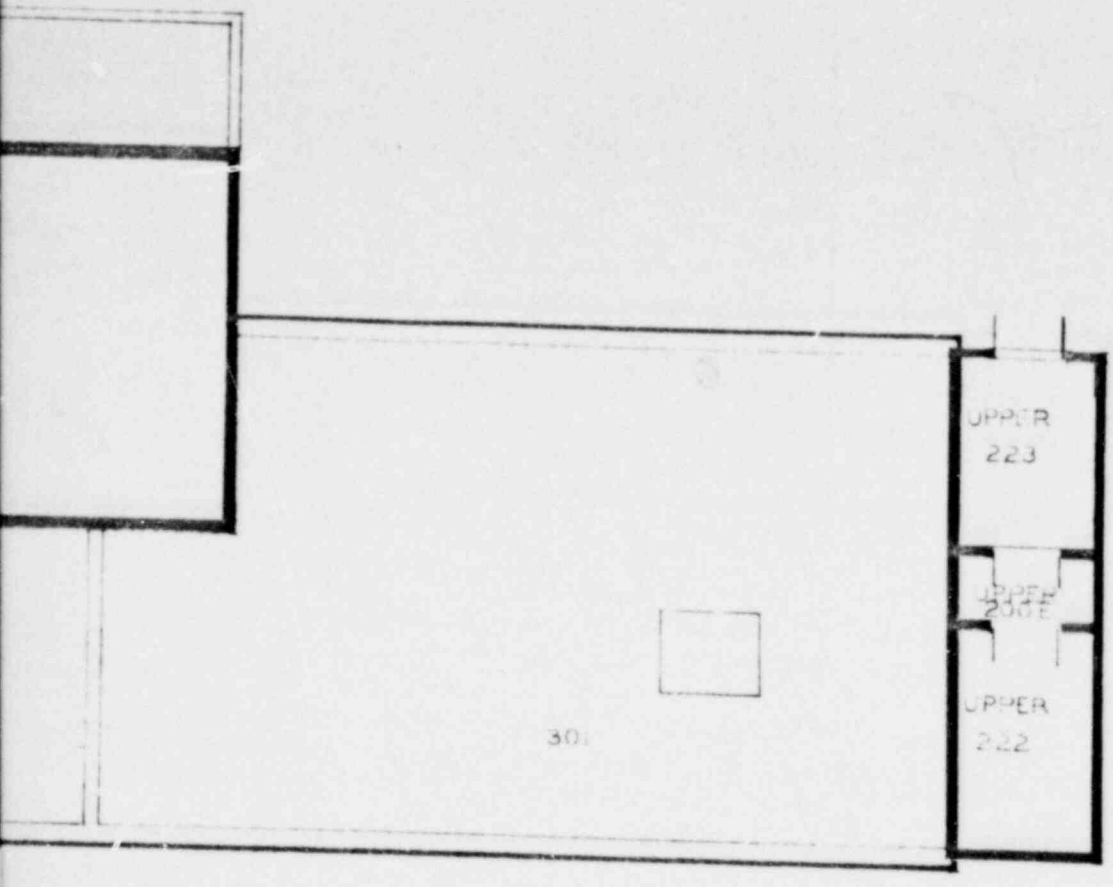

NORTH

R-4

N STATE UNIVERSITY. AN, WASHINGTON.	NUCLEAR RADIATION CENTER	BLDG. NO. 74

RE: 3.1d

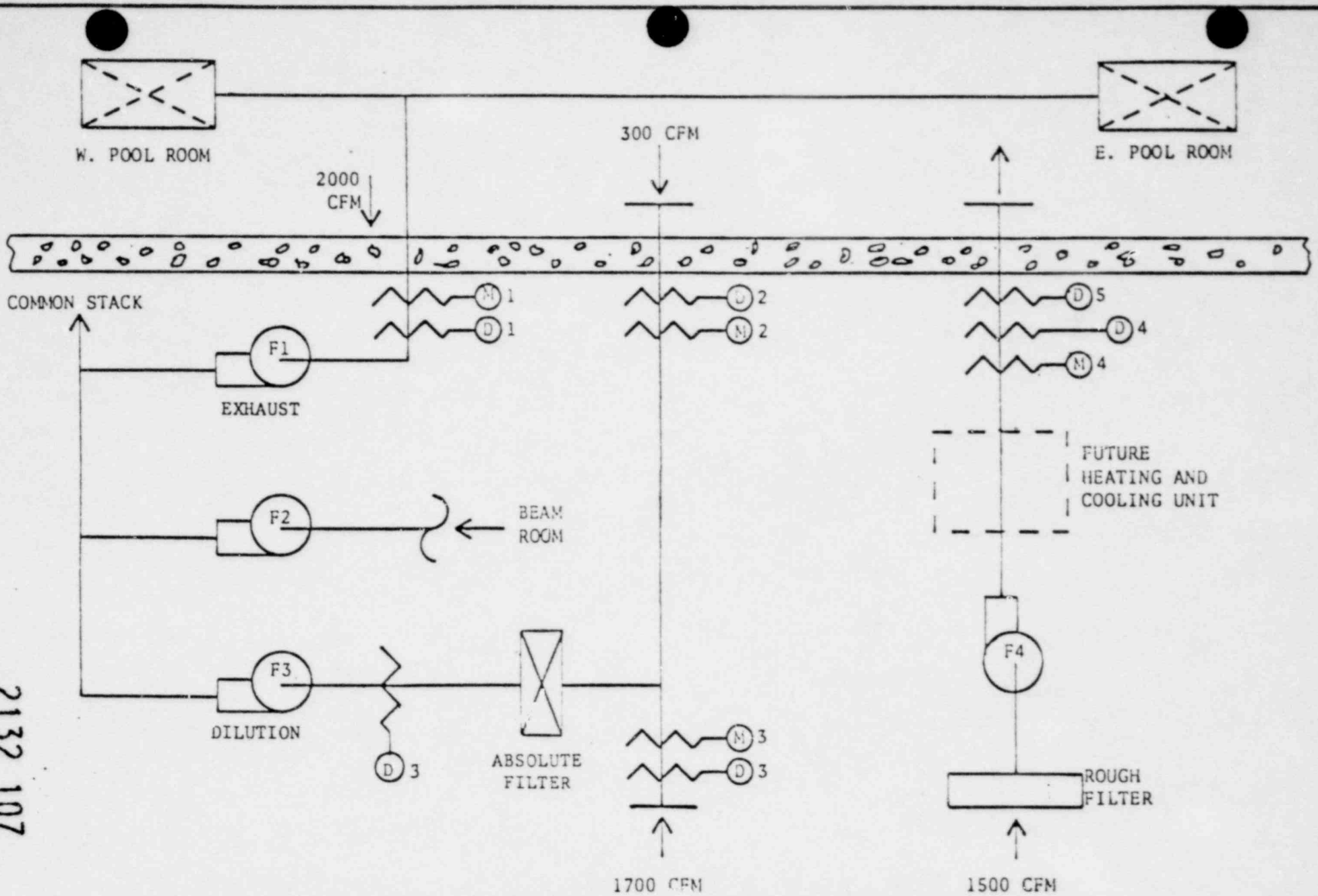

Reactor Ventilation System

FIGURE 3.2-1

(D) - AUTOMATIC DAMPER

(M) - MANUAL DAMPER

During normal operation, 9.44×10^5 cm^3/sec of air from the pool room is mixed with the beam room exhaust and discharges out the monitored exhaust. In the isolation mode, dampers on the pool room supply and exhaust lines serve to prevent all air flow into and out of the pool room. In the dilution mode, 1.42×10^5 cm^3/sec of pool room air is passed through an absolute filter, mixed with 8.02×10^5 cm^3/sec of outside air, and discharges up the exhaust stack. The main control panel for the system is located in the reactor control room and a set of emergency controls is located in the main office. The continuous air monitor and gaseous effluent monitors are shown in Figure 3.2-2 and 3.2-3.

3.3 Pool

The reactor pool is a reinforced, above ground, unlined concrete pool with a volume of 247,000 liters. The pool is penetrated by a thermal column and a number of beam ports as described in Section 4.11. A cross section of the pool is shown in Figure 3.3-1.

3.4 Liquid Waste Collection System

The Nuclear Radiation Center has two separate waste systems. The sanitary waste system handles all the normal non-radioactive liquids and the "hot drain" system handles all the radioactive liquids. The sanitary waste system connects all the washroom fixtures and cold laboratory drains to the campus sewer system. The "hot drain" system connects all the drains from the radiochemistry laboratories and reactor areas to a retention tank system. Radioactive effluents from the Center are collected in the retention tank system shown in Figure 3.4-1. Prior to discharge into the sanitary sewer, the contents of the retention tank are pumped to a sampling tank. The sampling tank is sampled, evaluated for activity content, and diluted as necessary during discharge.

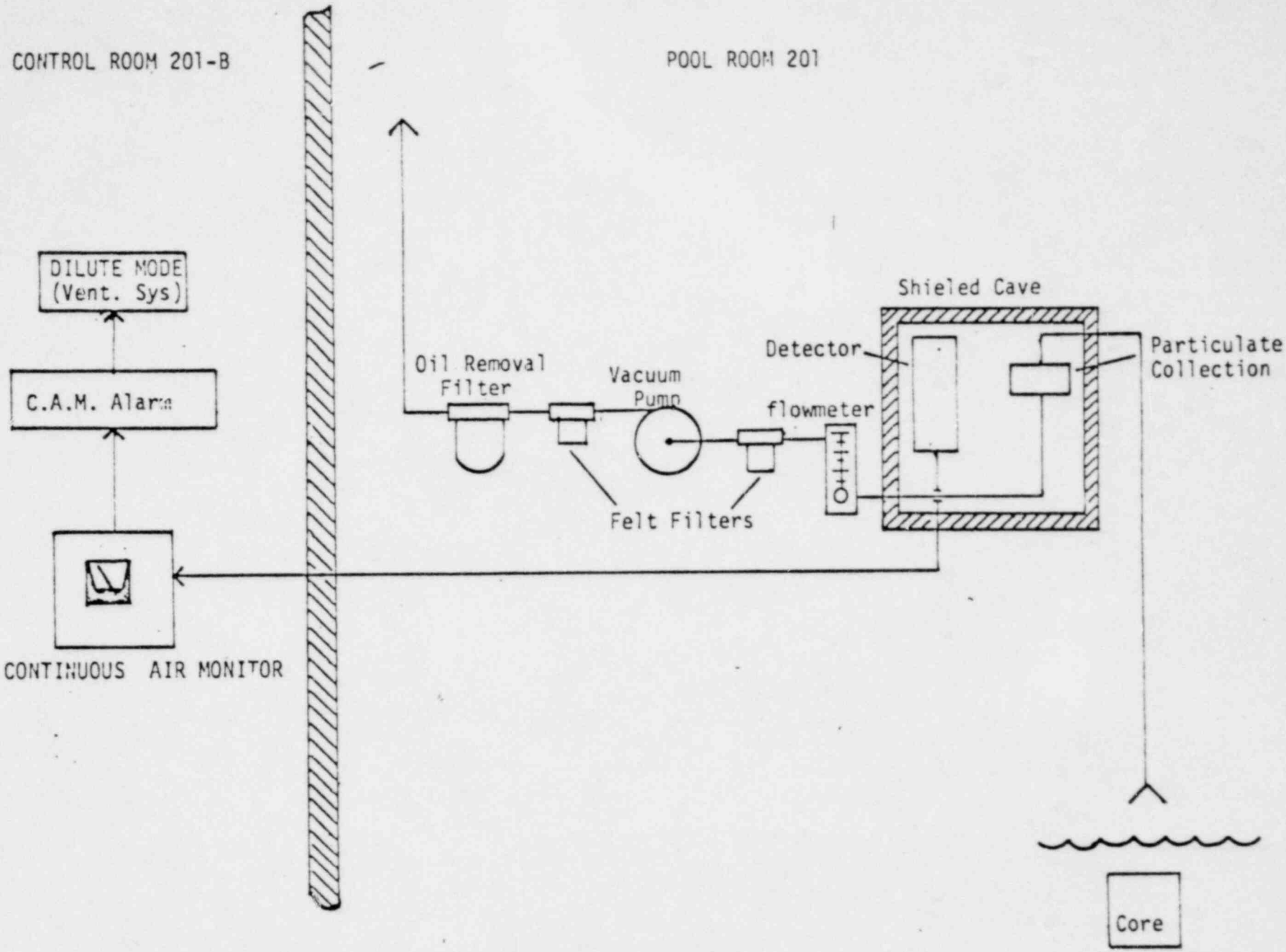

CONTINUOUS AIR MONITORING SYSTEM

FIGURE 3.2-2

2132 109

GASEOUS EFFLUENT

MONITORING SYSTEM

FIGURE 3.2-3

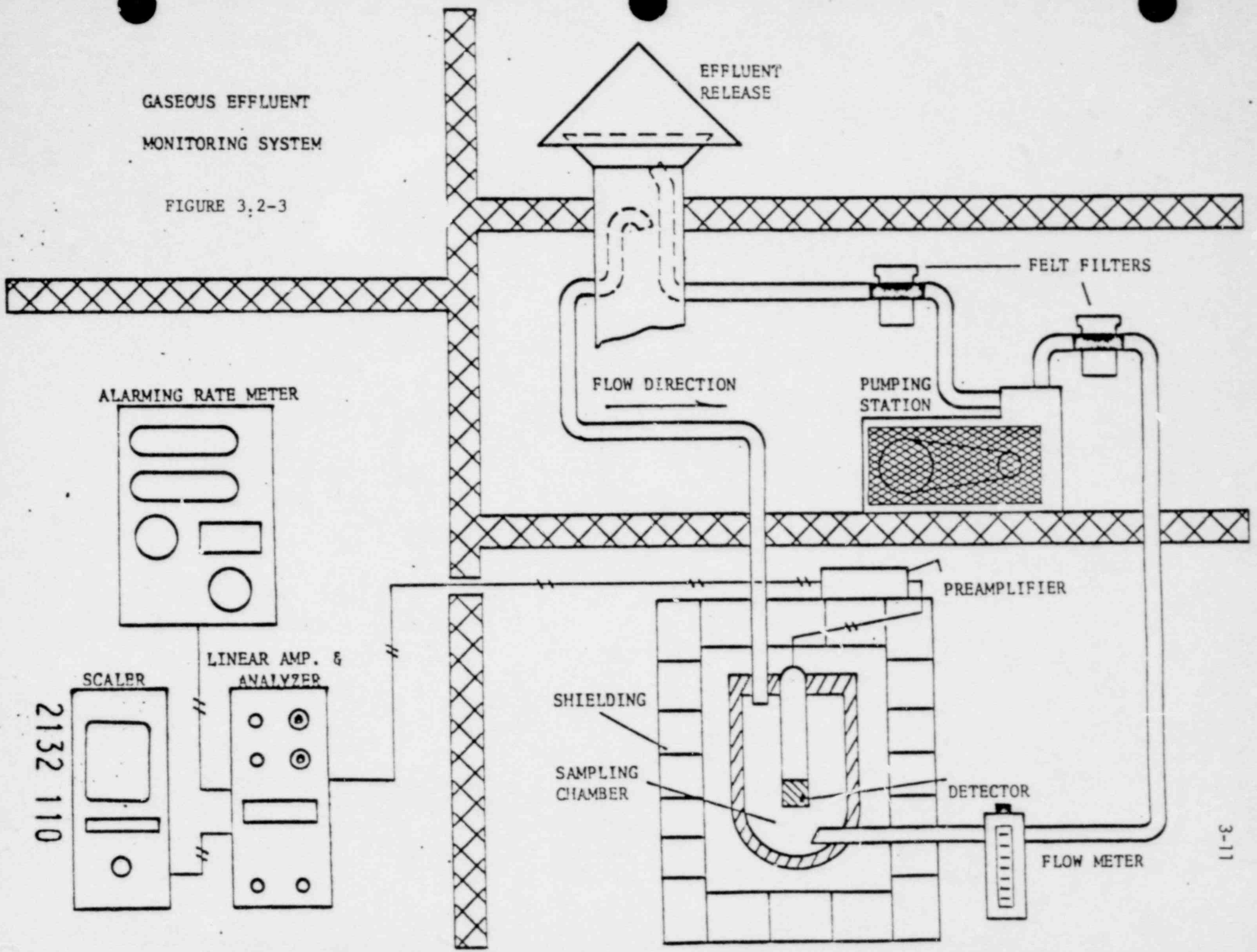

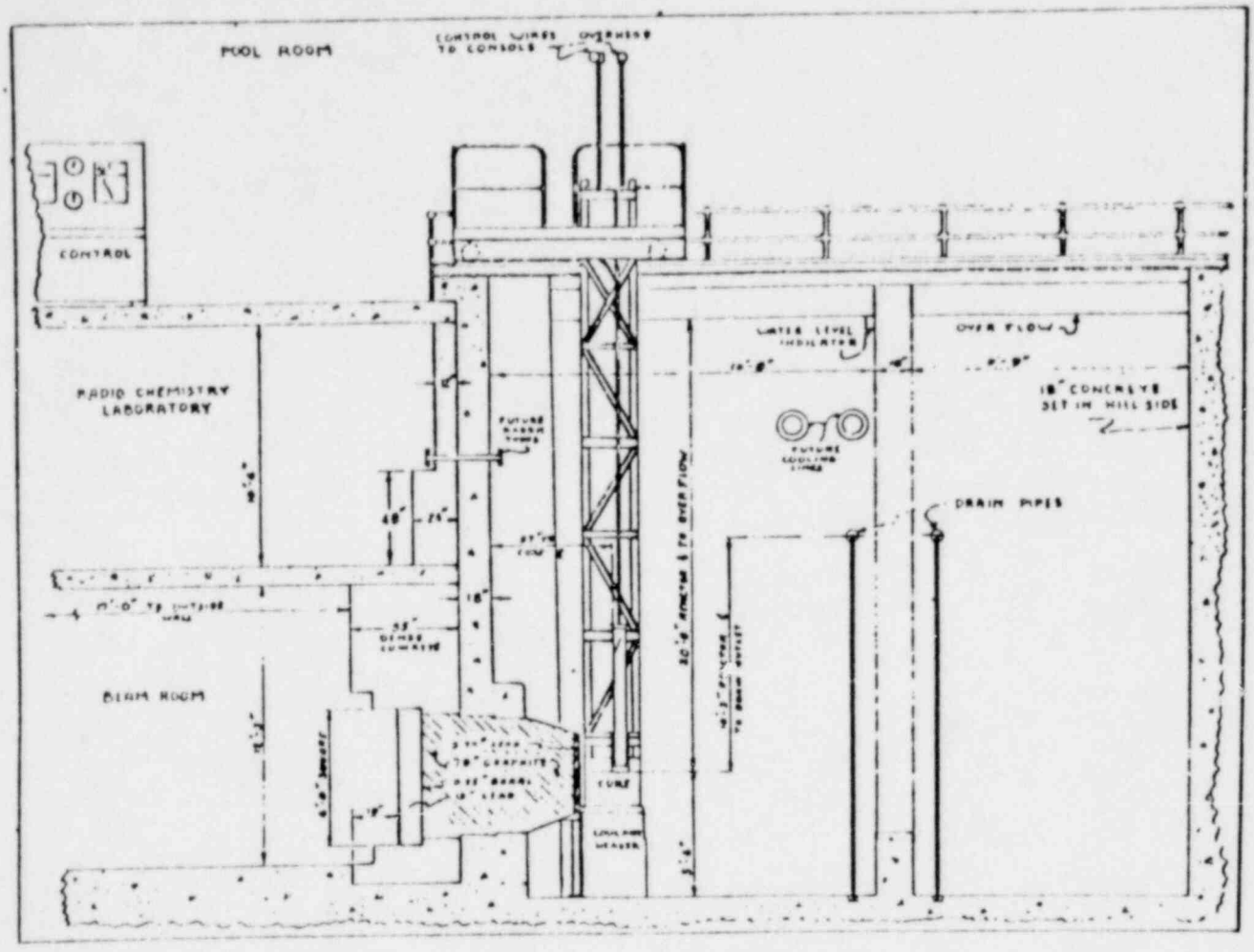

WSU REACTOR POOL STRUCTURE

FIGURE 3.3-1

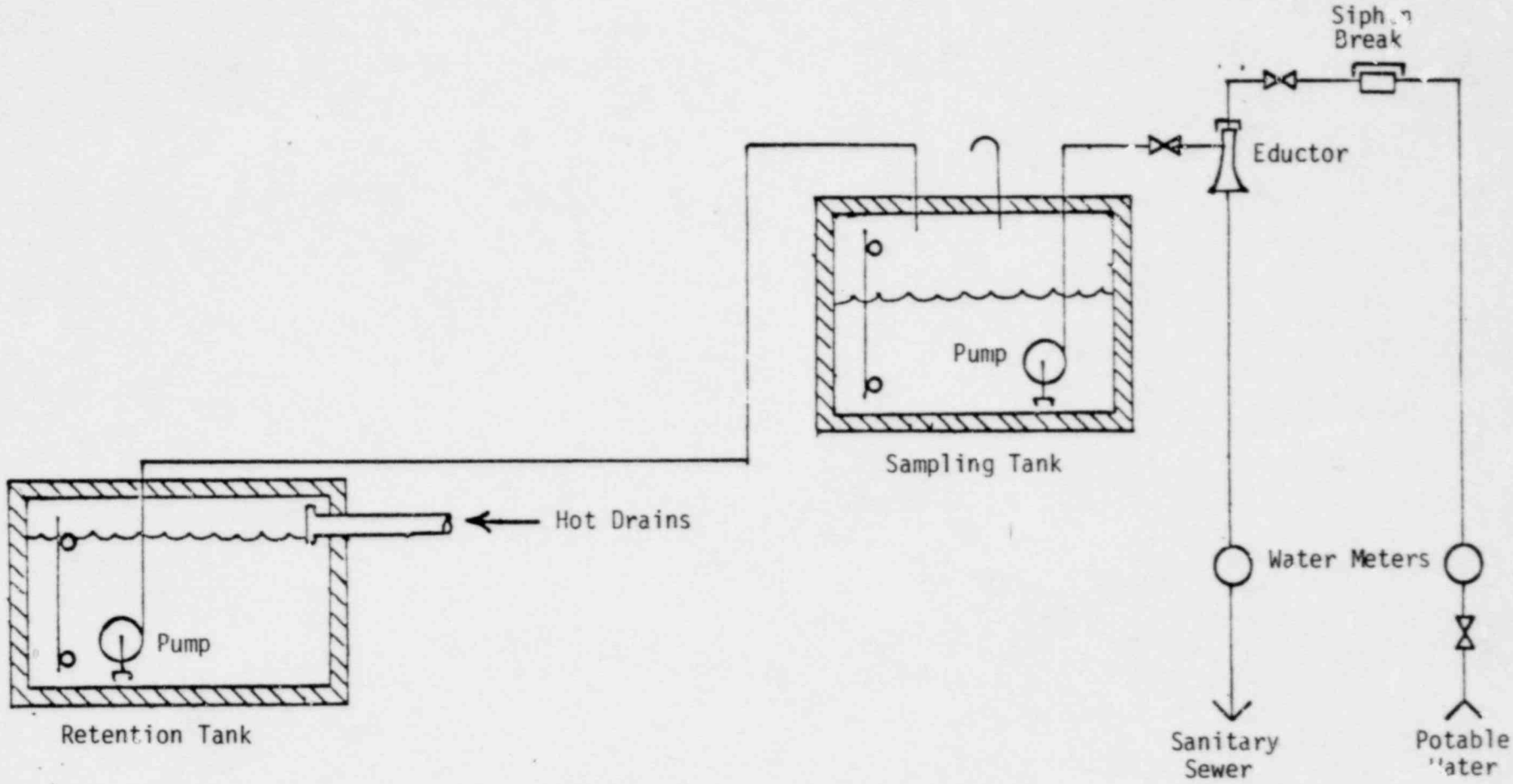

Retention Tank System

FIGURE 3.4-1

4.0 REACTOR DESCRIPTION

4.1 General Description

The WSU modified TRIGA reactor is a one megawatt pool-type research reactor using light-water as the moderator, coolant, and shield and TRIGA type solid fuel rods. The reactor core is immersed in a large concrete water-filled open-topped pool. The pool is spanned by a manually-operated bridge structure from which the core support structure is suspended. The core is situated in a grid box into which 4-rod clusters of TRIGA fuel are positioned.

Control over the reactor is exerted by inserting or withdrawing neutron absorbing control elements suspended from control drives mounted on the bridge. Heat generated by the fission process is transferred from the fuel to the pool water by natural convection cooling. The heat from the pool is dissipated to the atmosphere by means of a cooling tower-heat exchanger arrangement. A mixed bed demineralizer system maintains the purity of the pool water.

4.2 Bridge Structure

The WSU reactor is suspended in the pool from a movable bridge which is mounted on rails. The bridge and entire reactor structure may be moved laterally. The bridge and core suspension framework are shown in figure 4.2-1. The all-aluminum framework is suspended from the bridge and supports the grid box into which the fuel is inserted. The hollow corner posts of the suspension framework serve as guide tubes for the nuclear instrumentation detectors. The control element drives are connected to and supported by the bridge structure.

Deck plates mounted on the top side of the bridge structure form a floor area around the control drives. The floor area provides a work

FIGURE 4.2-1

space to use and maintain the reactor and associated facilities. A railing system is connected to the bridge floor to prevent personnel from accidently falling off the bridge structure.

4.3 Grid Box

The reactor core fuel rods are supported and enclosed in a rectangular grid box. The bottom of the grid box is a cast aluminum grid plate as shown in figure 4.3-1. The grid plate provides a 7 by 9 array of square holes for fuel and two slots for the control blades. The grid plate is suspended from the four corner posts of the suspension frame. The sides of the grid box are aluminum sheeting positioned to direct the convection current of cooling water through the core. The grid box accepts the 4-rod clusters described in section 4.4 or reflector elements shown in figure 4.3-2.

4.4 Fuel

The fuel elements consist of 3-rod or 4-rod clusters of TRIGA type fuel as shown in figure 4.4-1 and 4.4-2. The 4-rod fuel cluster was developed as a simple replacement for MTR-type plate fuel bundles. The top handle and bottom end fitting on the 4-rod cluster serve to adapt TRIGA rod type fuel to the square grid array used with plate type fuel.

The individual fuel rods are similar in construction to standard TRIGA fuel rods with the exception of the rod diameter and modified rod end fittings. Two types of TRIGA fuel rods, Standard and FLIP, with the parameters listed in table 4.4-1 are used in the WSU reactor. Each fuel rod is 1.41 inches in diameter, about 30 inches long, and clad in a .020 inch type 304 stainless steel cylinder as shown in figure 4.4-3.

The zirconium hydride active portion of the fuel rod is 1.37 inches in diameter and is composed of one or more cylinders to make a total

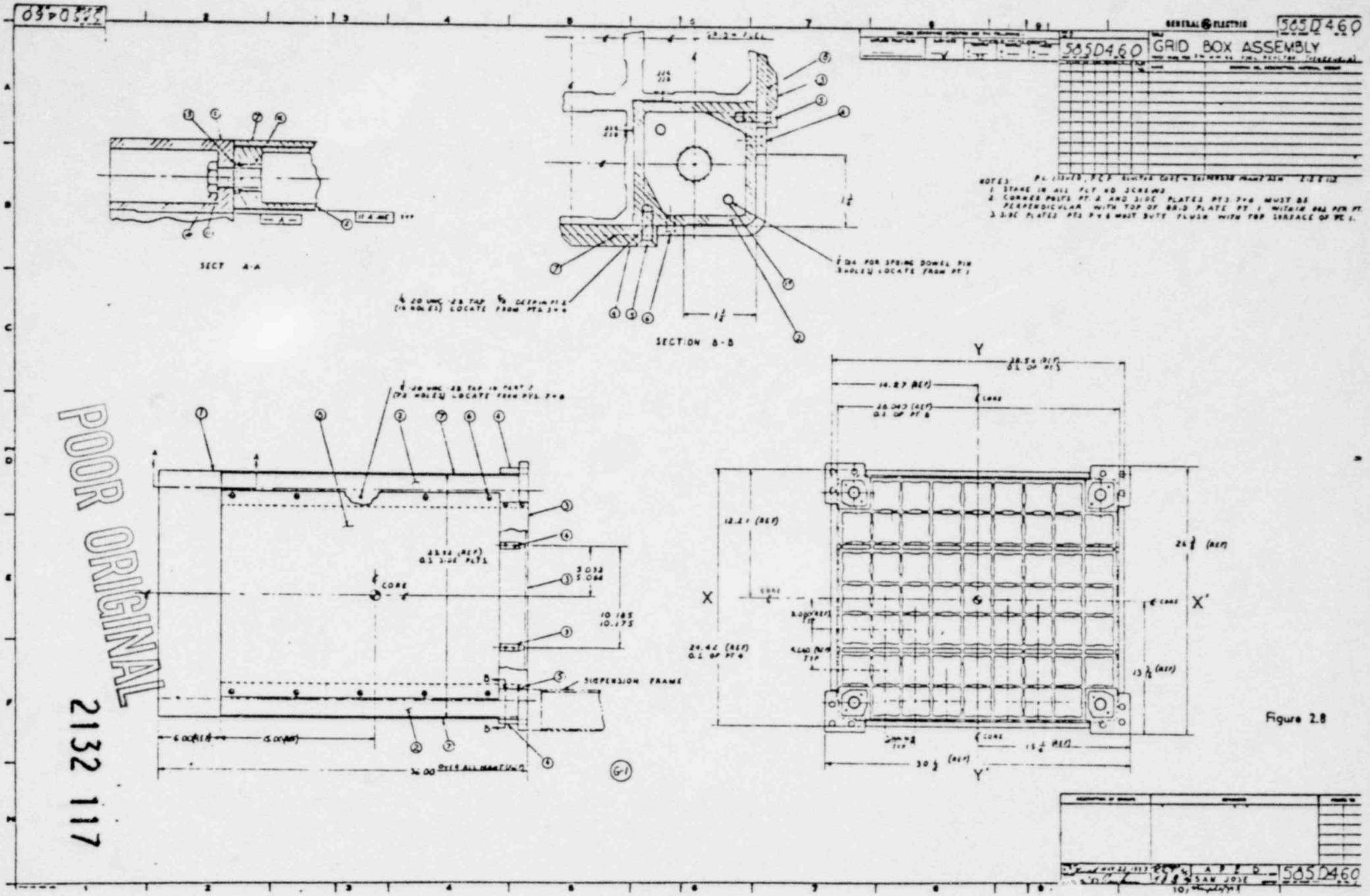

Figure 2.8

FIGURE 4.3-1

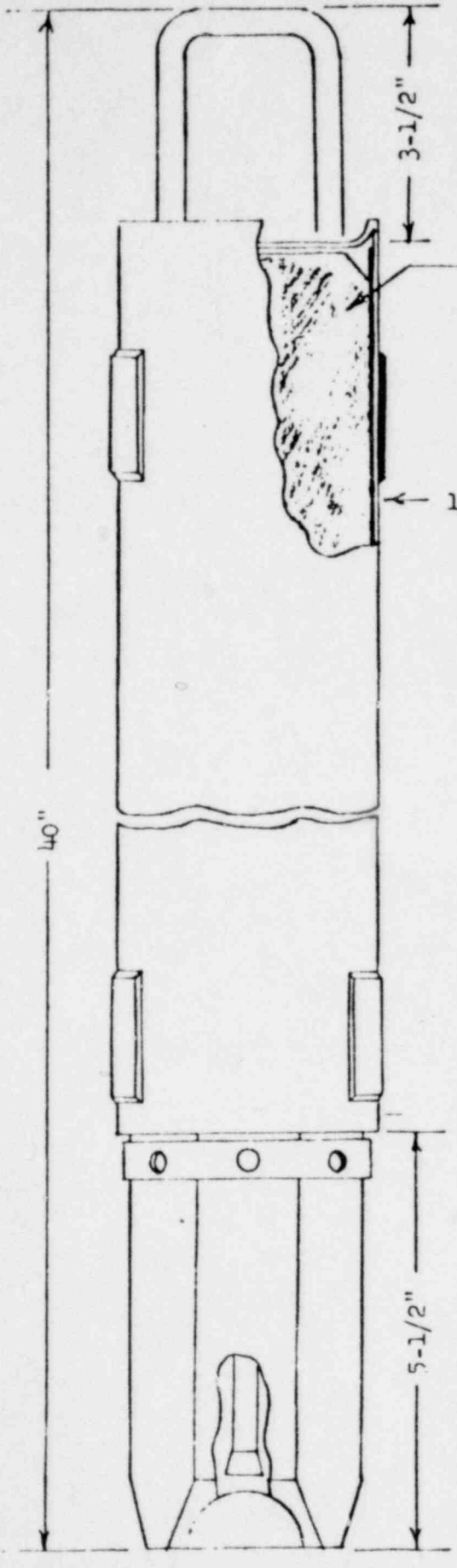

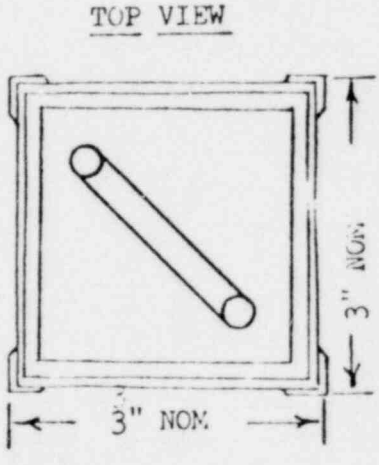

REFLECTOR ELEMENT

FIGURE 4.3-2

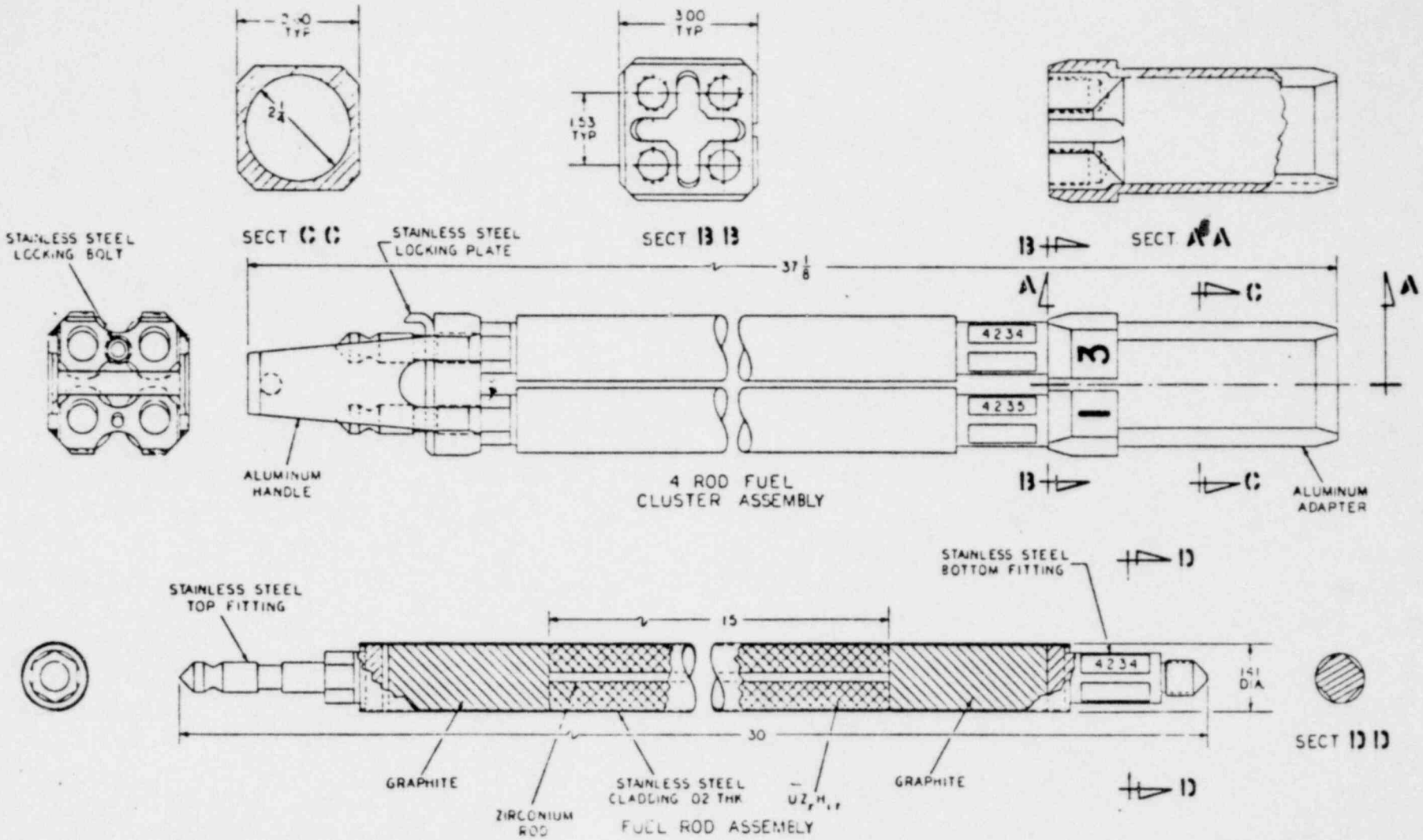

SECTIONAL VIEWS OF TRIGA STANDARD 4-ROD CLUSTER

FIGURE 4.4-1

FIGURE 4.4-2 Photograph of Four-Rod Fuel Element

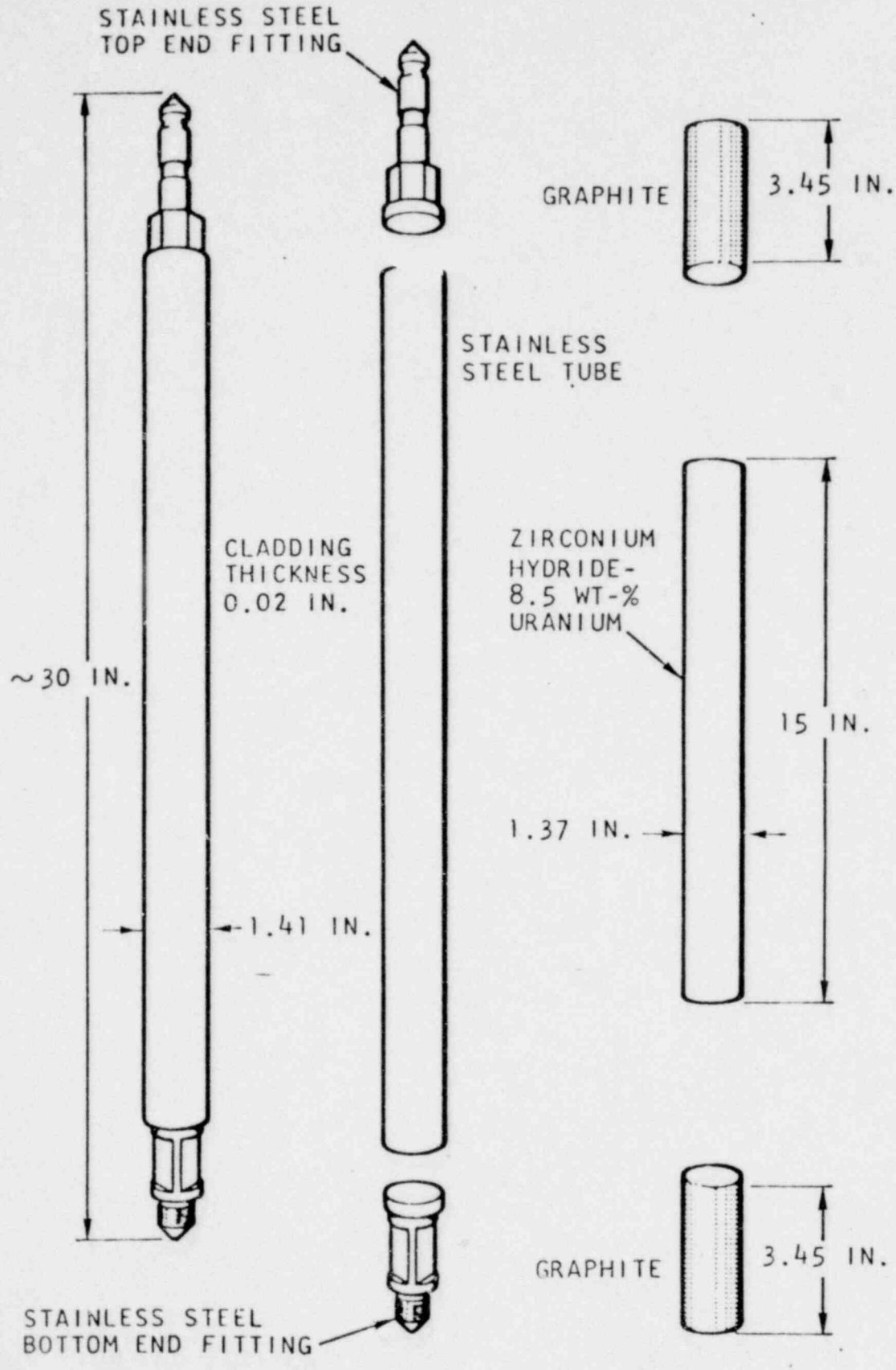

FIGURE 4.4-3

TABLE 4.4-1

Standard and FLIP Fuel Parameters

Fuel Element Type	FLIP	STANDARD
Fuel-moderator material	$U\text{-}ZrH_{1.6}$	$U\text{-}ZrH_{1.7}$
Uranium content	8.5 wt%	8.5 wt%
U-235 enrichment	70%	20%
U-235 content (avg) per element	123 g	35 g
Burnable poison	natural erbium	none
Erbium content	1.5 wt%	--
Shape	cylindrical	cylindrical
Length of fuel meat	15 in.	15 in.
Diameter of fuel meat	1.371 in.	1.371 in.
Cladding material	Type 304 SS	Type 304 SS
Cladding thickness	0.020 in.	0.020 in.

length of 15 inches. A 3.45 inch graphite reflector plug is positioned in each end of the fuel rod and top and bottom end fittings are welded onto the cladding.

In addition to standard fuel rods, one or more instrumented fuel rods as shown in figure 4.4-4 are used in the core. This type of fuel rod is fitted with three thermocouples used to measure the fuel temperature. A special 3-rod cluster with a transient rod guide tube as shown in figure 4.4-5 is positioned in the center of the reactor grid. The transient control rod is positioned inside the guide tube as described in section 4.6.

4.5 Control Blades

The safety and regulating control elements of the WSU reactor are blade type elements as shown in figures 4.5-1 and 4.5-2. The poison section of the safety blades is a boral sheet 40.5 inches long and 10.5 inches wide. The boral sheet is 3/8 inches thick and is clad with 1/8

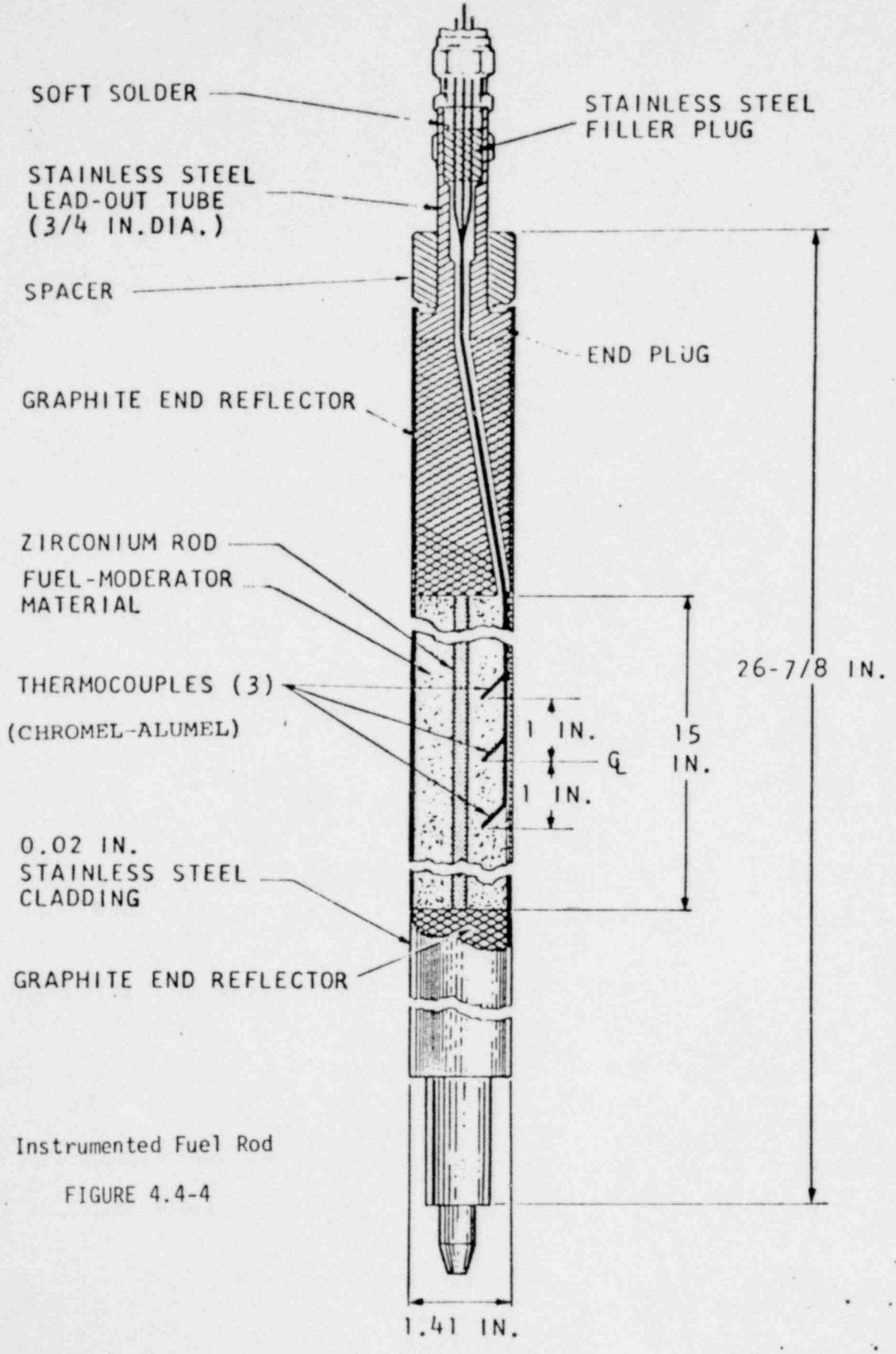

Instrumented Fuel Rod

FIGURE 4.4-4

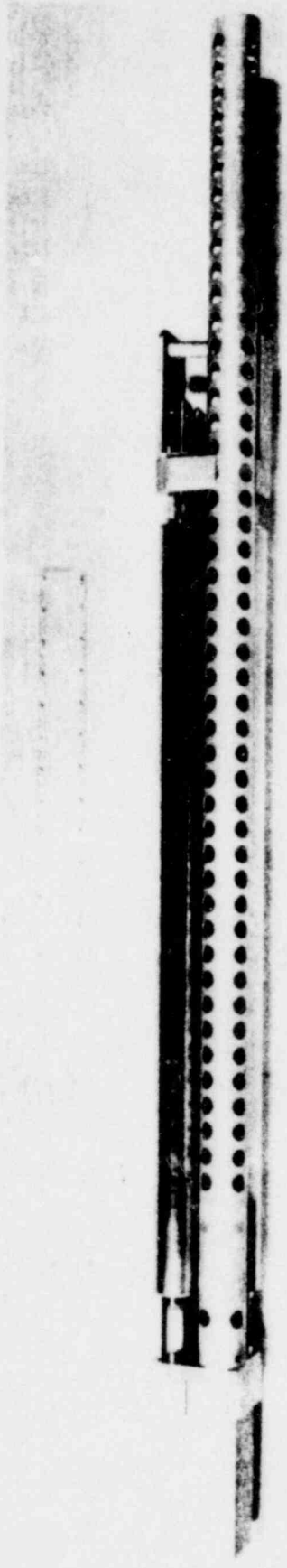

FIGURE 4.4-5 Transient Rod Guide Tube with 3-Rod Cluster

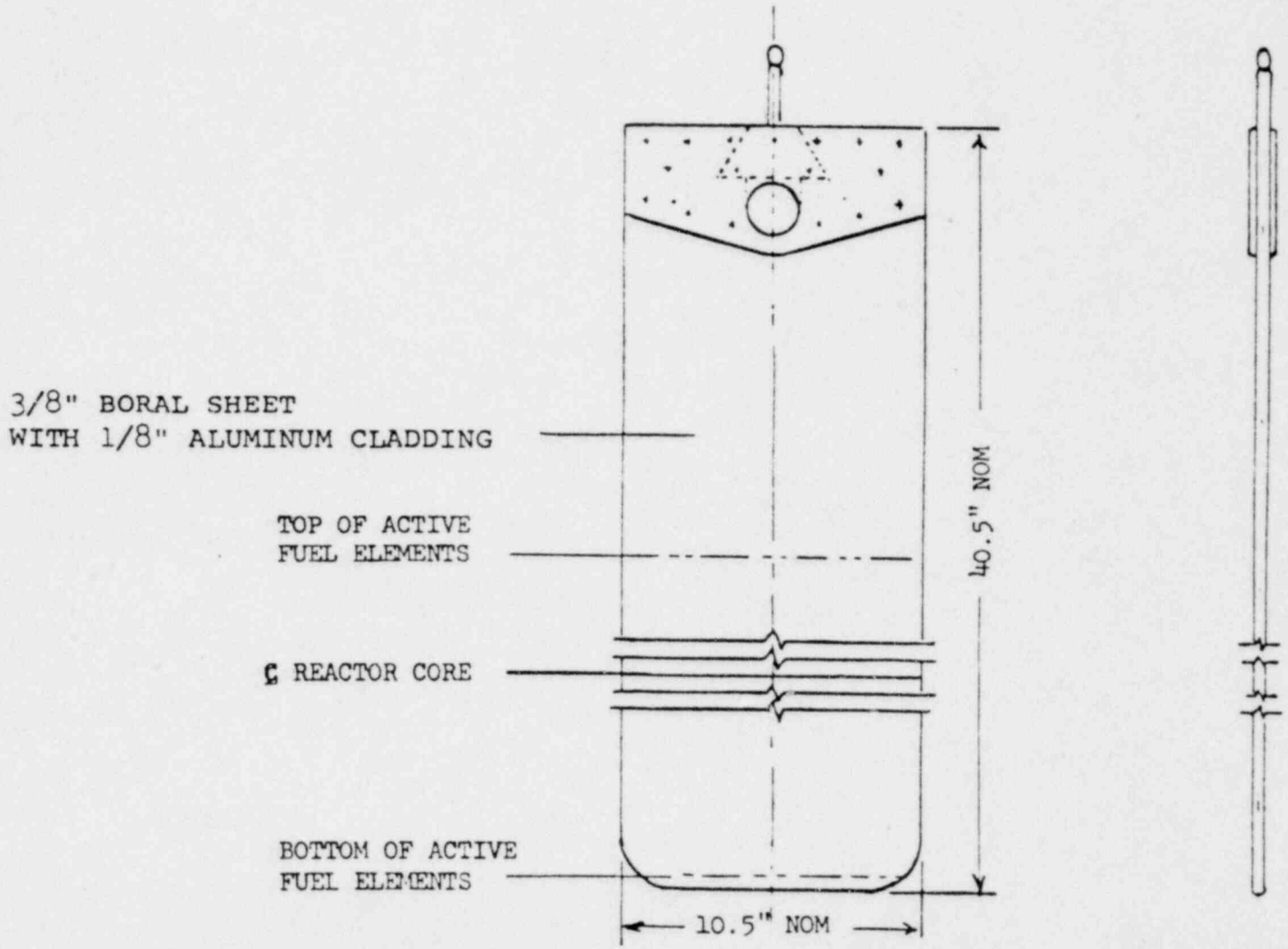

Safety Blade

FIGURE 4.5-1

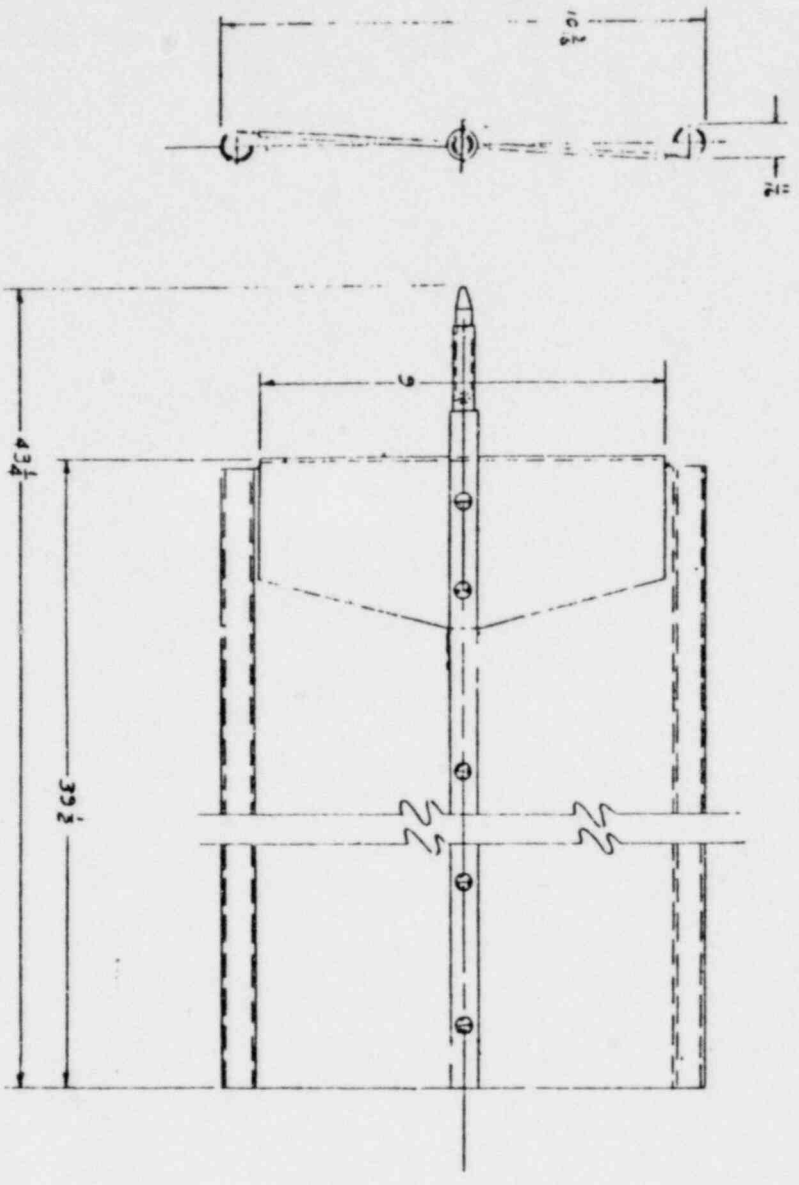

Regulating Blade

FIGURE 4.5-2

inch aluminum. The regulating blade is a stainless steel sheet about 11 inches wide and 40 inches long.

Each blade is guided through its travel by a shroud, as shown in figure 4.5-3. The shroud consists of two thin aluminum plates 38 inches high separated by aluminum spaces to provide a 3/4 inch control blade slot. Small flow holes are drilled at the bottom of the shroud to reduce the effects of viscous damping on the blade fall time.

4.6 Transient Control Rod

The transient control rod is a solid borated graphite cylinder contained in a 1-1/4 inch diameter stainless steel or aluminum tube as shown in figure 4.6-1. The poison section of the transient rod is 15 inches in length. The transient rod is connected to the transient rod drive via an end fitting welded on the top end of the rod. The rod is held in position laterally by the guide tube inserted into a 3-rod cluster. A hold-down tube extends from the top of the guide tube up to the bottom of the transient rod drive, as shown in figure 4.7-3.

4.7 Control Element Drive

The drive mechanism for the blade type control elements are shown in figure 4.7-1 and are activated by reversible electric motors with an integral worm-gear drive mechanism. The worm-gear assembly serves to reduce the drive speed and to minimize over-travel of the drive after power is removed from the drive motor. A mechanical slip clutch on the output shaft limits the force on the blade to approximately 75 pounds. A ball-bearing screw and nut system is used to raise and lower the control element.

Each safety blade is coupled to its associated drive mechanism by means of an electromagnet and steel armature disk, as shown in figure 4.7-2. De-energizing the electromagnet allows the safety blade to fall into the

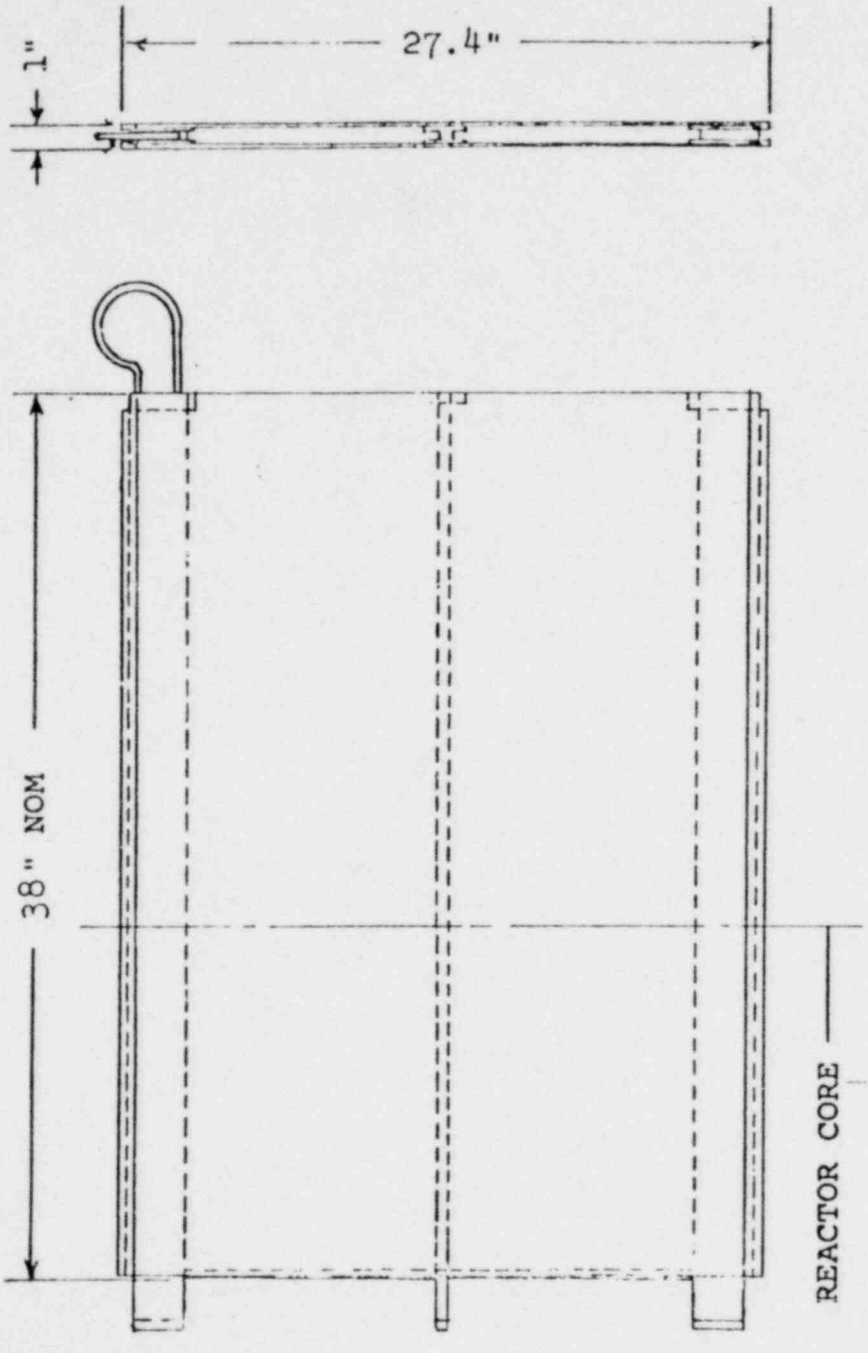

SHROUD ASSEMBLY

FIGURE 4.5-3

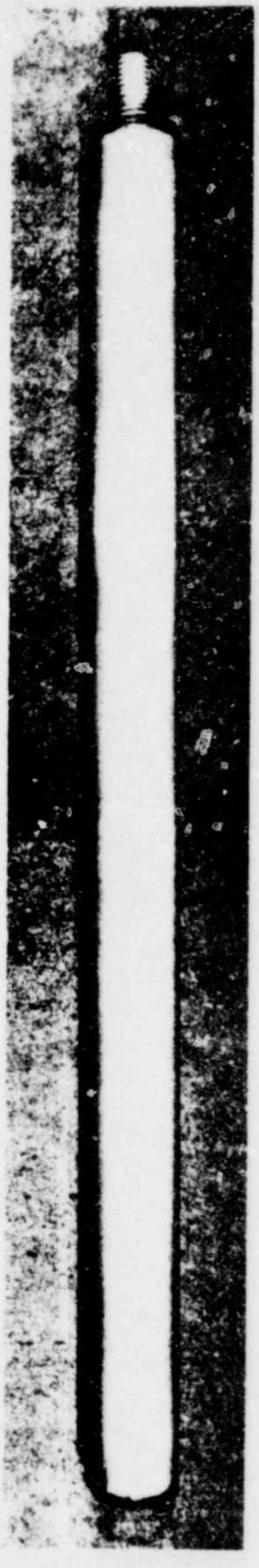

Photograph of Transient Control Rod

FIGURE 4.6-1

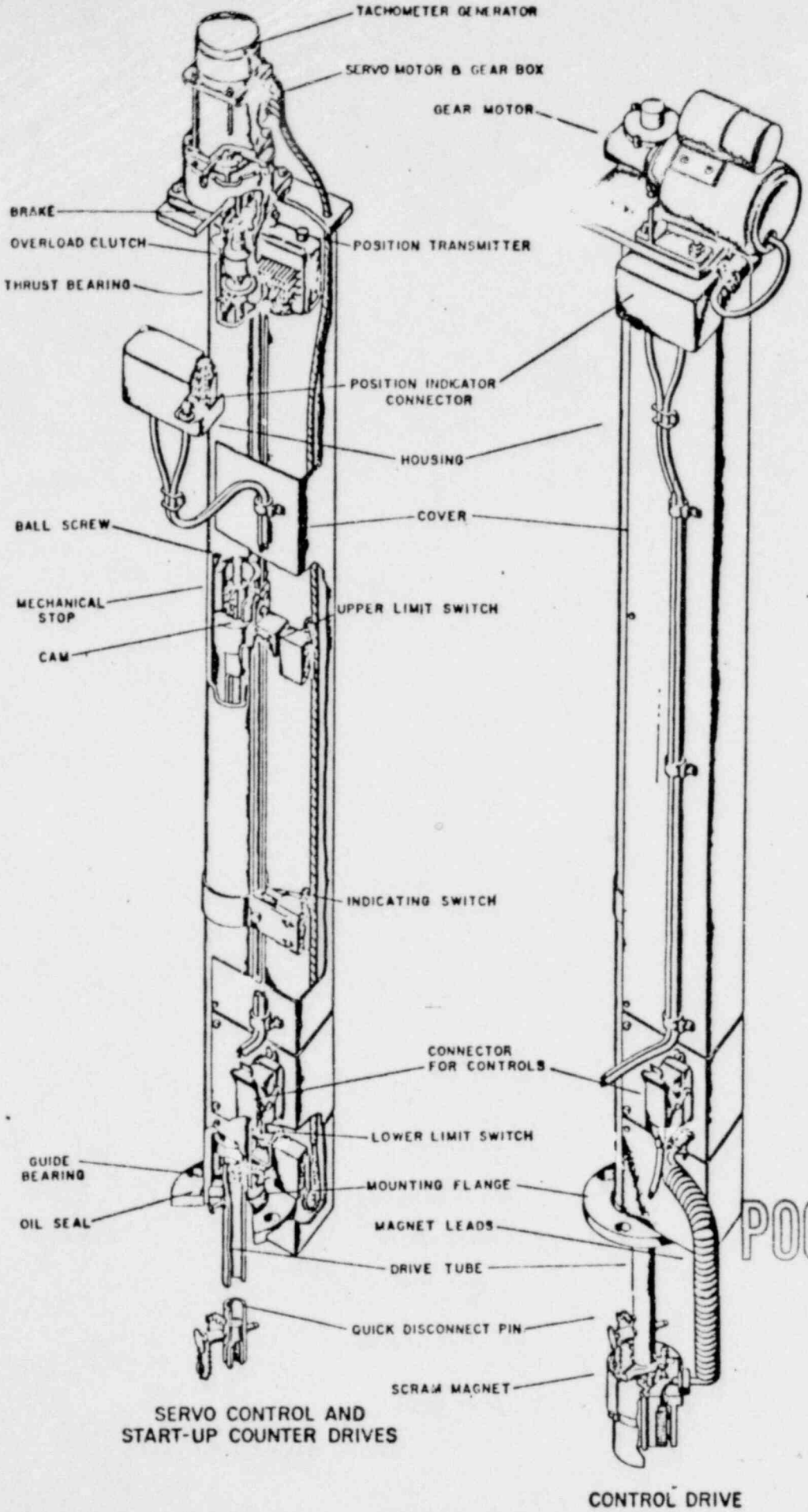

DRIVE MECHANISMS

FIGURE 4.7-1

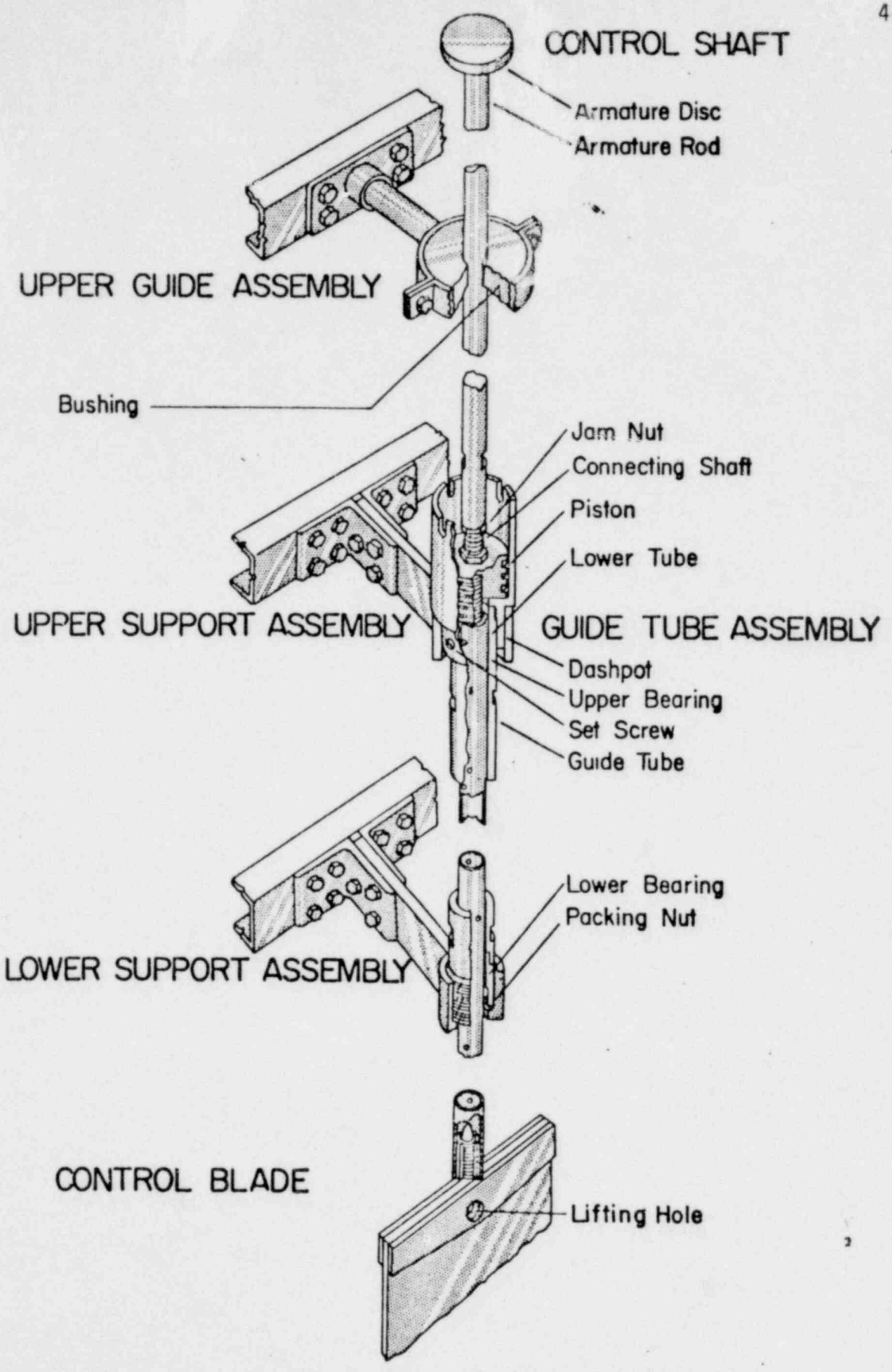

CONTROL SHAFT, DASH POT, & BEARING DETAILS

FIGURE 4.7-2

core by the action of gravity within 700 milliseconds. A shaft connects the armature disk to the blade and is fitted with polyethylene sleeve-bearings which control the lateral position of the blade drive shaft. A dashpot is positioned at the end of the shaft travel to decelerate the last 5 inches of fall. The blades are recovered after a scram by running the drive mechanism down and re-energizing the electromagnets.

The transient control rod drive employs a combination pneumatic-electromechanical drive assembly shown in figures 4.7-3 and 4. The mechanism is designed to allow the rod to be used both as a control rod and a transient rod.

The pneumatic portion of the pneumatic-electromechanical drive, referred to herein as the "transient" rod drive, is basically a single-acting pneumatic cylinder. A piston within the cylinder is attached to the transient rod by means of a connecting rod. The piston rod passes through an air seal at the lower end of the cylinder. Compressed air is admitted at the lower end of the cylinder to drive the piston upward. As the piston rises, the air being compressed above the piston is forced out through vents at the upper end of the cylinder. At the end of its stroke, the piston strikes the anvil of a shock absorber. The piston is thus decelerated at a controlled rate during its final inch of travel. This action minimizes rod vibration when the piston reaches its upper-limit stop.

An accumulator tank mounted on the movable bridge stores the compressed air that operates the pneumatic portion of the transient rod drive. A three-way solenoid valve, located in the piping between the accumulator tank and the cylinder, controls the air supplied to the pneumatic cylinder. De-energizing the solenoid valve interrupts the

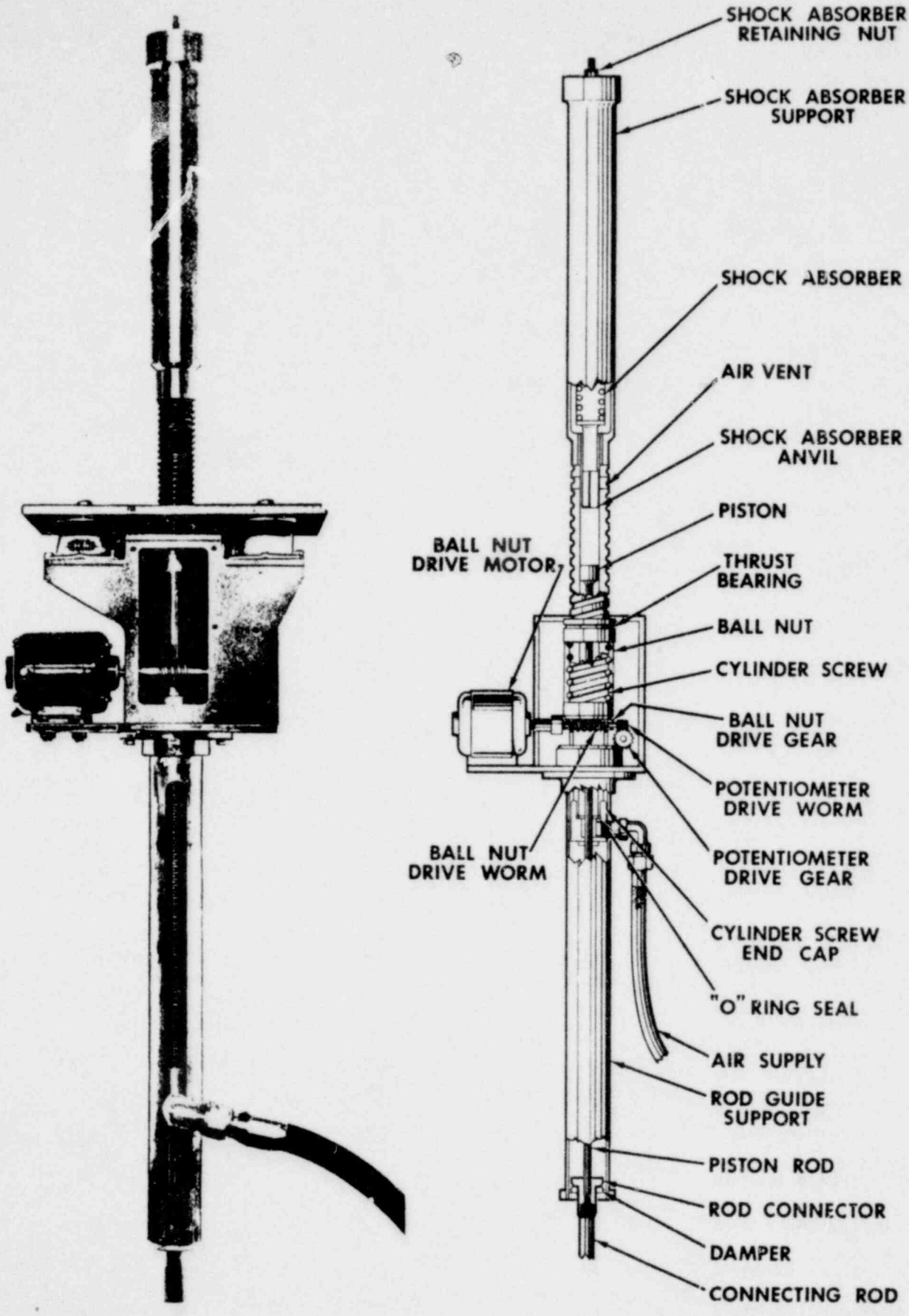

Pneumatic-Electromechanical Transient-Rod Drive

FIGURE 4.7-3

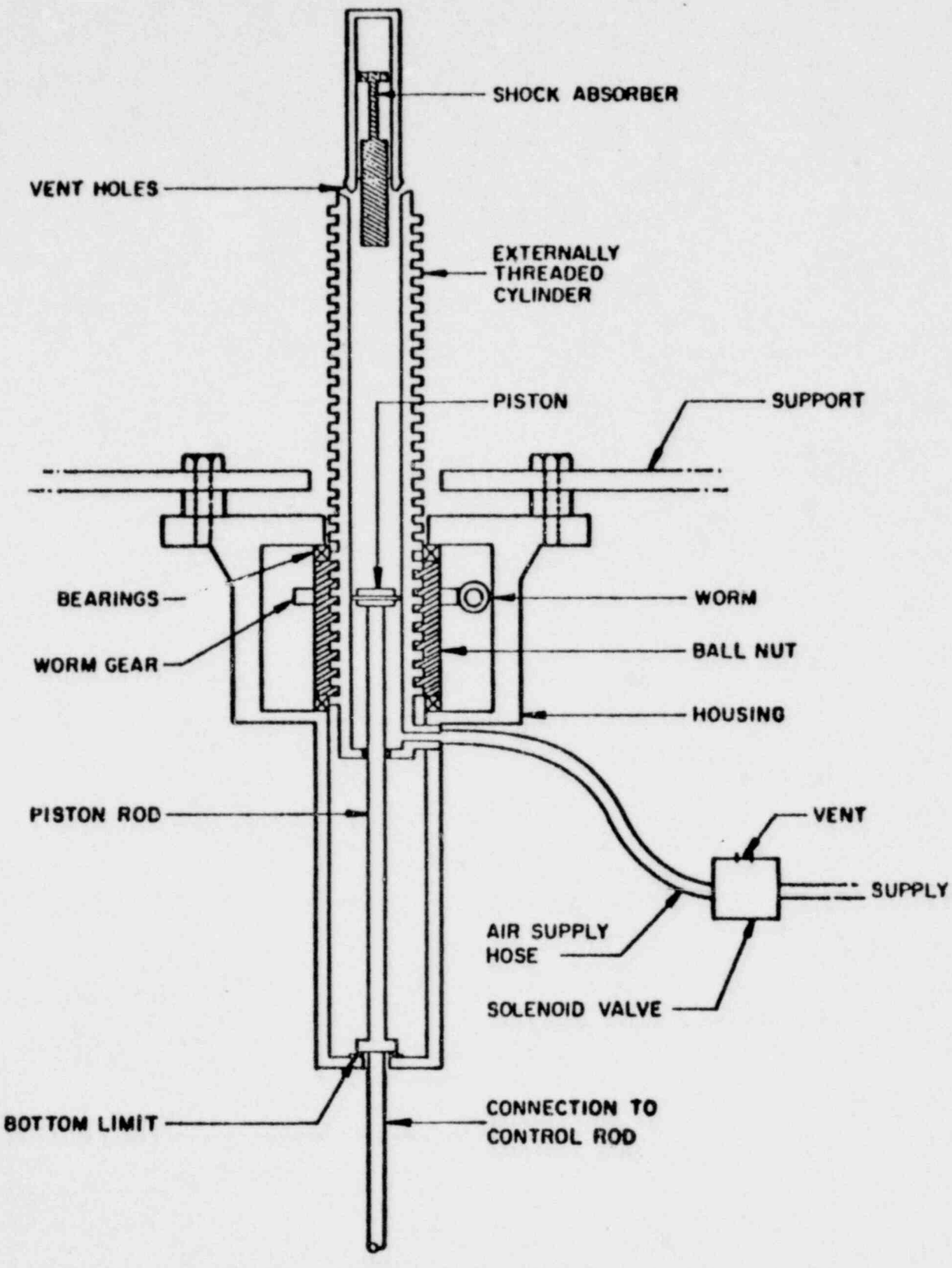

Schematic Drawing of Transient Rod Drive

FIGURE 4.7-4

air supply and relieves the pressure in the cylinder so that the piston drops to its lower limit by gravity. With this operating feature, the transient rod is inserted in the core except when air is supplied to the cylinder.

The electromechanical portion of the transient rod drive consists of an electric motor, a ball-nut drive assembly, and the externally threaded air cylinder. During electromechanical operation of the transient rod, the threaded section of the air cylinder acts as a screw in the ball-nut drive assembly. These threads engage a series of balls contained in a ball-nut assembly in the drive housing. The ball-nut assembly is in turn connected through a worm-gear drive to an electric motor. The cylinder may be raised or lowered independently of the piston and control rod by means of the electric drive. Adjustment of the position of the cylinder controls the upper limit of piston travel, and hence controls the amount of reactivity inserted for a pulse.

A system of limit switches is used to indicate the position of the air cylinder and the transient rod. Two of these switches, the Drive Up and Drive Down switches, are actuated by a small bar attached to the botton of the air cylinder. A third limit switch, the Rod Down switch, is actuated when the piston reaches its lower limit of travel. During steady state operation the transient rod may be withdrawn and used as a control rod by means of the ball-nut drive.

4.8 Control and Instrumentation

4.8.1 Control Console

The Control System for the WSU TRIGA reactor consists of a Control Console and associated instrumentation. The Control Console is pictured in figure 4.8-1 and was designed and constructed by the

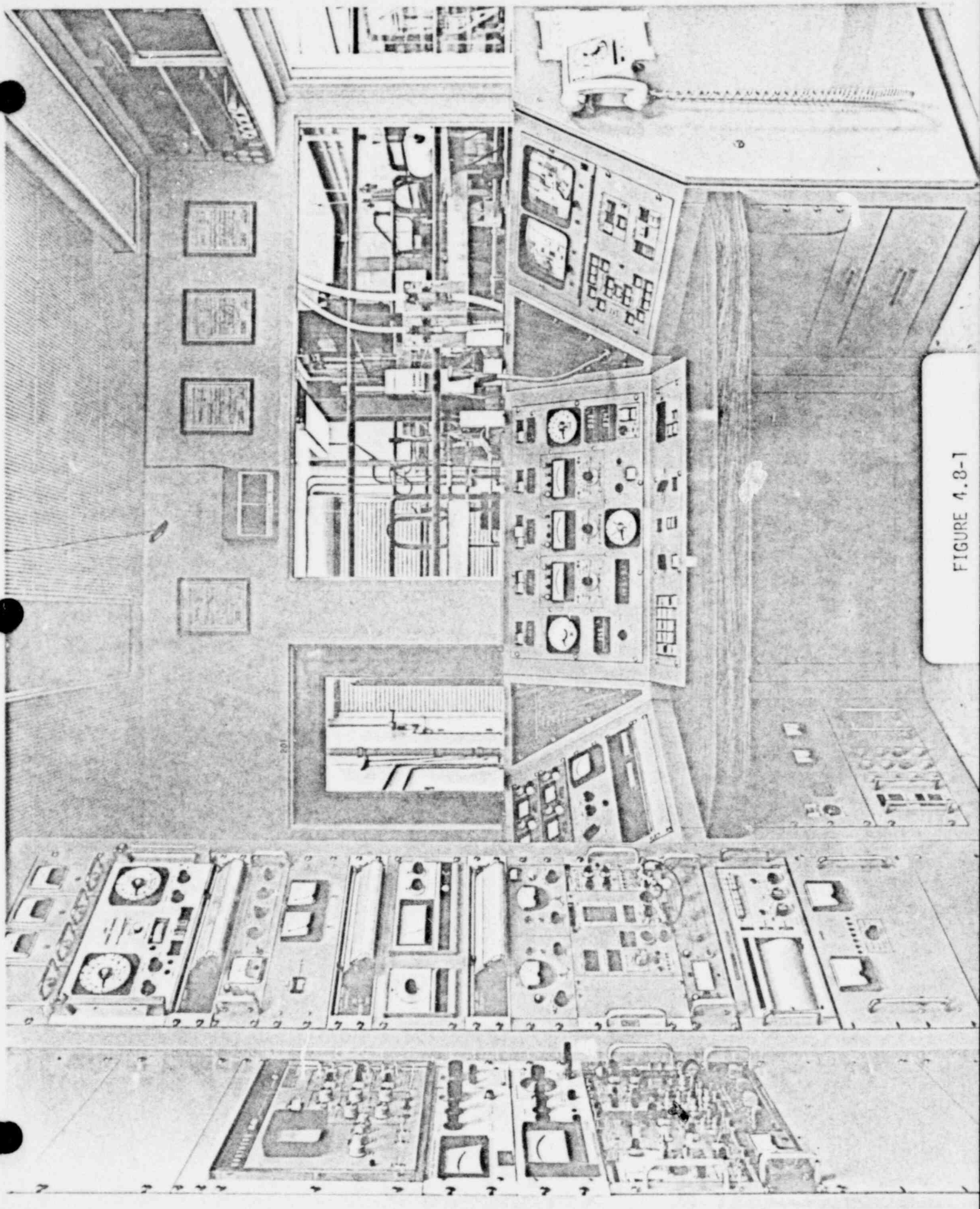

FIGURE 4.8-1

Nuclear Radiation Center Staff. Considerable thought and experience went into the human engineering aspects of the console layout. All indicating devices are placed for optimum readability and accessibility. All the alarm and interlock functions are in a single block of dual color back-lighted switches. The controls for the control elements are grouped together and located for ease of use. The console is positioned to allow the operator to not only watch the console but also to view the activities on the reactor bridge. A closed circuit TV system allows the operator to view the activity in the radiochemistry laboratory and beam rooms.

The electronic systems use solid-state circuitry and high reliability components wherever possible. All essential relays and terminal boards are mounted on slide-out trays for easy maintenance. A permanent record of the important parameters is provided by strip-chart recorders mounted in a rack on the left side of the console. Ready access to communications facilities are provided for operator convenience.

The control system instrumentation contains electronic subsystems to perform the functions listed in table 4.8-1. A block diagram of the Linear Power indication and safety subsystems is shown in figure 4.8-2. A block diagram of the pulse mode instrumentation is shown in figure 4.8-3. A block diagram of the scram circuitry and wide range channel are shown in figures 4.8-4 and 4.8-5.

4.9 Cooling System

The heat generated within the fuel during operation of the reactor is transferred to the pool water by natural convection heat transfer. The heated pool water is pumped through the tube side of a conventional

TABLE 4.8-1

MINIMUM REACTOR SAFETY CHANNELS

Safety Channel	Function	Number Operable in Specified Mode S.S.	Number Operable in Specified Mode Pulse
Fuel Temperature	Scram if fuel temperature exceeds 500°C	1	1
Power Level	Scram if power level exceeds 125% of full licensed power	1	
Manual Scram		1	1
Wide Range	a. prevent initiation of a pulse above 2 kw		1
	b. prevent control element withdrawal when neutron count is less than 2 cps	1	
High Voltage Monitor	Scram on loss of high voltage to power channels	1	1
Pulse Mode Switch	Prevent withdrawal of standard control and regulating elements in pulse mode		1
Preset Timer	Transient rod scram 15 seconds or less after pulse		1
Pool Level	Alarm if pool level falls below 16 feet over the core	1	1
Transient Rod Control	Prevent application of air unless fully inserted	1	

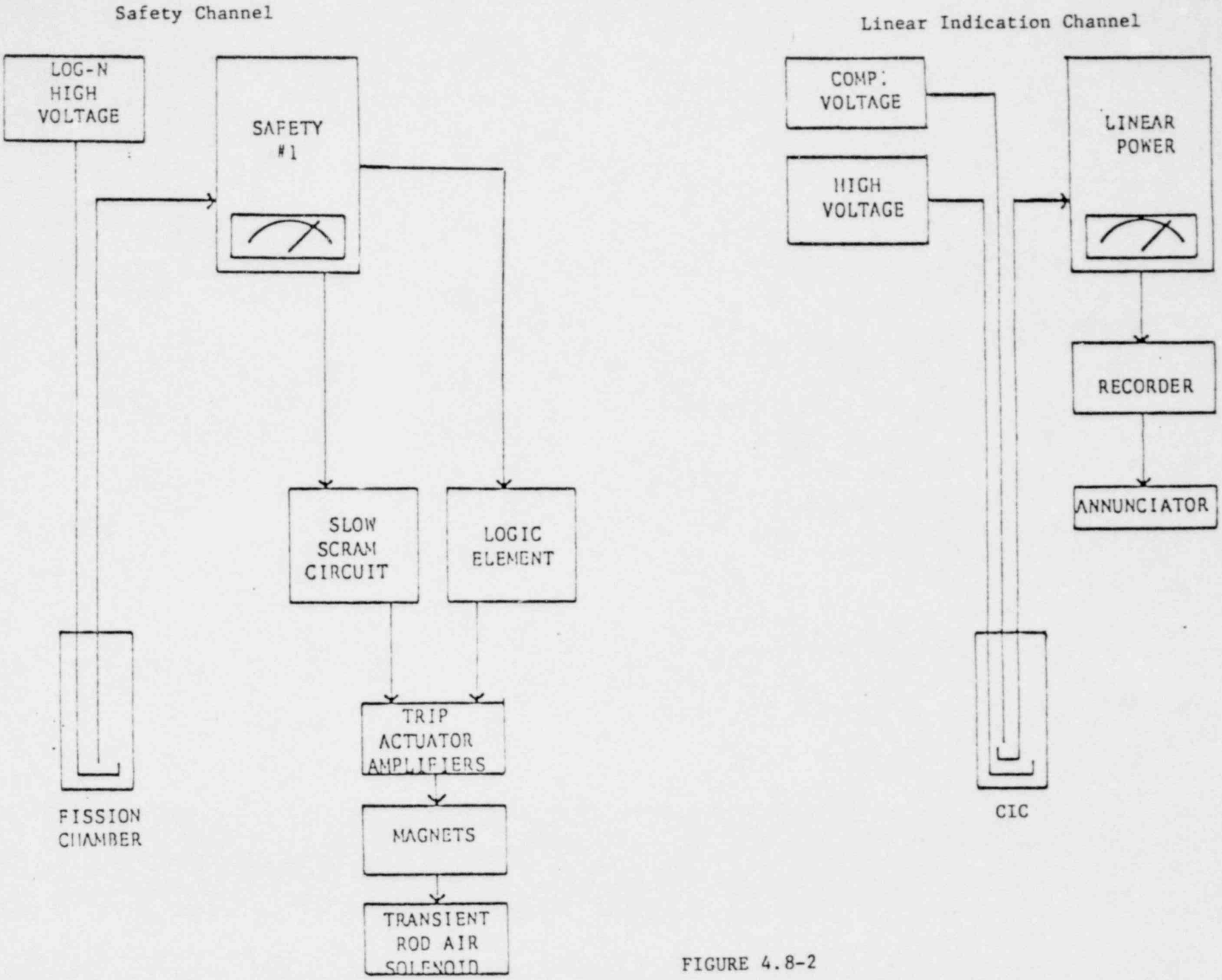

FIGURE 4.8-2

A) FUEL TEMPERATURE CHANNEL

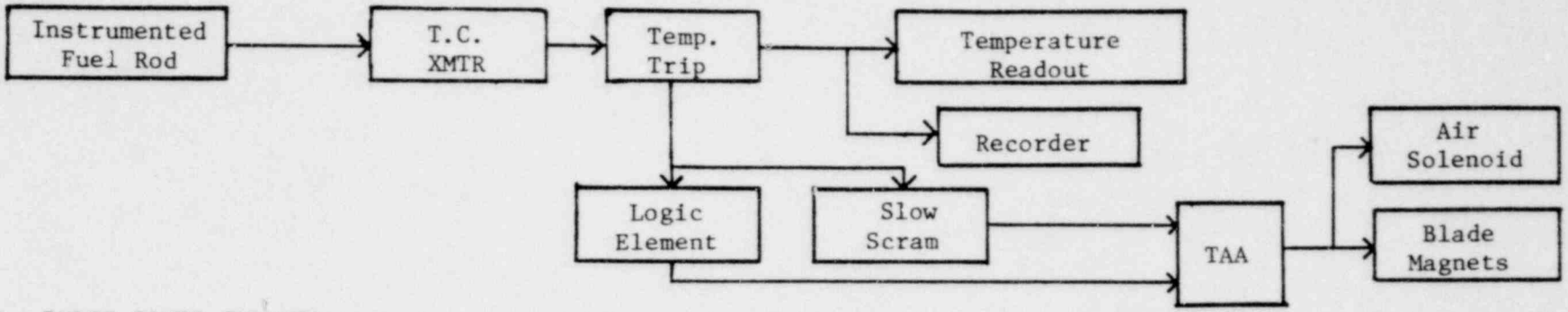

B) PULSE POWER CHANNEL

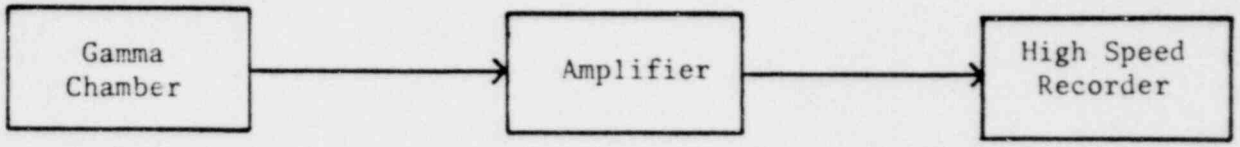

C) PULSE MODE CONTROL CHANNEL

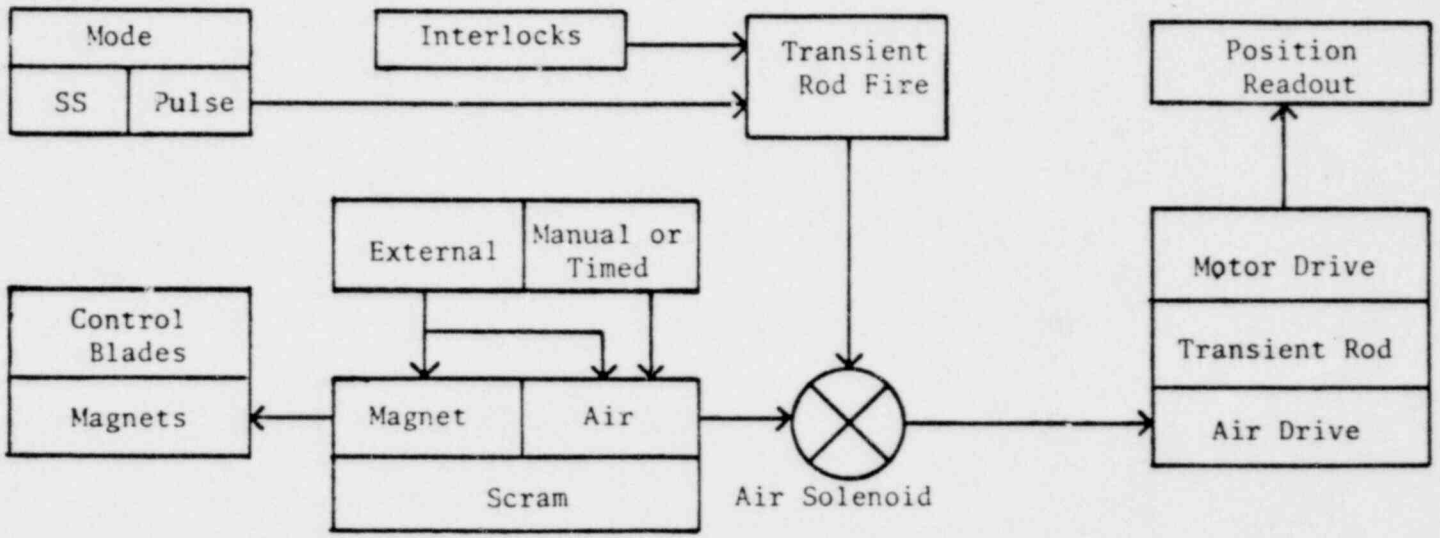

Pulsing Mode Instrumentation

FIGURE 4.8-3

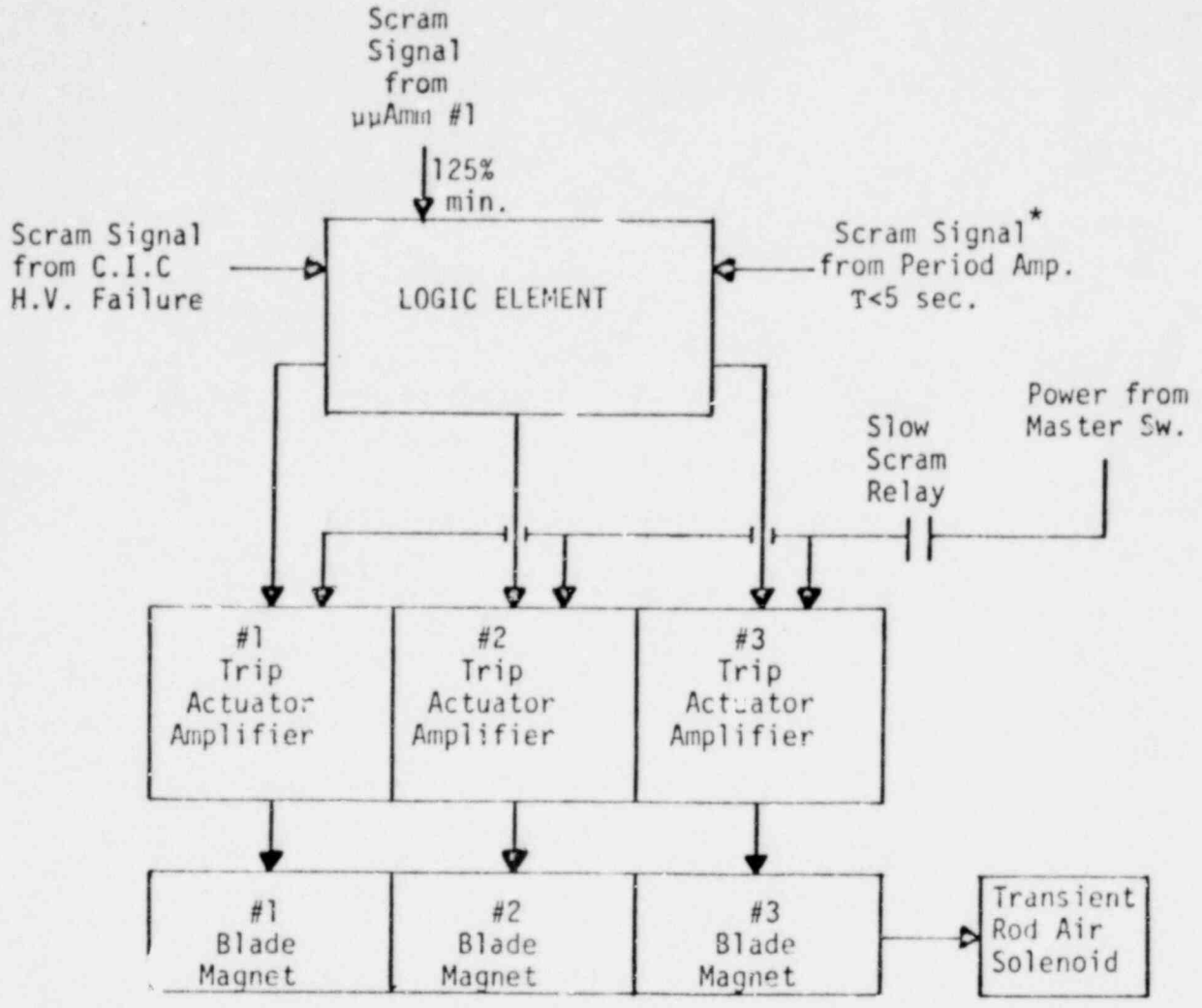

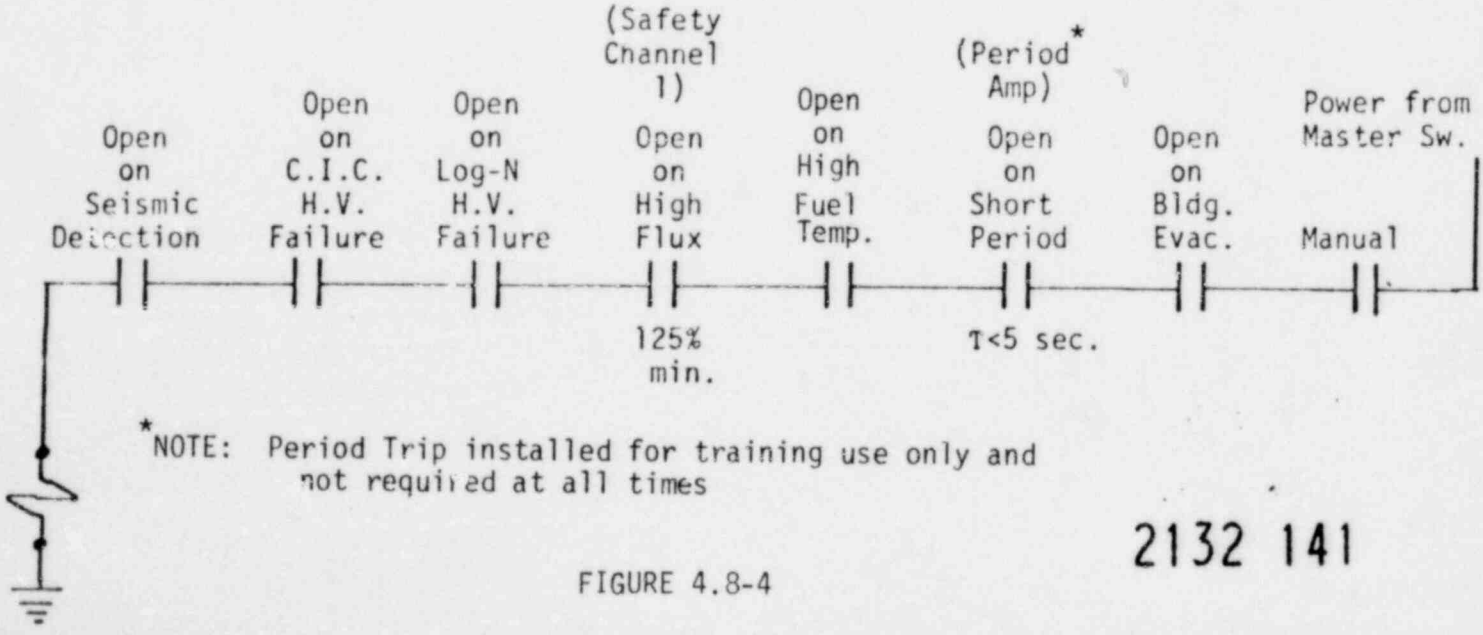

*NOTE: Period Trip installed for training use only and not required at all times

2132 141

FIGURE 4.8-4

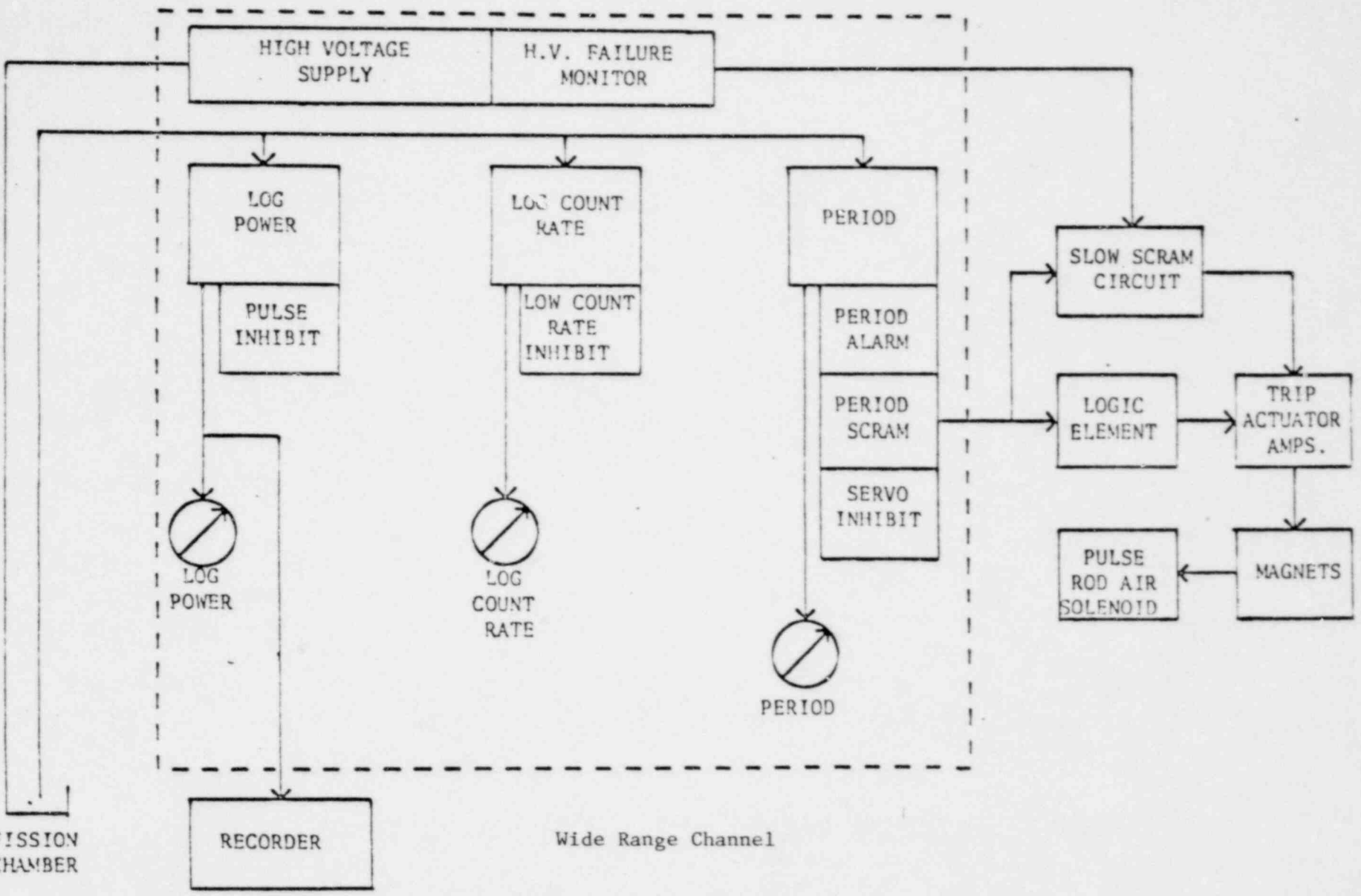

Wide Range Channel

FIGURE 4.8-5

shell-and-tube heat exchanger constructed with stainless-steel tubes. The primary pump has a stainless steel pump housing and rotor, and the primary piping is aluminum. A secondary side pump takes water from the sump of an induced draft type cooling tower and passes it through the shell side of the heat exchanger. The heat generated is dissipated to the atmosphere through the latent heat of vaporation of water in the cooling tower. A schematic diagram of the cooling system is shown in figure 4.9-1.

The physical layout of the cooling system is shown in figures 4.9-2 and 4.9-3. The system includes appropriate siphon breaks in the pool to prevent draining of the pool in the event of a piping rupture. A thermostatically controlled heater is installed in the cooling tower sump to prevent freezing during cold weather. Instrumentation for the cooling system in the control room allows the operator to control the system pumps as well as to monitor the conductivity, temperature, and pressure at various points in the system.

4.10 Pool Make-up and Demineralizer System

The pool water makeup and pool water demineralizer system is shown in figure 4.10-1. Water is circulated from the surface of the pool, through a mixed bed demineralizer, and then discharged at the botton of the pool. This loop maintains the purity of the pool water and collects the majority of the radionuclides created in the pool water by activation. Make-up feed water to compensate for pool evaporation is supplied by a Culligan demineralizer system. A float switch in the pool controls a solenoid valve in the make-up water line which automatically maintains the pool level.

4.11 Experimental Facilities

Experimental facilities are provided in the WSU TRIGA reactor for

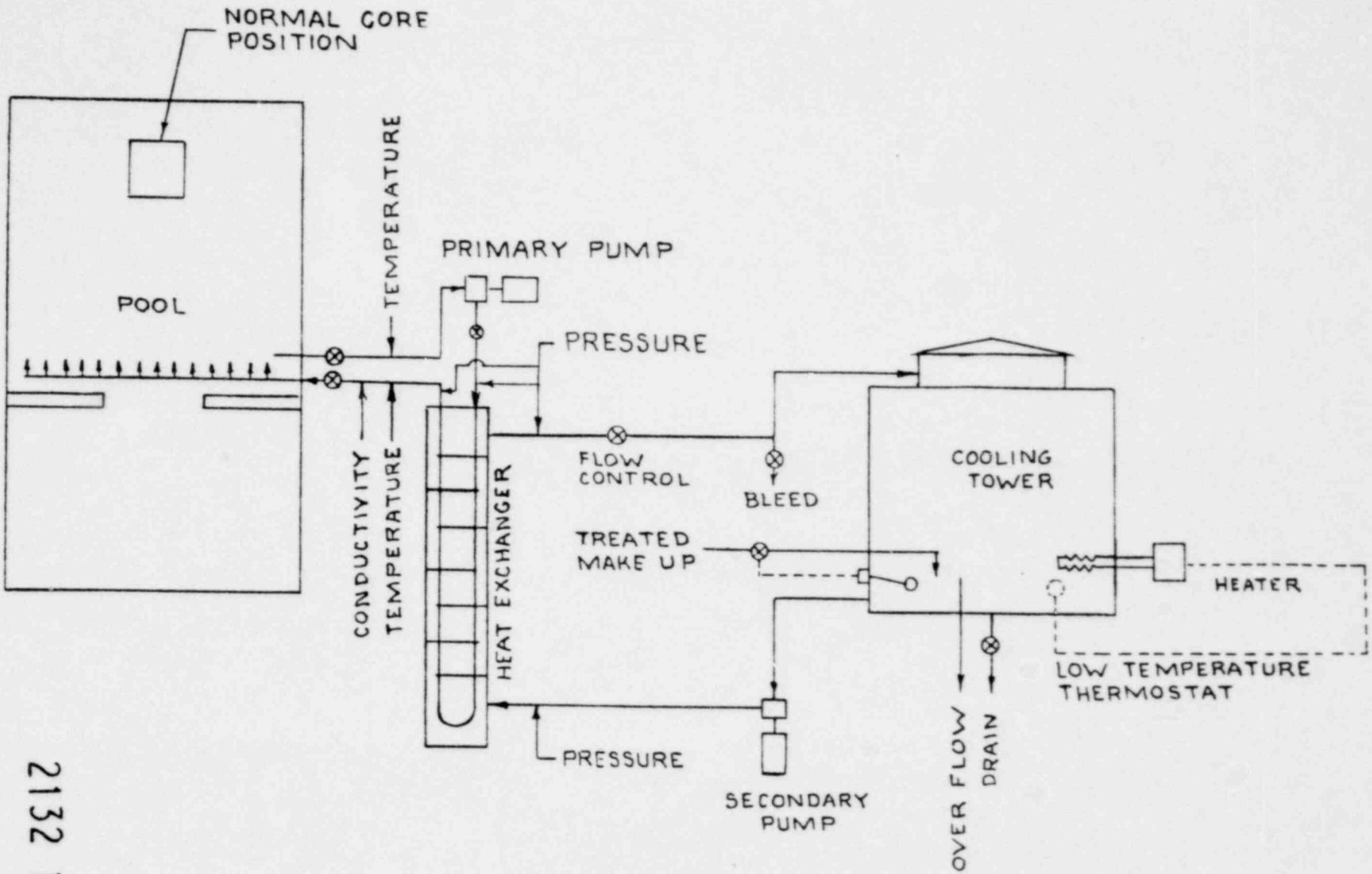

Cooling System Schematic

FIGURE 4.9-1

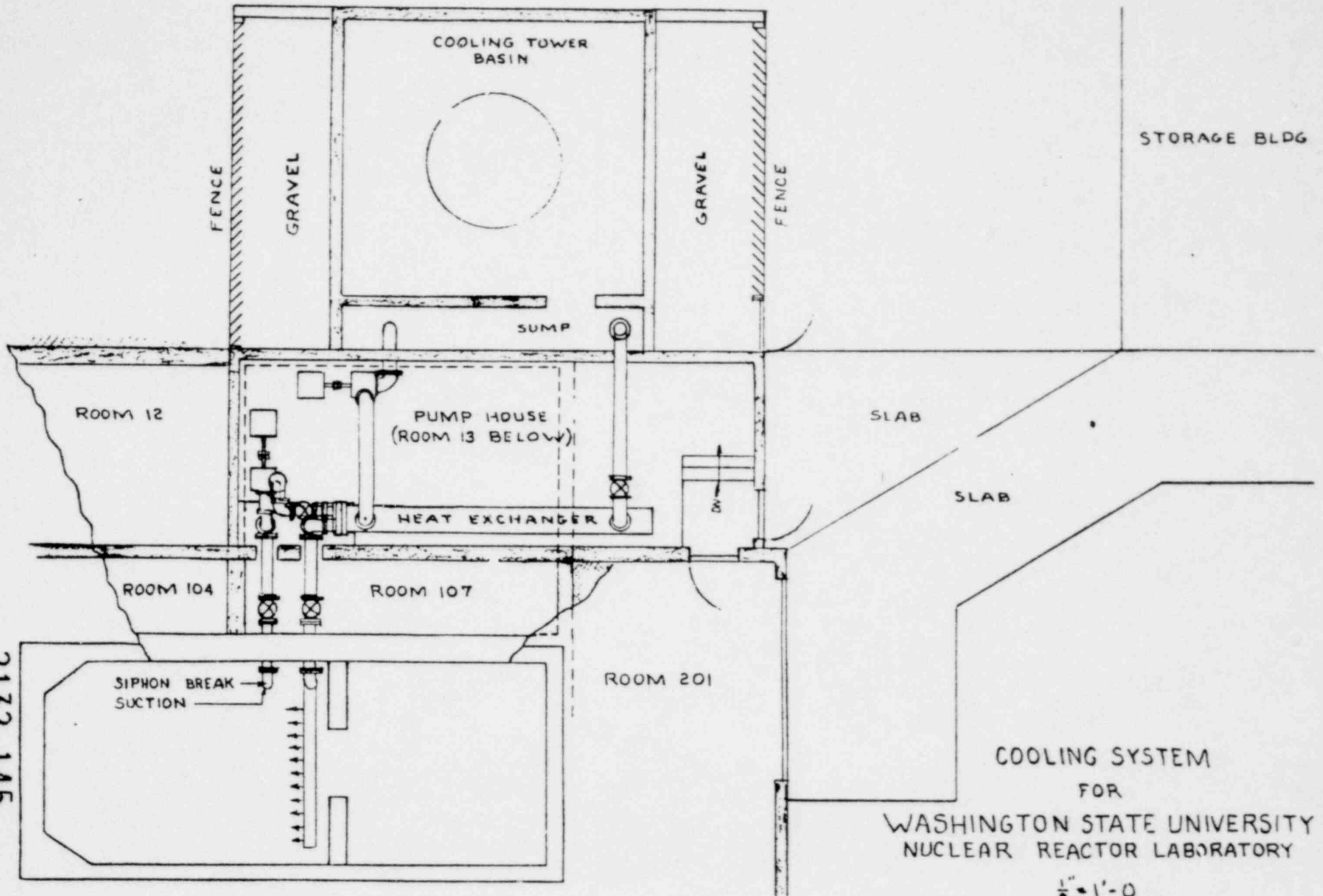

FIGURE 4.9-2

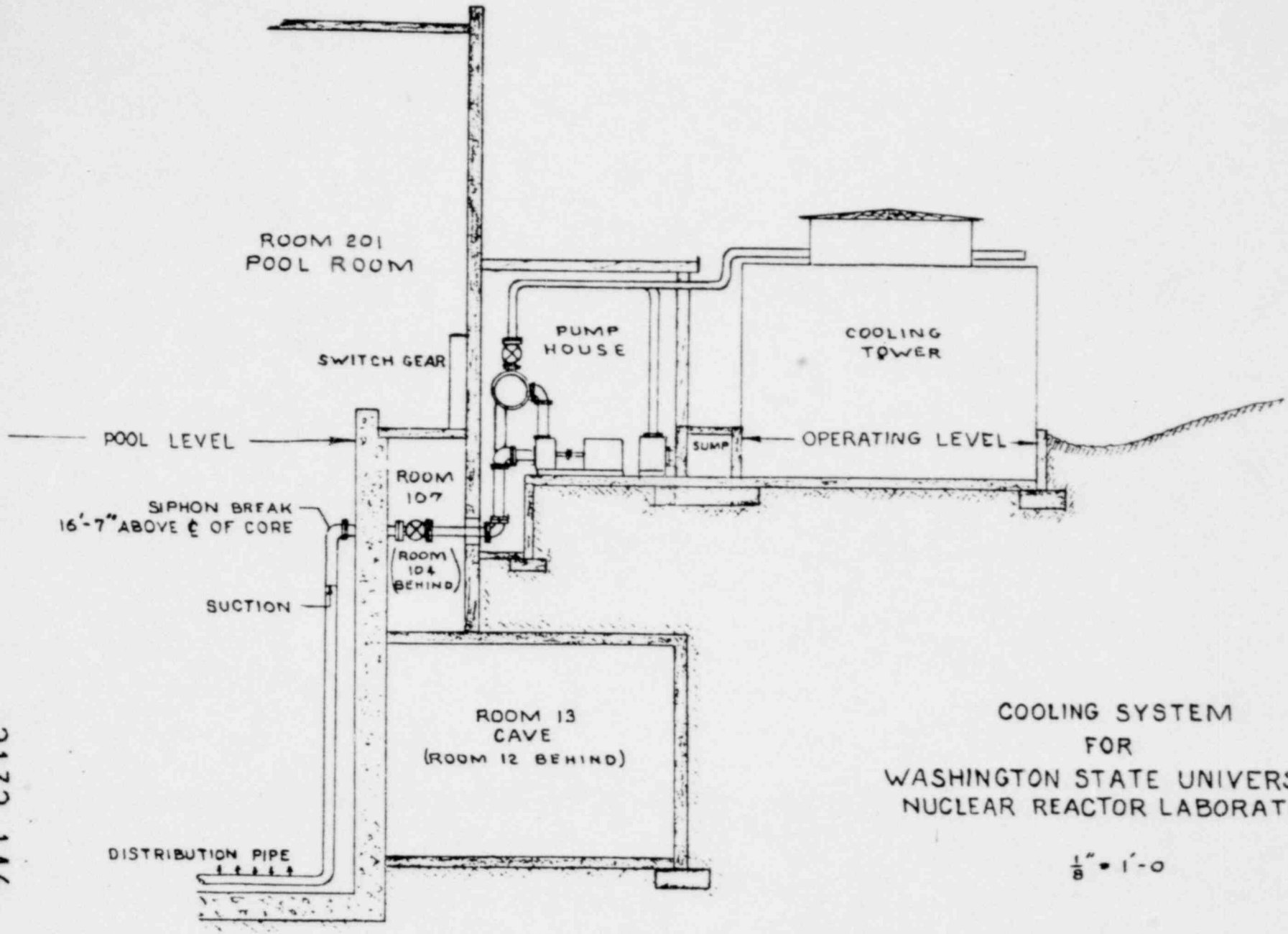

COOLING SYSTEM
FOR
WASHINGTON STATE UNIVERSITY
NUCLEAR REACTOR LABORATORY

$\frac{1}{8}$" = 1'-0

FIGURE 4.9-3

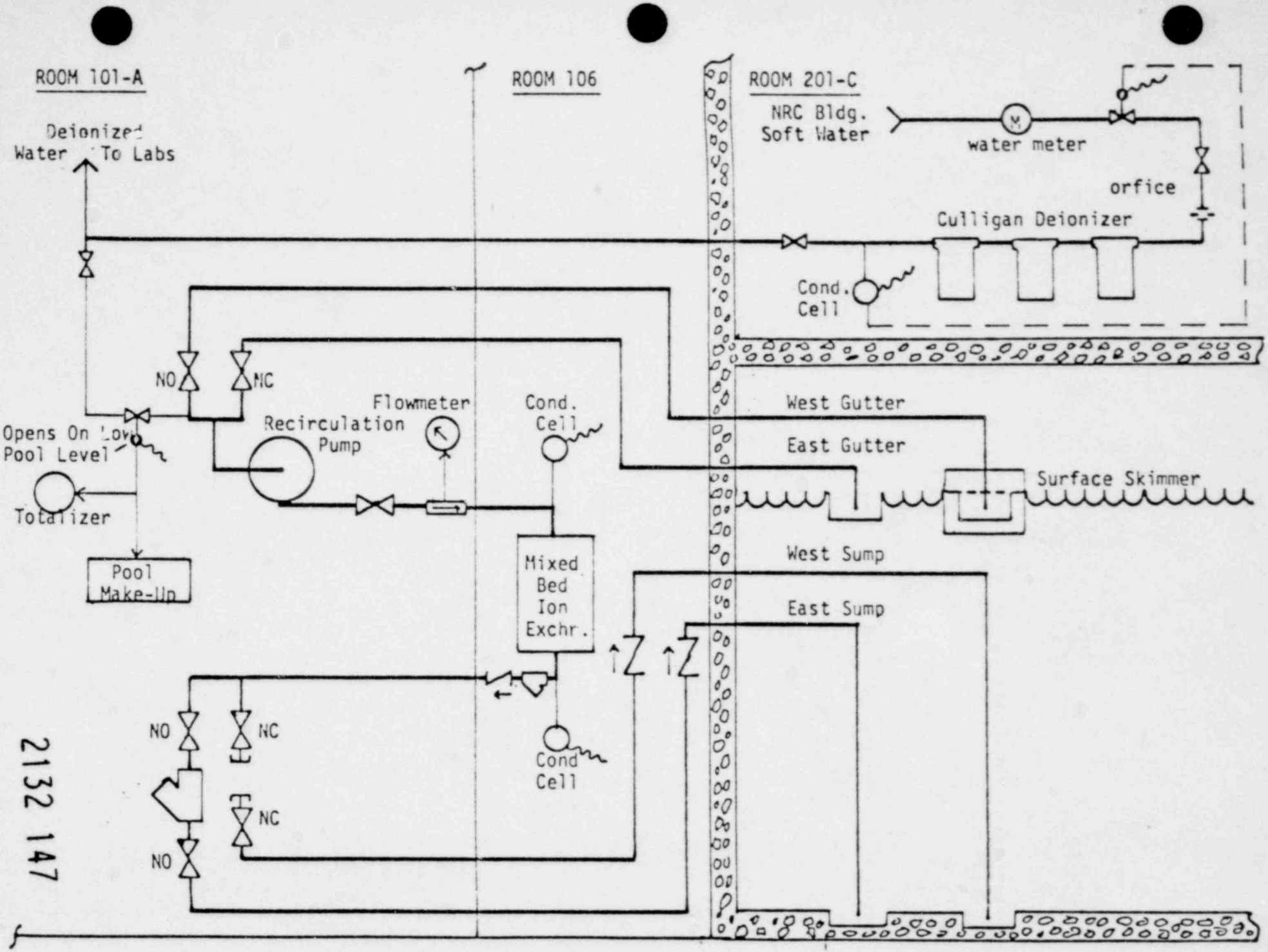

POOL WATER PURIFICATION & MAKE-UP SYSTEM

FIGURE 4.10-1

research purposes. These include a pneumatic transfer system, a thermal column, and numerous beam ports. The layout and dimension of the thermal column and beam ports is shown in figure 4.11-1. A schematic of the pneumatic transfer system is shown in figure 4.11-2. The pneumatic transfer system discharges into the monitored facility ventilation system. The ventilation system also maintains a negative pressure on the thermal column cavity to insure that air flows into the thermal column cavity and up the monitored exhaust.

4.12 N-16 Diffuser

A fraction of the oxygen present in the pool water is activated to nitrogen-16 by a fast neutron (n,p) reaction as the water passes upward through the core. To reduce the dose rate on the bridge caused by the upward migration of N-16, a diffuser system consisting of a centrifugal pump and discharge nozzle was installed. This system pumps water from the surface of the pool and discharges it downward and across the top of the core. The net result is an increase in the transport time of N-16 to the surface and a significant reduction of the N-16 related dose rate at the bridge level.

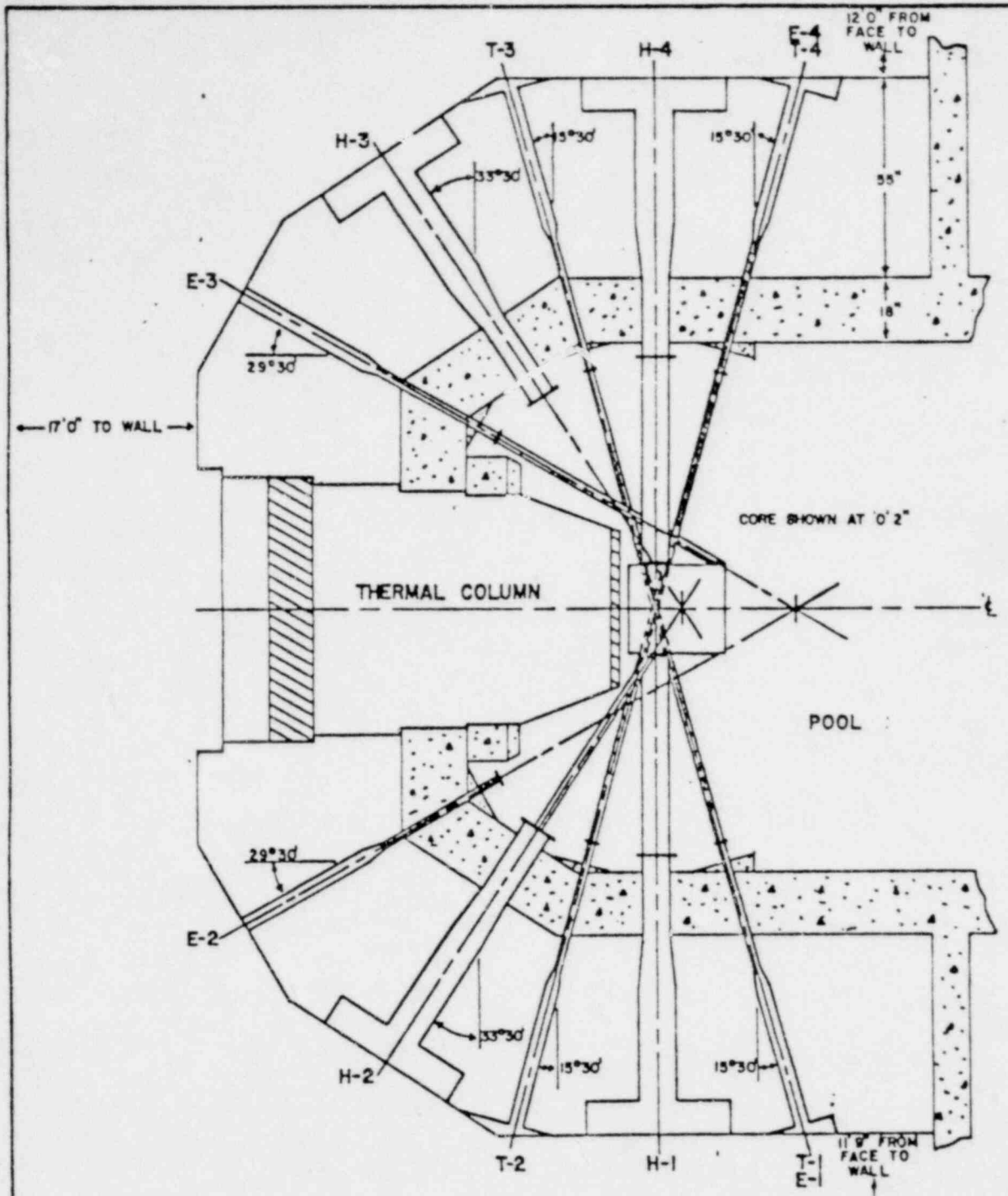

BEAM PORT SCHEDULE

BEAM PORT	LENGTH, INCHES 10" I.D. SECTION	10" to 8" REDUCER	8" I.D. SECTION	EXTENSION	℄ HEIGHT, INCHES FROM CORE ℄	FROM POOL FLOOR	FROM BEAM RM. FLOOR
H-1	31.50	15.50	21.75	55.13	-0.75	60.50	33.50
H-2	31.50	15.50	21.75	56.00	8.25	69.50	42.50
H-3	31.50	15.50	21.75	- - - -	8.25	69.50	42.50
H-4	31.50	15.50	21.75	54.63	-0.75	60.50	33.50

BEAM PORT	4" I.D. SECTION	4" to 2" REDUCER	2" I.D. SECTION	EXTENSION	FROM CORE ℄	FROM POOL FLOOR	FROM BEAM RM. FLOOR
E-1	38.40	4.50	37.00	55.38	- 5.75	55.50	28.25
E-2	39.19	4.50	37.00	69.75	-10.25	51.00	23.63
E-3	39.19	4.50	37.00	70.50	-10.25	51.00	24.13
E-4	38.40	4.50	37.00	54.50	- 5.75	55.50	28.13
T-1	38.40	4.50	37.00		-25.25	36.00	9.00
T-2	38.40	4.50	37.00		-20.25	41.00	13.75
T-3	38.40	4.50	37.00		-25.25	36.00	9.25
T-4	38.40	4.50	37.00		-20.25	41.00	13.87

NOTES:

1. THE H-1 EXTENSION IS 5.50" I.D., 0.25" WALL THICKNESS.
2. THE H-2 EXTENSION IS 2.067" I.D., 2.375" O.D.
3. THE H-4 EXTENSION IS TAPERED WITH AN INNER DIMENSION OF 5.00" SQ. AT THE CORE END & 3.625" SQ. AT 53.00" FROM THE END. THE SIDES ARE 0.50" PLATE AND THE END IS 0.25" PLATE.
4. THE E-SERIES AND T-SERIES EXTENSIONS ARE 2.067" I.D., 2.375" O.D.
5. THE ℄ OF H-1 & H-4 IS 9.50" FROM THE THERMAL COLUMN FACE.
6. THE POINT WHERE THE ℄'S OF E-2 & E-3 CROSS THE POOL ℄ IS 48.00" FROM THE THERMAL COLUMN FACE.
7. THE POINT WHERE THE ℄'S OF H-2 & H-3 CROSS THE POOL ℄ IS 17.00" FROM THE THERMAL COLUMN FACE.

2132 149

NUCLEAR RADIATION CENTER
WASHINGTON STATE UNIVERSITY
PULLMAN, WASHINGTON

TITLE: PLAN VIEW OF BEAM PORT FACILITIES

SCALE: 1/4"=1'	DRAWN BY: J. OGREN	DRAWING NO.
DATE: 8/25/71	CK'D. BY: W. HENDRICKSON	

FIGURE 4.11-1

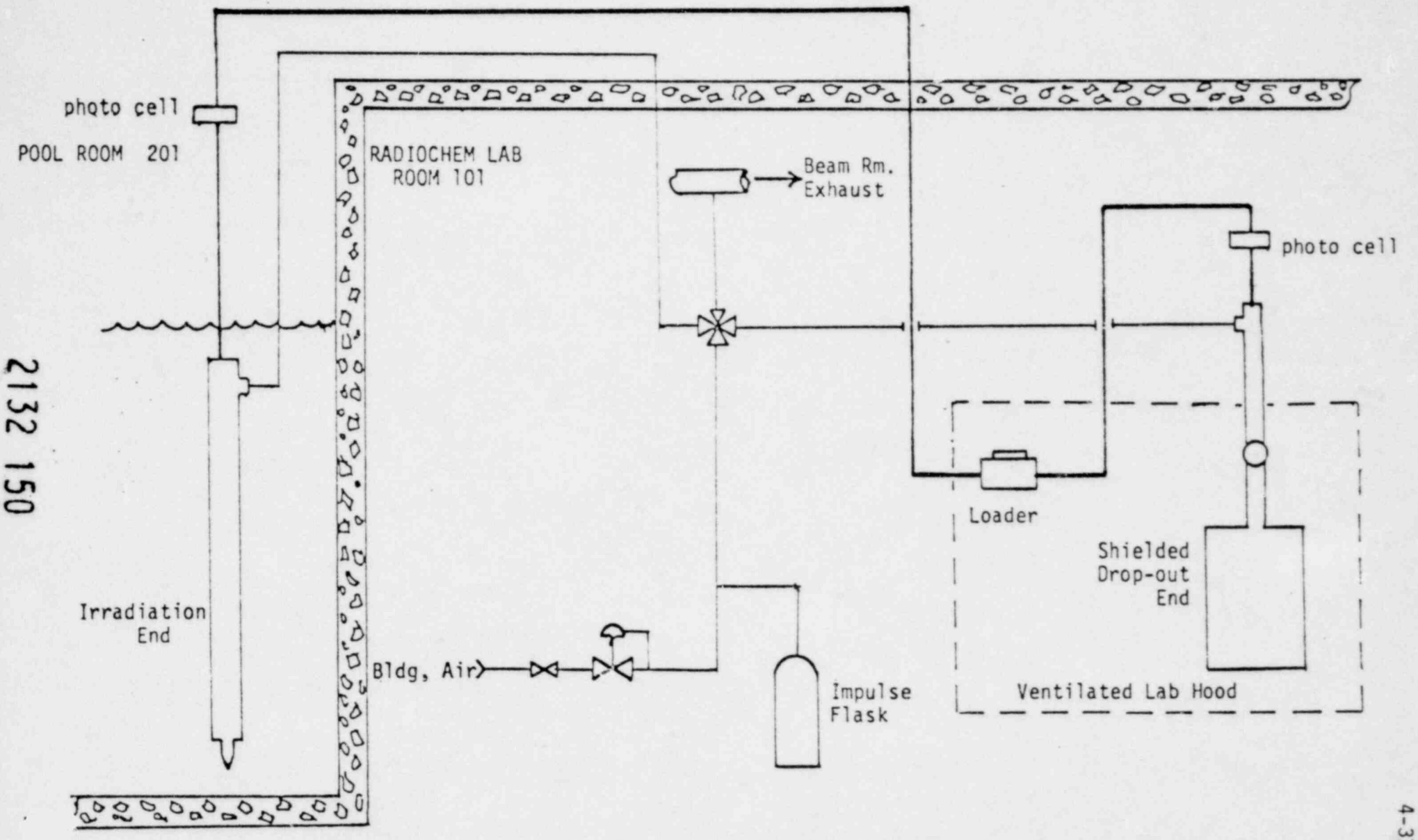

Pneumatic Transfer System

FIGURE 4.11-2

5.0 OPERATIONAL PERFORMANCE

5.1 General Reactor Data

This section covers the operational performance of the W.S.U. TRIGA reactor as fueled with a mixture of Standard and FLIP type fuel. On January 23, 1976 the W.S.U. TRIGA reactor fueled with all-Standard fuel was shut down after accumulating 6337 Mw-hours of steady-state operation and 535 pulsed reactivity insertions up to a maximum of $3.00 per pulse. The core was subsequently unloaded and minor modifications were made to the control system prior to loading new fuel. Fuel loading commenced on February 9, 1976 and a critical loading was obtained at 0955 on February 17, 1976. The approach to the critical loading is shown in Figure 5.1-1.

Additional fuel was loaded into the core to obtain operational core 30-A shown in Figure 5.1-2. This core had a shutdown margin of $.68 with the transient and servo blades withdrawn. The control elements were calibrated using the doubling time method and the total worth amounted to $14.39 as shown in Table 5.1-1. Integral control element worth curves for core 30-A are given in Figures 5.1-3 to 5.1-7. The reactivity worth of selected 4-rod clusters in core 30-A are tabulated in Table 5.1-2.

TABLE 5.1-1

Control Element Worths in Core 30-A

Element Number	Worth in Dollars
1	$ 2.54
2	3.57
3	4.39
4 (regulating) (Servo Blade)	.44
5 (transient)	3.45
Total	$ 14.39

Approach To Critical Experiment Core 30A

Inverse multiplication vs. fuel rod addition

FIGURE 5.1-1

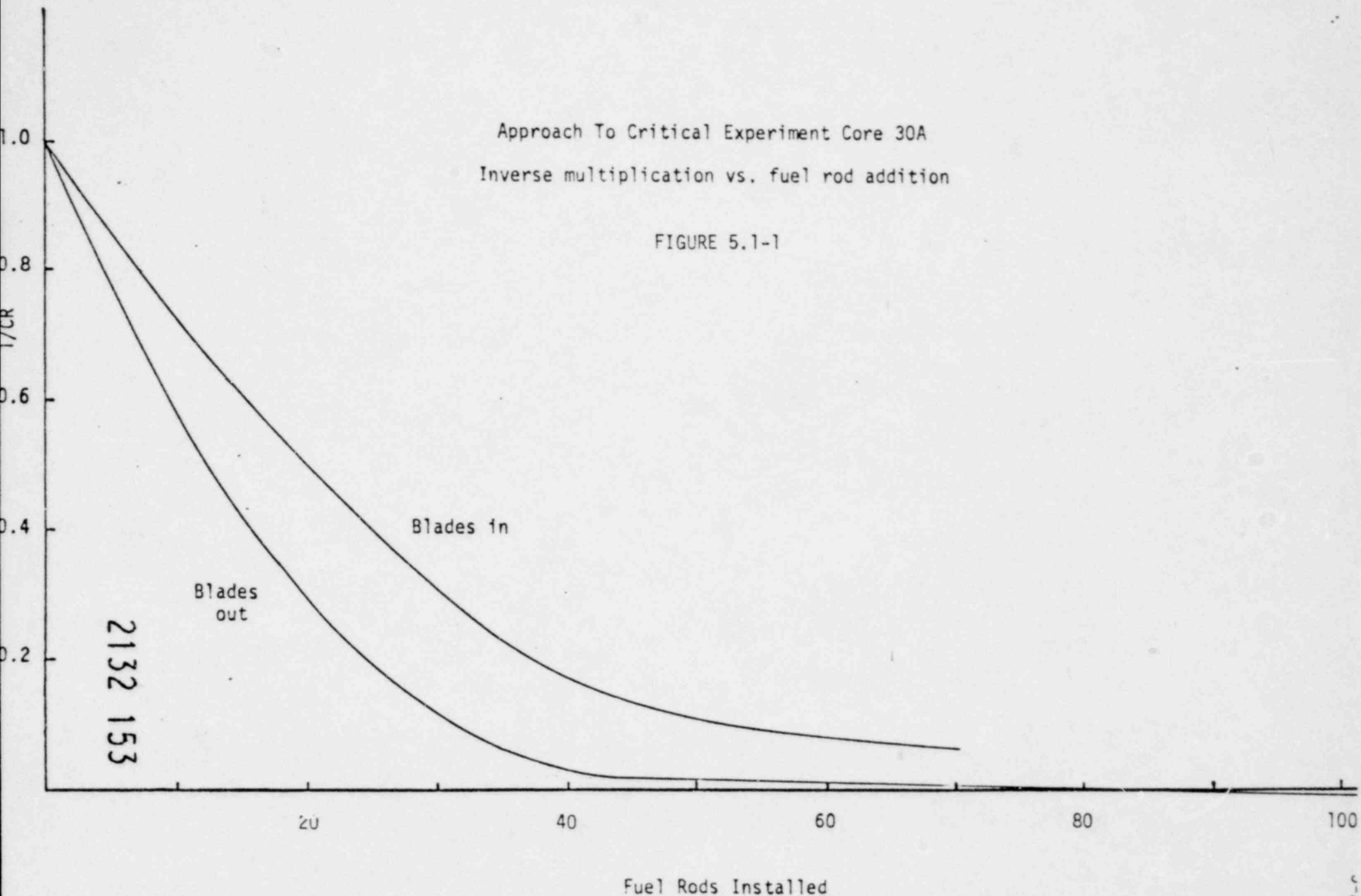

2132 153

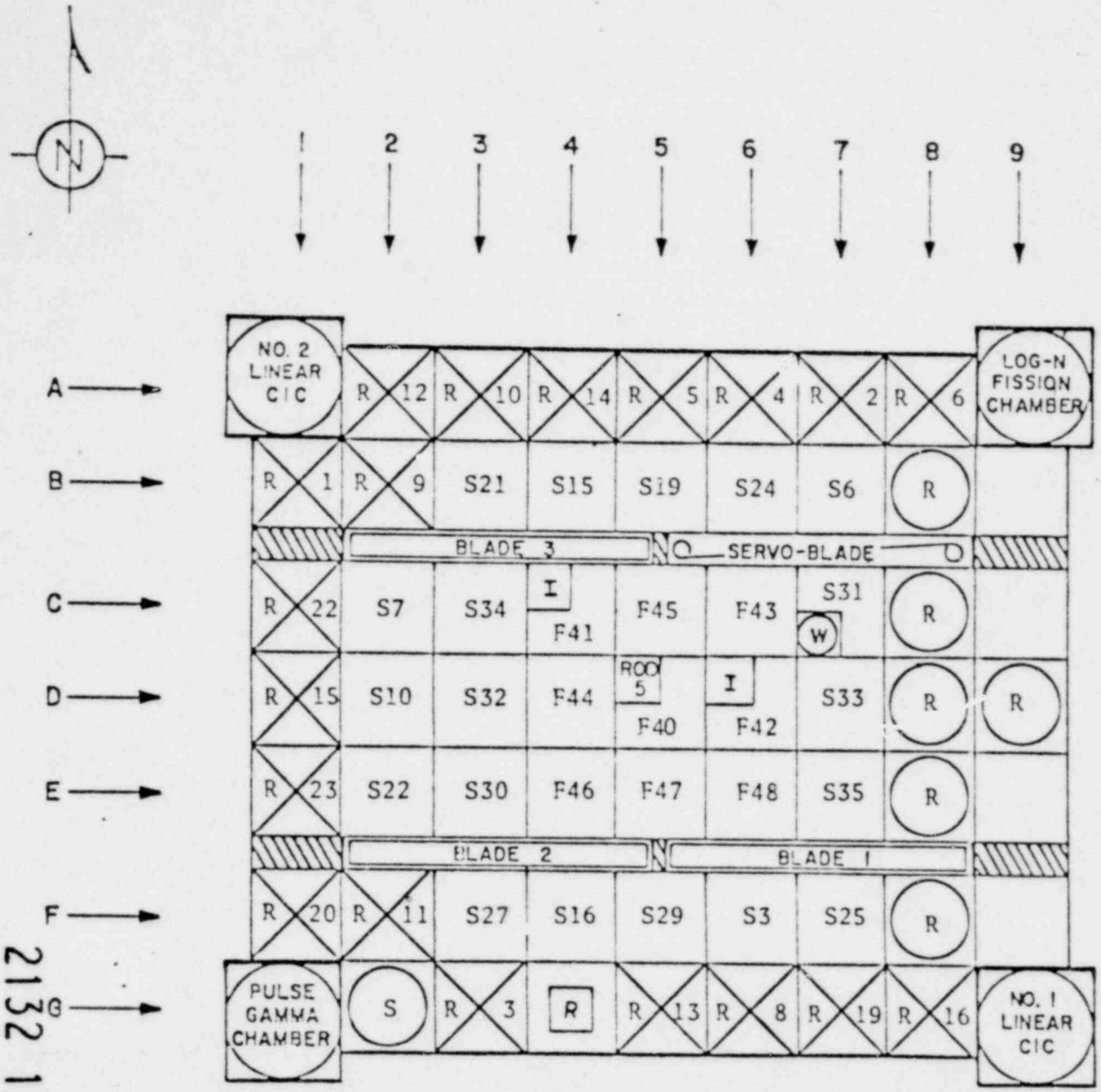

FIGURE 5.1-2

CORE LAYOUT

CORE NO. 30-A

DATE: Feb. 25 ,19 76

- S — STD. ELEMENT
- F — FLIP ELEMENT
- REFLECTOR
- R — ROTATOR TUBE
- D — DRY TUBE
- W — WET TUBE
- R — RABBIT TUBE
- RADIATION BASKET
- S — NEUTRON SOURCE
- I — INSTRUMENTED FUEL ROD

2132 154

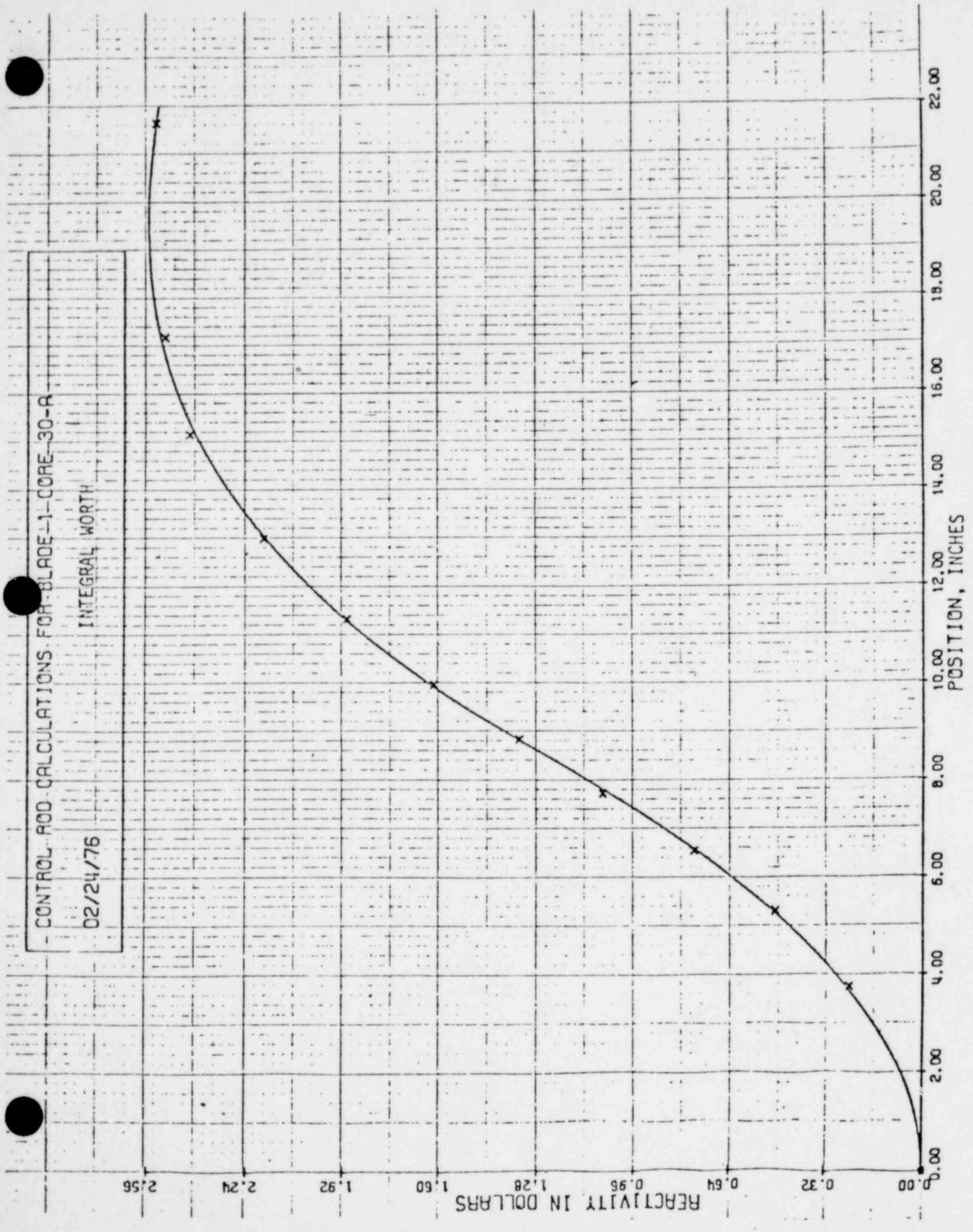
CONTROL ROD CALCULATIONS FOR BLADE-1-CORE-30-A
INTEGRAL WORTH
02/24/76
REACTIVITY IN DOLLARS
0.00
0.32
0.64
0.96
1.28
1.60
1.92
2.24
2.56
POSITION, INCHES
0.00
2.00
4.00
6.00
8.00
10.00
12.00
14.00
16.00
18.00
20.00
22.00

FIGURE 5.1-3

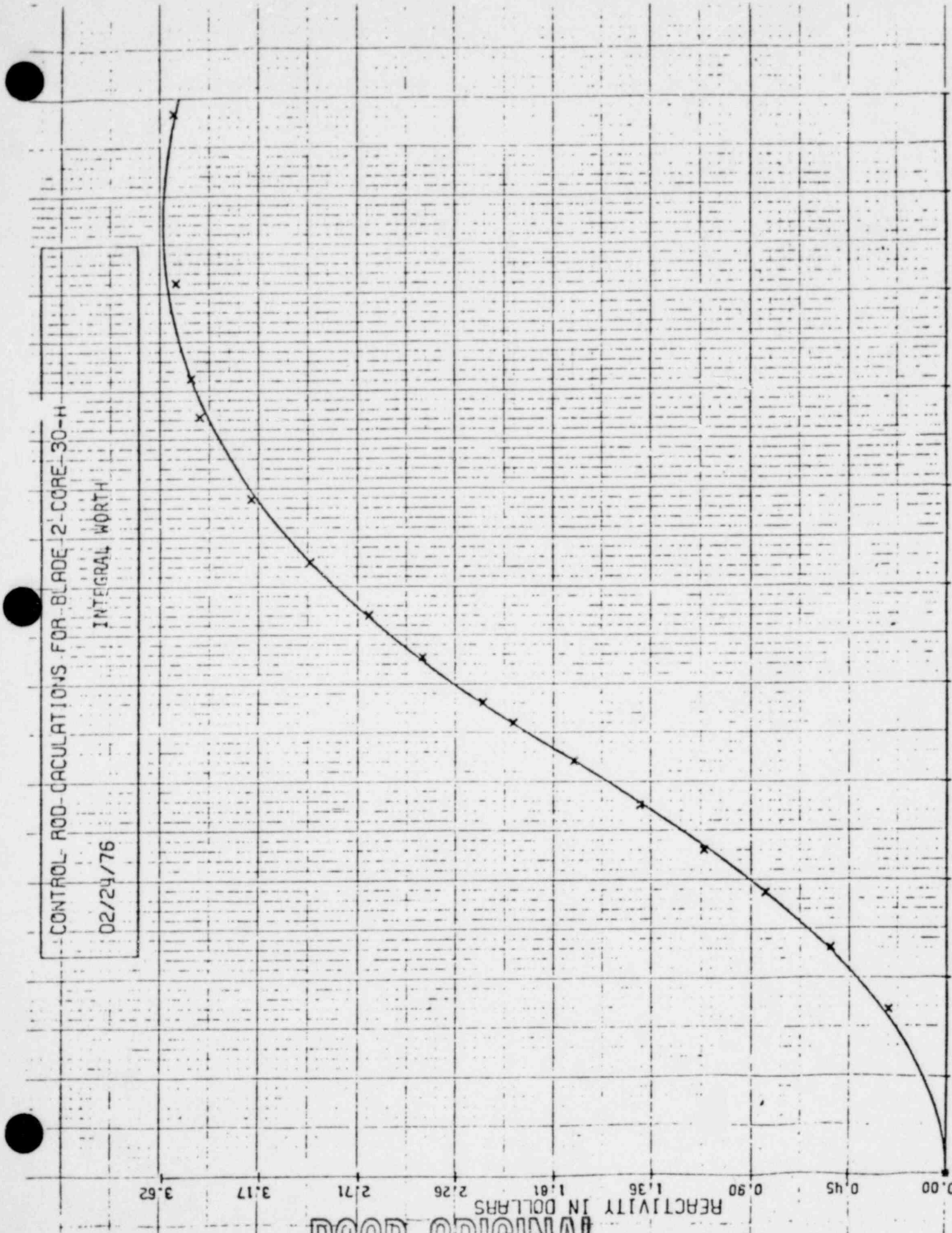

FIGURE 5.1-4

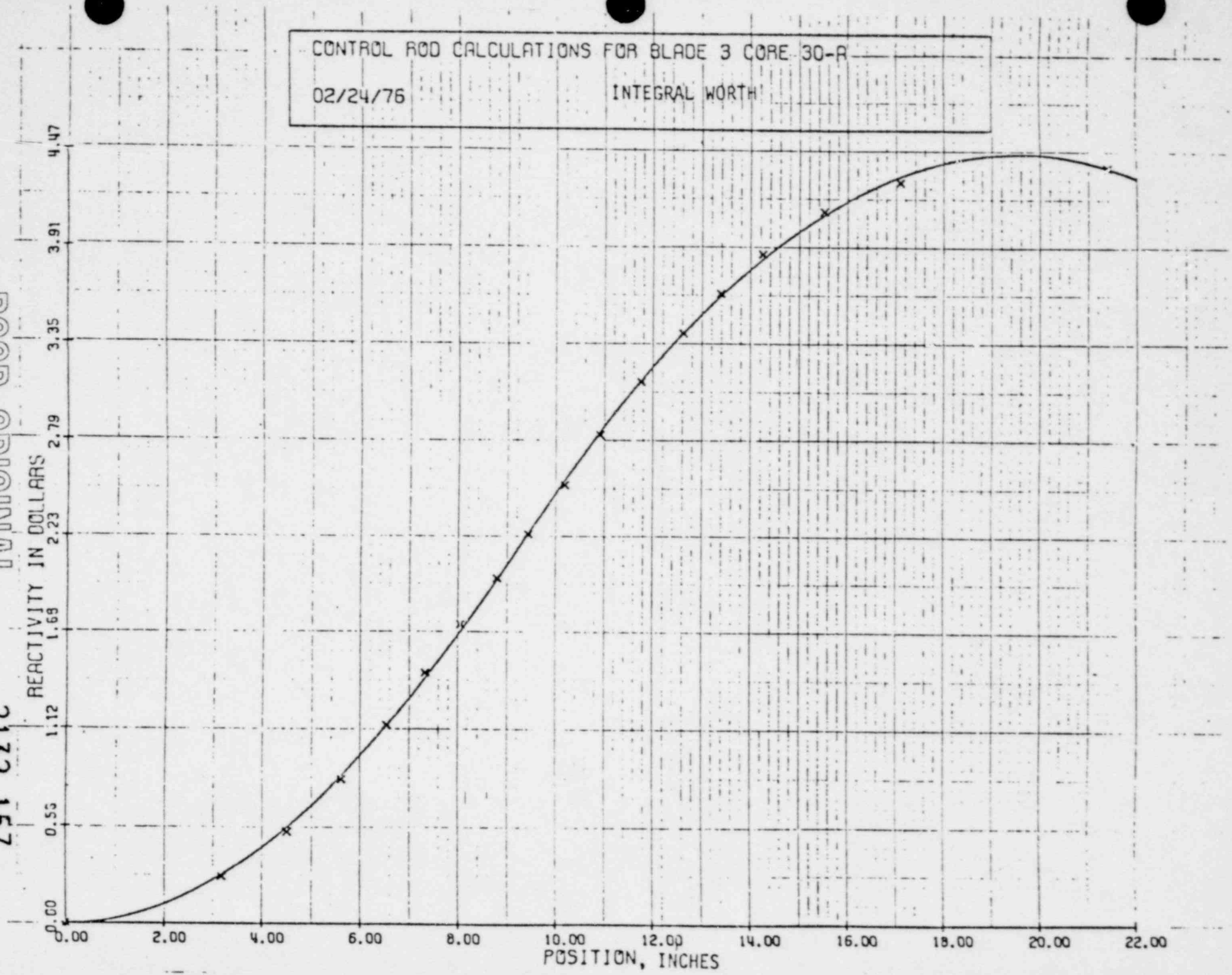

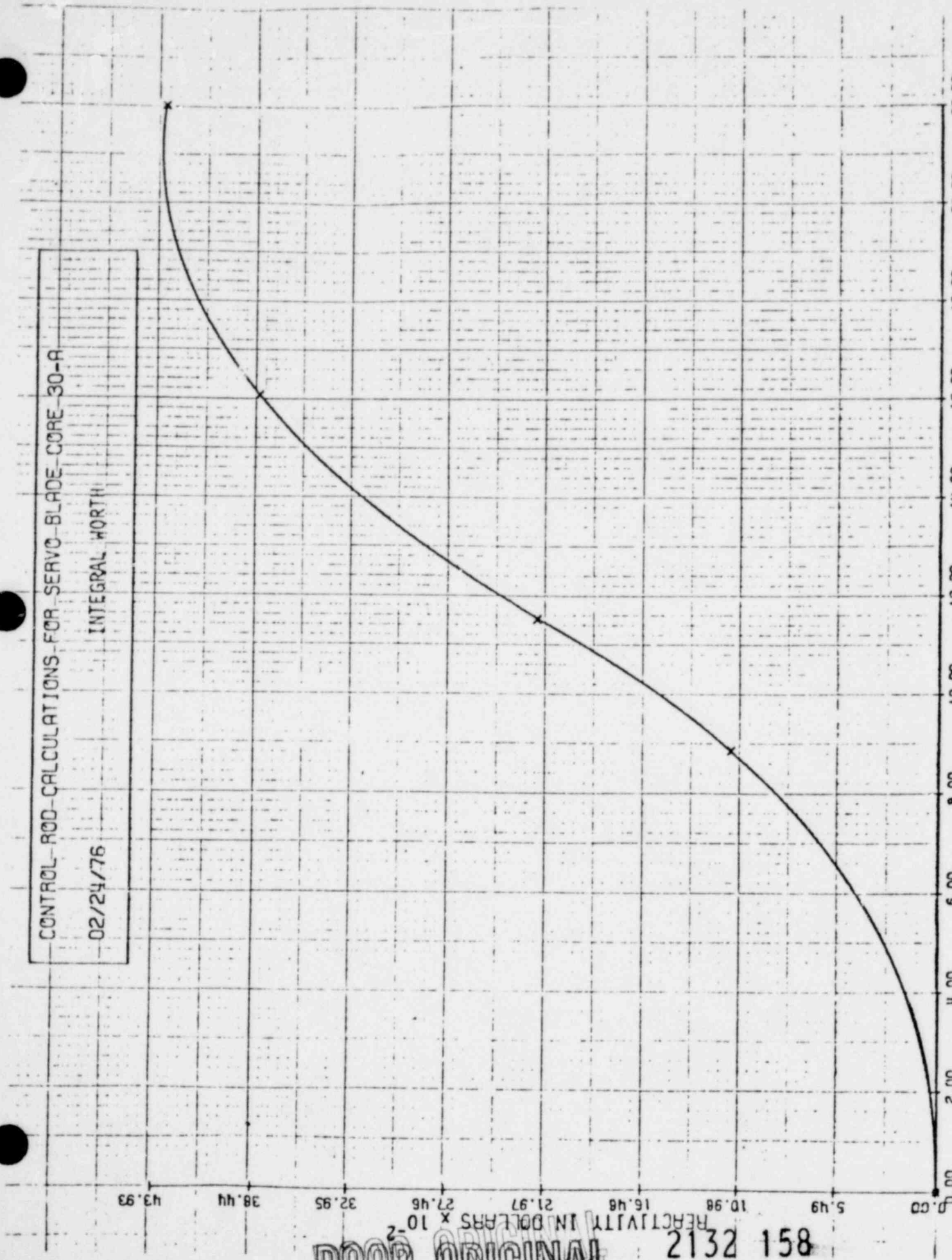

FIGURE 5.1-6

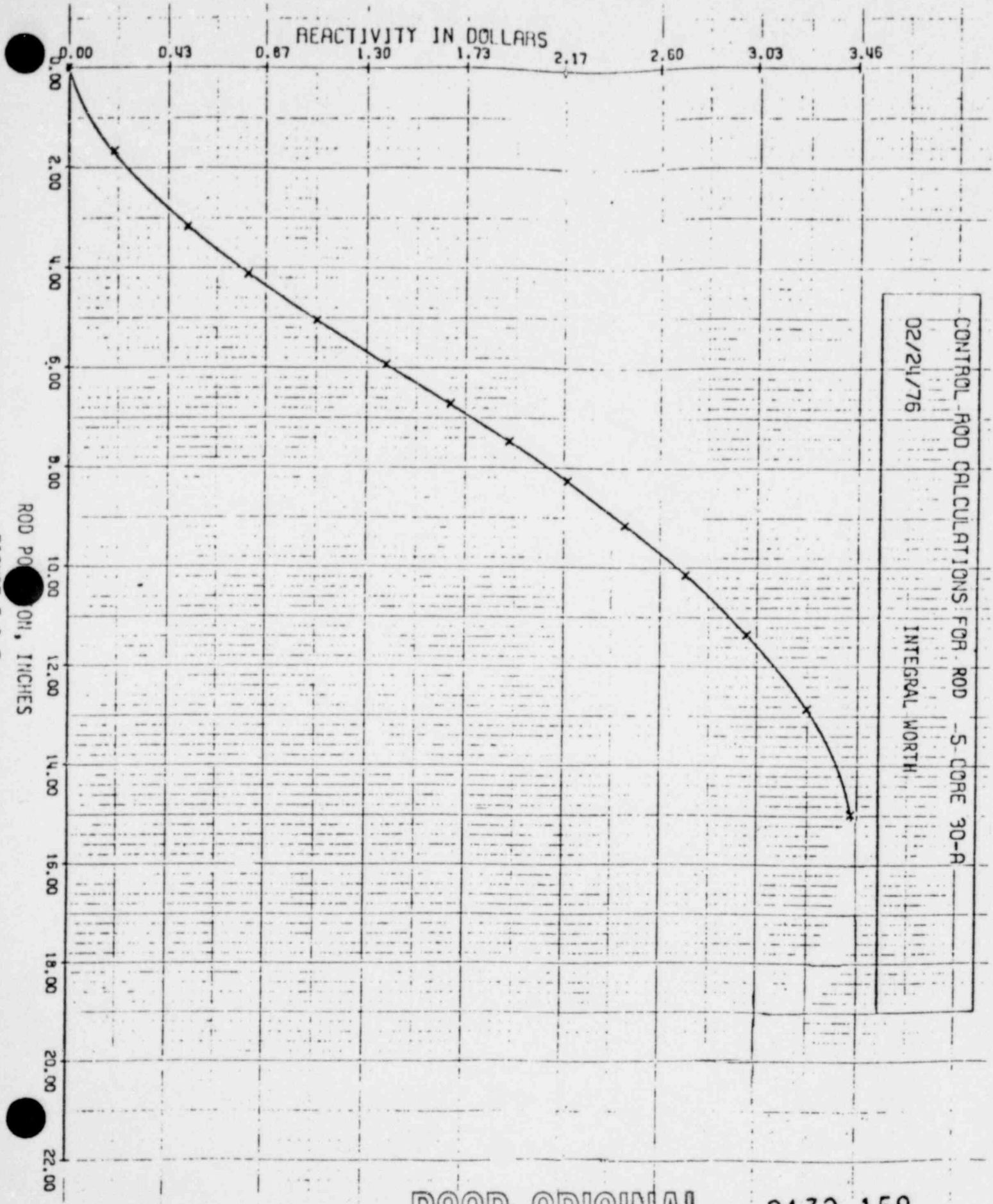

FIGURE 5.1-7

TABLE 5.1-2

Four-Rod Fuel Cluster Reactivity Worths

Core Position	Cluster No.	Reactivity in Dollars
C-6	F43 (FLIP)	$ 2.80
E-6	F48 (FLIP)	2.13
E-3	S30 (Standard)	1.79

5.2 Steady State Operation

Escalation to full power on mixed core 30-A was commenced on February 20, 1976 using 100 kw steps. Routine full power operations on this core began on March 12, 1976. As of May 1, 1979, a total of 2700 Mw-hrs of operation without a single significant problem has been accumulated on the W.S.U. TRIGA reactor fueled with a mixture of FLIP and Standard type fuels.

The fuel temperature as measured by the instrumented FLIP fuel rod in core position F42 versus reactor power level is shown in Figure 5.2-1. The measured excess reactivity loss due to heating of the fuel versus power level is shown in Figure 5.2-2. The measured excess reactivity of the core as a function of megawatt hours of operation is shown in Figure 5.2-3. The indicated fuel temperature and average core temperature versus excess reactivity is shown in Figure 5.2-4. The average core fuel temperature versus average temperature coefficient of reactivity is shown in Figure 5.2-5.

No unusual or significant problems have been encountered during the three years that the W.S.U. TRIGA reactor has been operated in the steady state mode at a maximum power level of one megawatt. Future plans call for the replacement of one of the FLIP instrumented fuel rods due to the

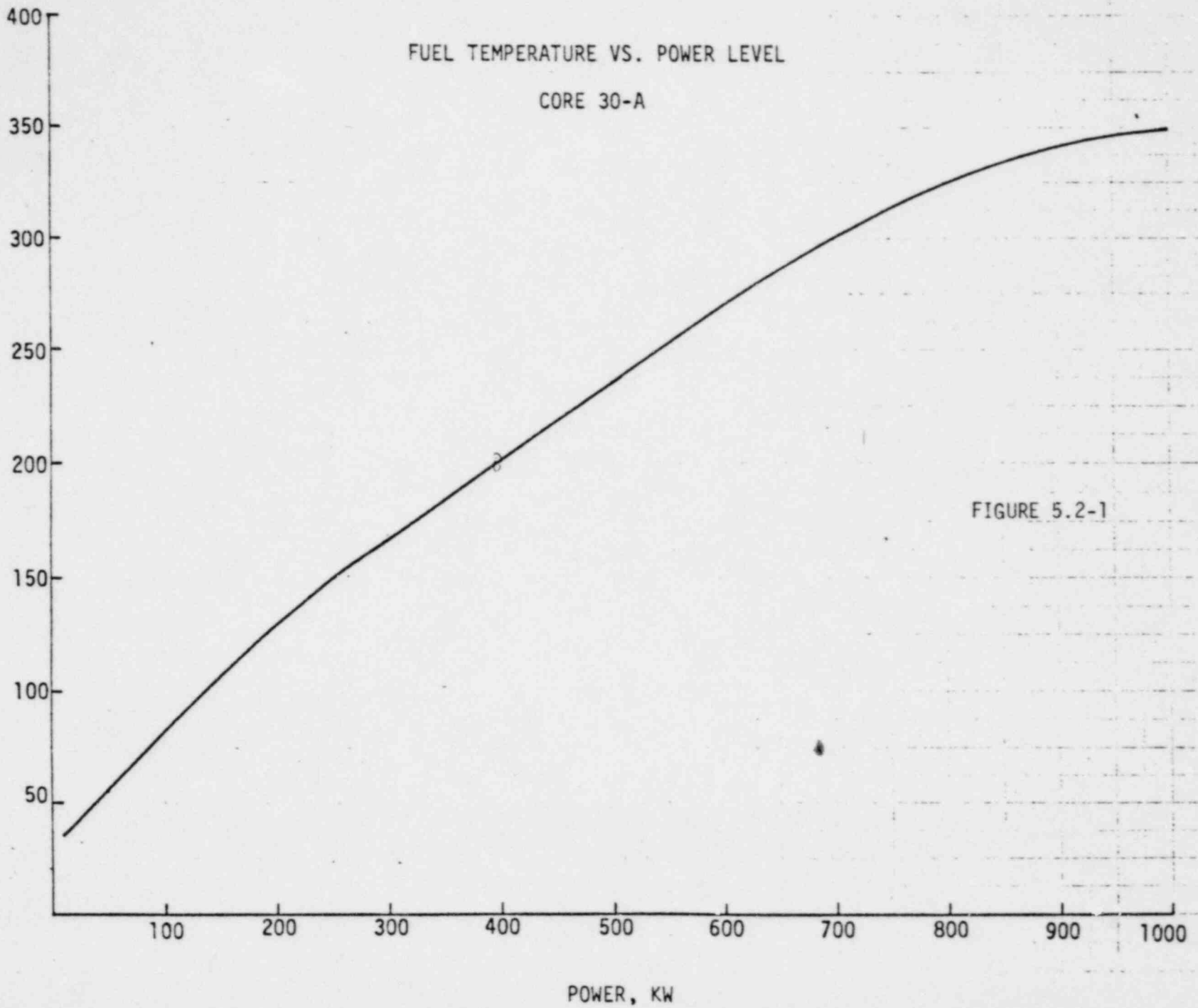

FIGURE 5.2-1

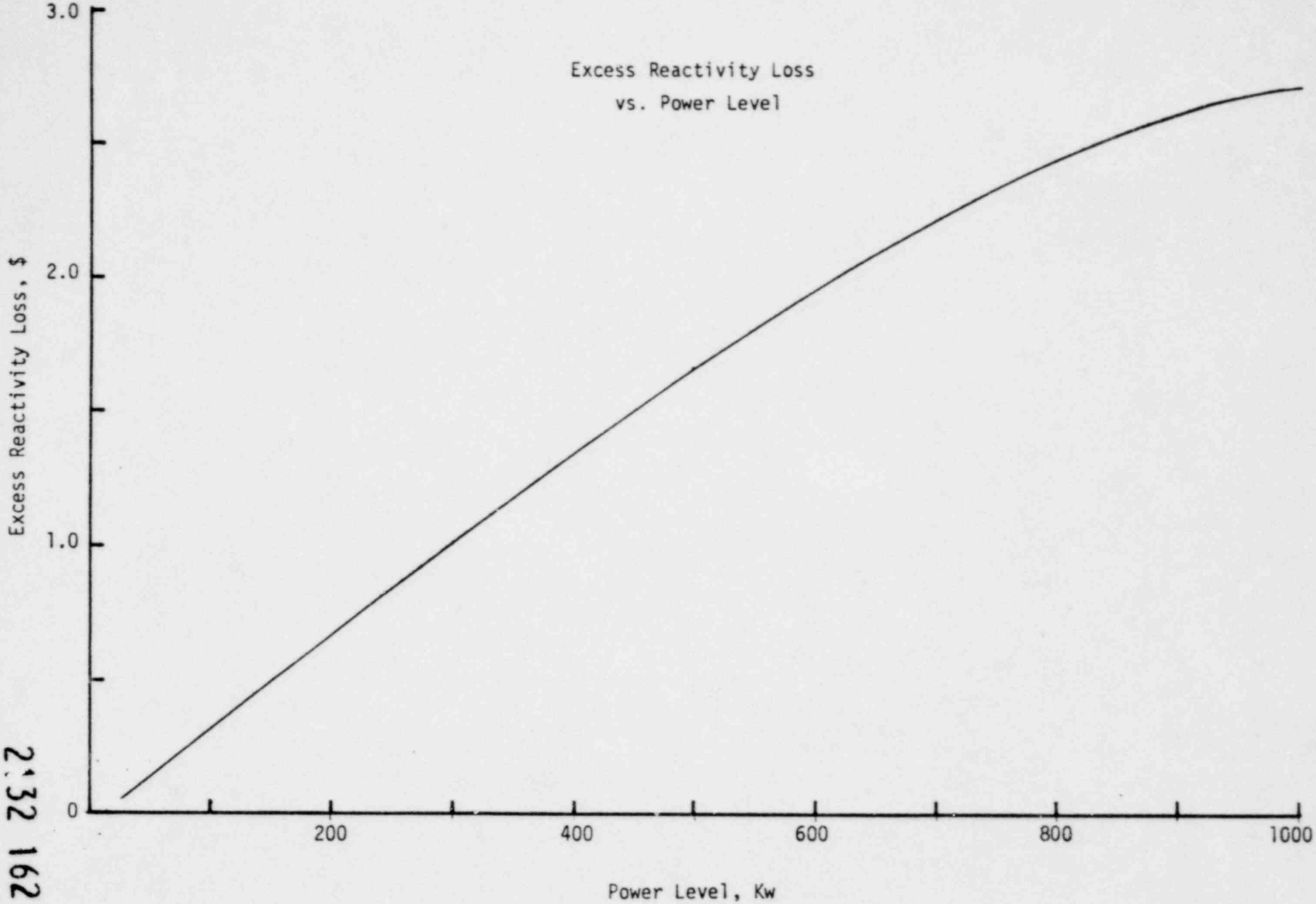

FIGURE 5.2-2

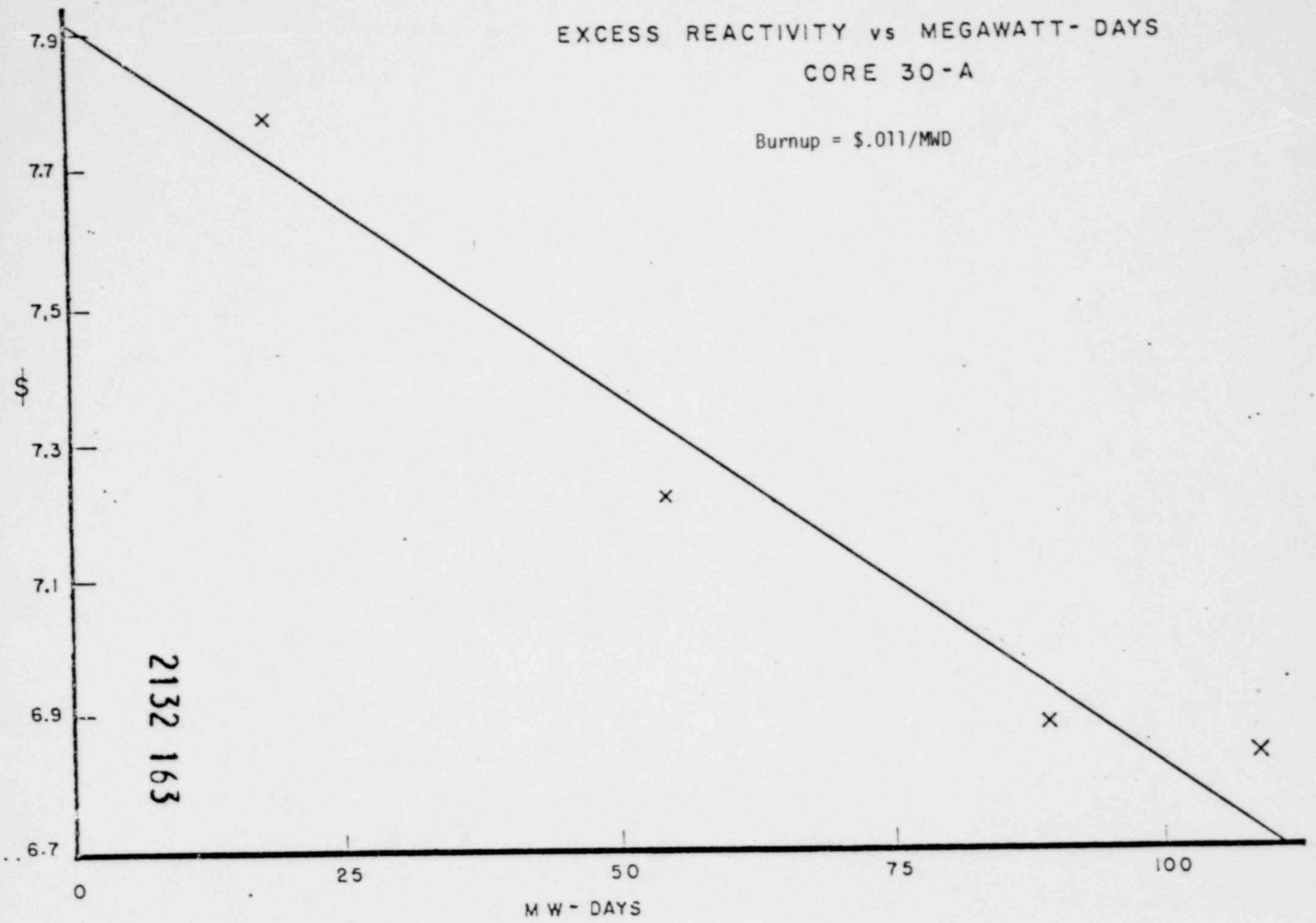
EXCESS REACTIVITY vs MEGAWATT- DAYS
CORE 30-A
Burnup = $.011/MWD
7.9
7.7
7.5
$
7.3
7.1
6.9
6.7
0
25
50
75
100
M W - DAYS
2132 163

FIGURE 5.2-3

Excess Reactivity vs. Indicated
and Average Core Temperature

FIGURE 5.2-4

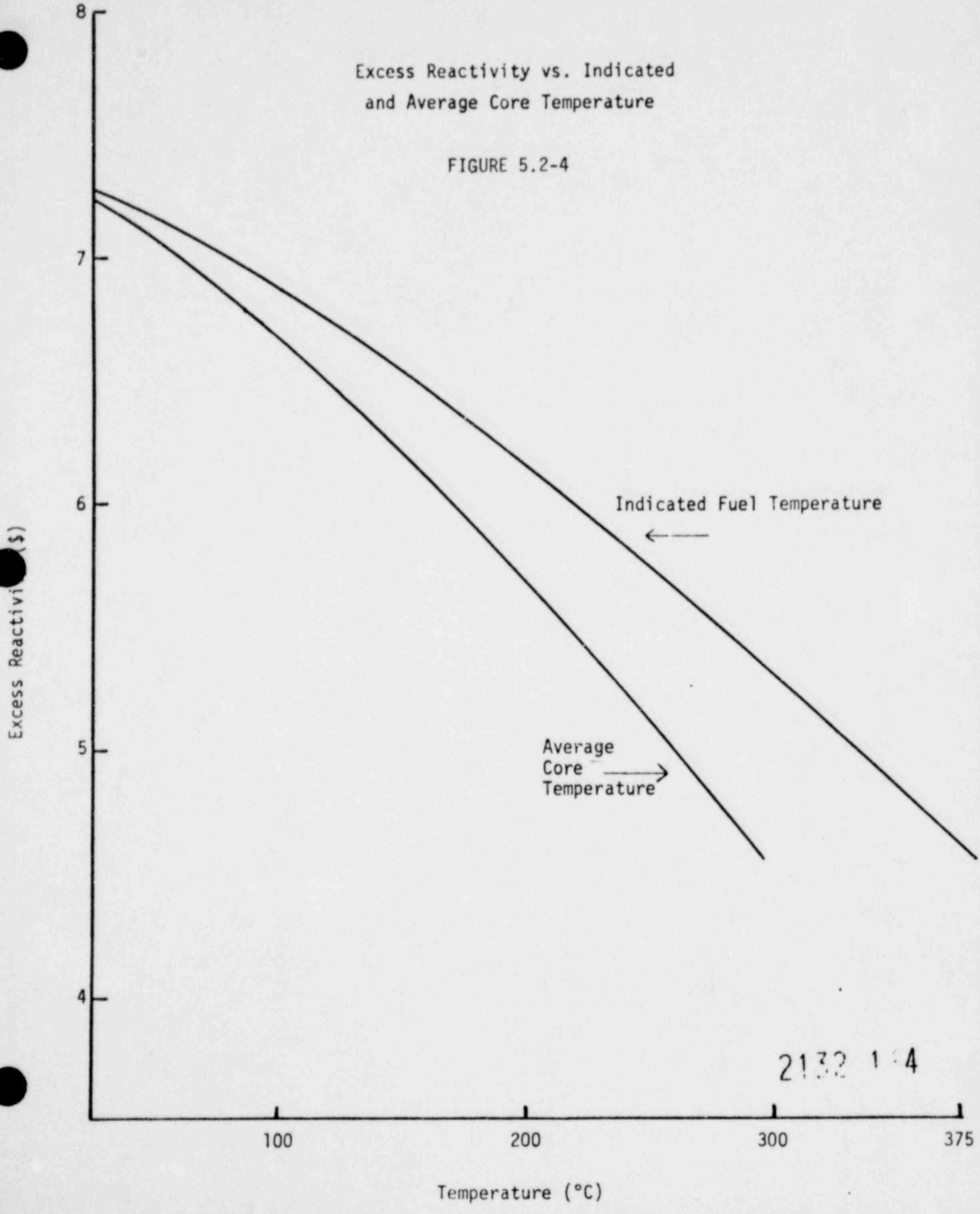

Average Temperature Coefficient vs.
Average Core Temperature

FIGURE 5.2-5

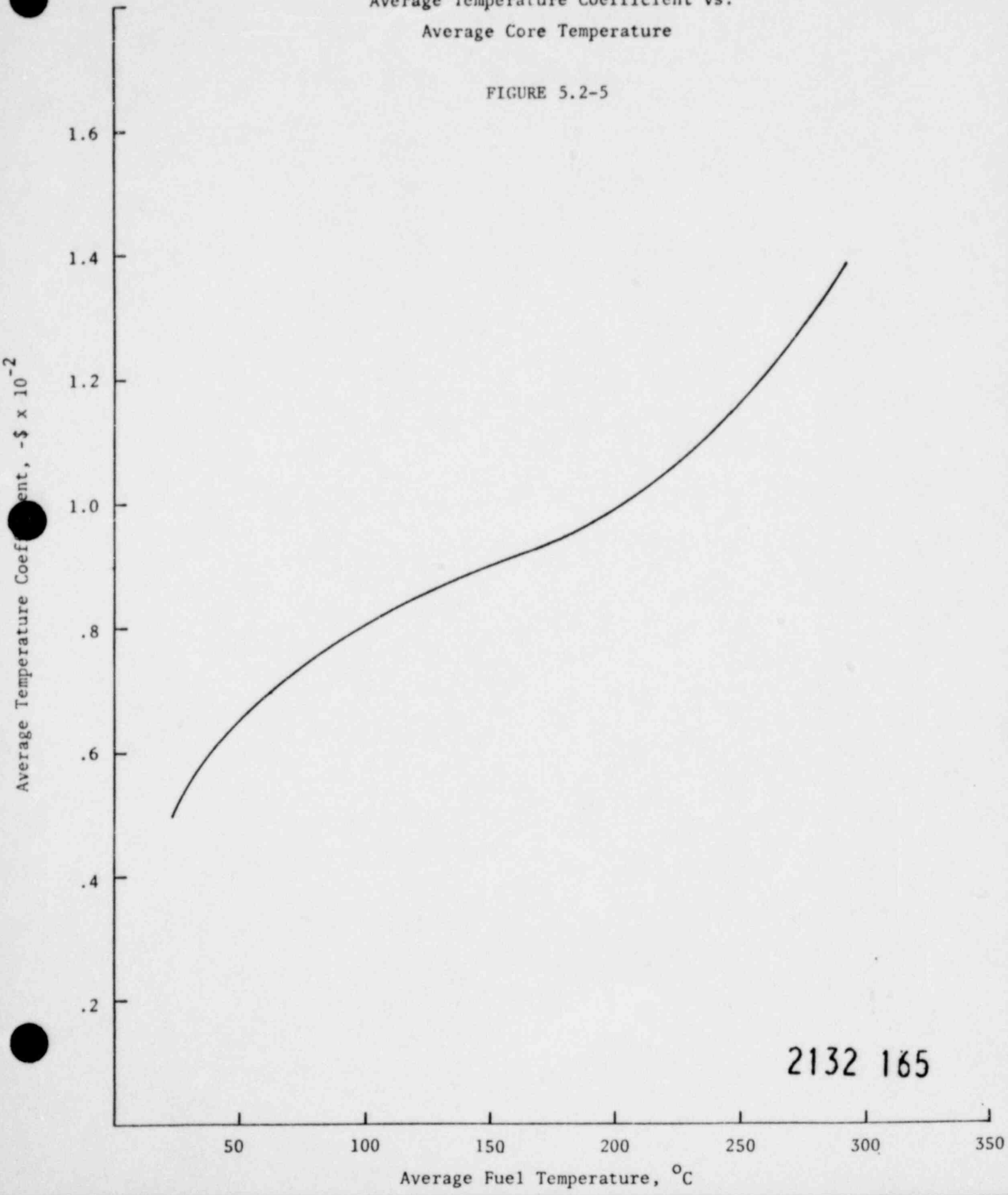

failure of two of the thermocouples. This type of failure is common in TRIGA reactors and the only solution is replacement. An increase in the number of FLIP fuel rods in the core is also planned to lengthen the core life. The performance and safety considerations for mixed cores with more FLIP fuel than that of the current core was previously considered in the original S.A.R. for conversion to FLIP fuel. The information is contained in Appendix A of this revised S.A.R.

5.3 Pulsing Characteristics

Pulsing tests for core 30-A began on February 23, 1976, starting with a $1.25 insertion and increasing up to the license limit of $2.50 in $.25 increments. The results of this initial series of pulses is shown in Table 5.3-1 below. The measured peak power and energy released in a

TABLE 5.3-1

Core 30-A Pulse Testing Data

ρ, $	No. of Pulses	Avg. Peak Fuel Temp., °C	Avg. Peak Power, Mw
1.10	2	235.5	7.11
1.15	1	248	16.59
1.25	3	271.7	60.0
1.50	6	309.3	155.3
1.75	4	333.8	304.8
2.00	3	367.3	622.3
2.25	3	403	1197.3
2.50	11	442.4	1850.5

pulse versus the reactivity insertion for core 30-A is shown in Figure 5.3-1. The peak indicated fuel temperature in core 30-A versus the reactivity insertion is shown in Figure 5.3-2. The measured pulsing

Peak Power and Energy

Release vs. Reactivity Insertion

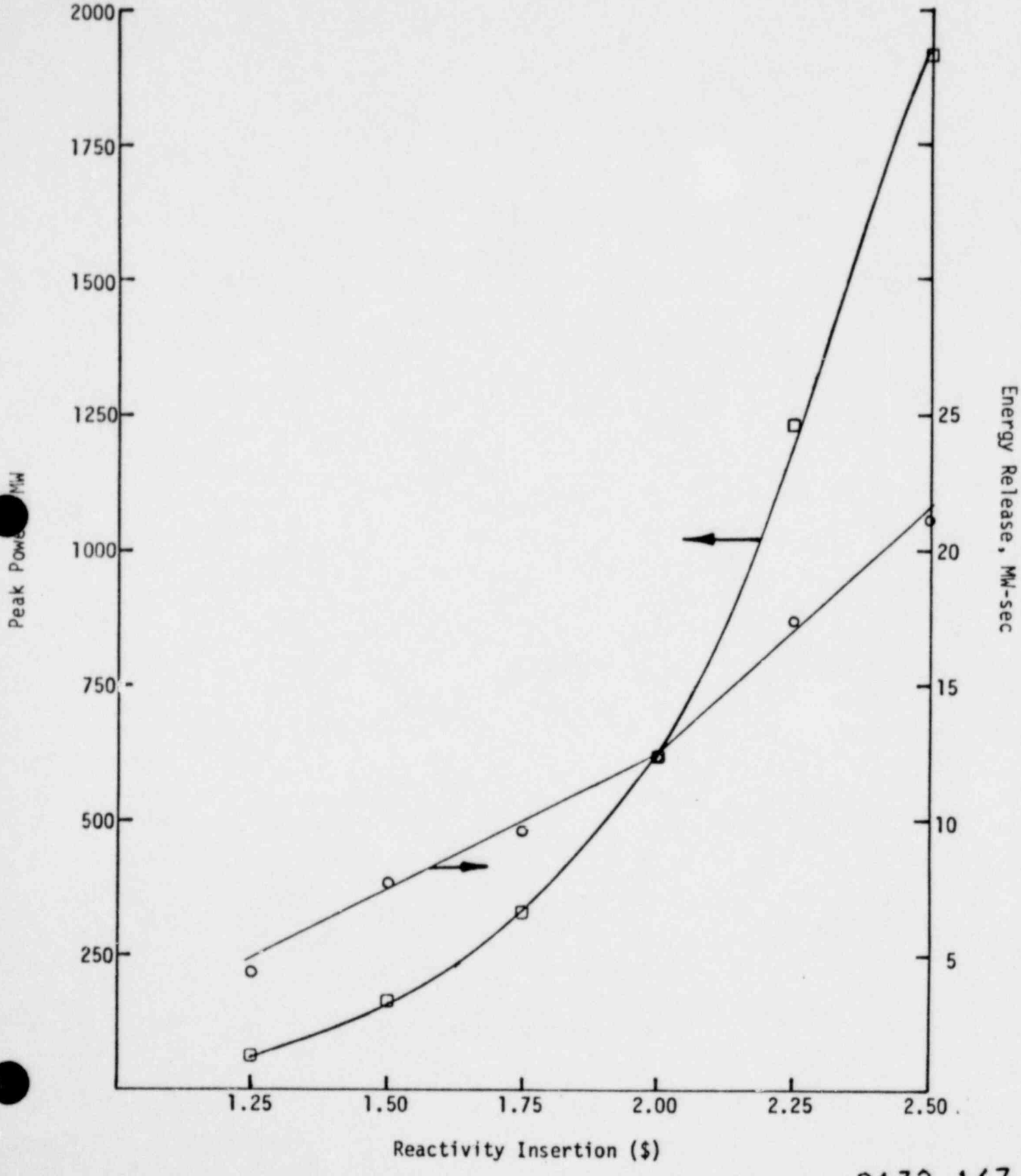

FIGURE 5.3-1

Peak Indicated Fuel Temp vs. ρ

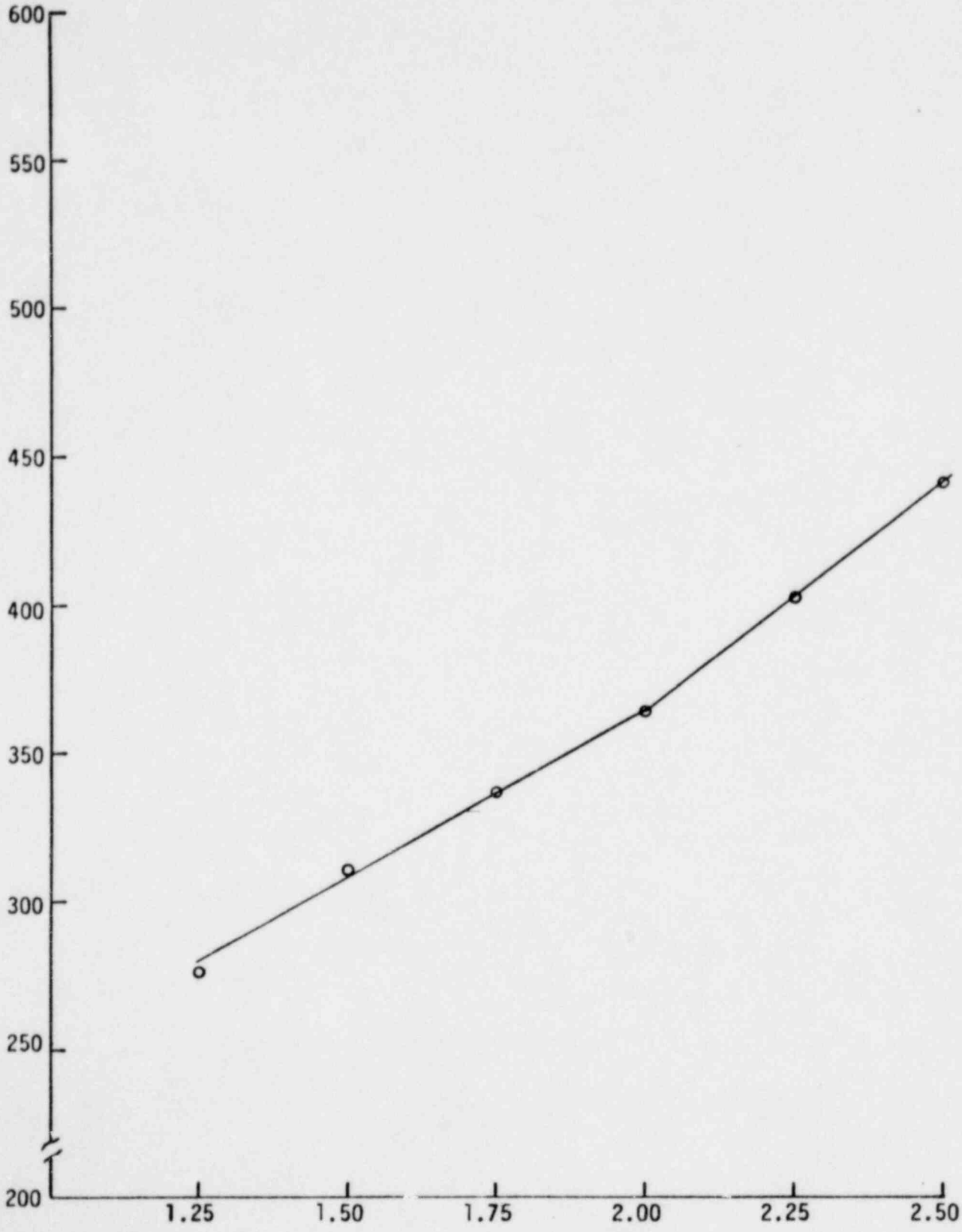

FIGURE 5.3-2

characteristics of the W.S.U. TRIGA reactor fueled with a mixed core of Standard and FLIP fuels were as expected. No significant pulsing performance changes have been observed to date.

In September of 1976 a fuel problem developed in the FLIP fuel region of a mixed core fueled TRIGA reactor similar to the W.S.U. reactor. The reactor involved was being pulsed with insertions up to $2.70. At the request of the Commission, the FLIP fuel in the central portion of the W.S.U. reactor was inspected but no damage was discovered. At the time of the inspection the W.S.U. reactor had been pulsed 55 times at a maximum insertion of $2.50. The current number of pulses on core 30-A is 141. A detailed comparison of the two reactors revealed the fact that the water gap between the transient rod guide tube and the adjacent fuel rods varied from .050 to .0204 in the reactor with the damaged fuel whereas it is a constant .0825 inches in the W.S.U. reactor. Thus the fuel damage problem is due in part to water-gap peaking effects not present in the W.S.U. reactor. Additional information is contained in the report of December 6, 1976 filed with the Commission on this subject.

6.0 SAFETY ANALYSIS

6.1 General Considerations

The safety related aspects of the operation of the W.S.U. Modified TRIGA reactor will be considered in this section. First we will examine the fundamental characteristics and operational parameters of a TRIGA-type reactor as they relate to safety. Then we will examine the consequences of a number of postulated accidents.

6.2 Design Bases

The primary design criteria for the Washington State University TRIGA reactor are determined by the maximum safe operational capabilities of the solid-fuel moderator elements used to fuel the W.S.U. modified TRIGA reactor and the core configuration described in this report. The combination of fuel and core configuration must be selected to provide a high degree of operational safety independent of mechanical, electrical, or human errors. To attain this, the following characteristics and properties must be inherent in the reactor system.

a. Large prompt negative temperature coefficient of sufficient magnitude to control the effects of a sudden large insertion of positive reactivity.

b. Metallurgical properties of the fuel-moderator alloy that would insure integrity of the fuel-moderator alloy during either a sudden increase in temperature or prolonged periods of operation at high temperatures.

c. A suitable cladding that would contain the fuel-moderator material and associated fission products under all operating conditions. Cladding integrity must be maintained under the expected thermal and mechanical stresses and strains resulting from sudden increases in temperature and prolonged periods of operation at high temperature.

d. A core configuration that is slightly undermoderated to provide a negative void coefficient and to insure safety in case of a loss-of-water accident.

6.3 Design Limits

A considerable amount of theoretical analysis has been performed and a large amount of operational experience has been accumulated on TRIGA-type reactors over the past decade. This accumulation of knowledge and experience has led to the establishment of certain design limits for TRIGA-type reactors. These limits may be categorized as (1) shutdown margin limit, (2) reactivity addition rate limit, (3) fuel operating temperature limit, (4) operating power limit, (5) reactivity addition limit during pulsing, and (6) Fuel dimensional variation limit.

6.3.1 Shutdown Margin

The aggregate worth of the control elements of a reactor must be set so that a safe shutdown margin is obtained with the highest worth control element fully withdrawn from the core. This requirement insures that the reactor remains subcritical during core changes with one control element withdrawn. The total control element worth necessary is obviously determined by the excess reactivity available and the worth of

the individual control elements. The safe shutdown margin for TRIGA reactors has been set at 0.2% ΔK/K or about $.25. The highest worth control element in most TRIGA reactors is the pulse rod which generally has a maximum worth limit of $4.00 as determined by pulsing considerations. Accordingly in normal operation a TRIGA reactor is shut down by $4.25 with all the control elements inserted.

6.3.2 Reactivity Addition Rate

The reactivity addition rate to a reactor during normal operation is a function of the worth of the control elements, the speed of element withdrawal, and the number of elements being withdrawn at one time. In a TRIGA reactor the control system is generally designed to allow the withdrawal of only one element at a time. Thus the maximum reactivity addition rate is equal to the product of the maximum differential worth of the most reactive element in dollars per inch times the element speed in inches per second.

In practice the maximum reactivity insertion rate is set at a level where an operator can retain control of power changes during steady-state operation. No limit is set on the transient rod during pulsing as the transient rod must be removed in a very short time to prevent clipping of the power transient resulting from the pulse. The normal reactivity insertion rate limit that has been set for TRIGA reactors is about 0.2% ΔK/K per second or $.25 per second.

6.3.3 Fuel Operating Temperature

The thermal limit for the fuel used in the W.S.U. TRIGA reactor is based on the combined characteristics of the fuel-moderator alloy and the associated cladding material. The limit depends upon the metallurgical properties of the fuel-moderator alloy, the pressure of the gases in the cladding gap, and the yield stress of the cladding (see page 63 of Appendix A).

For TRIGA reactors using high hydride fuel it is a well established and documented fact that the limiting factor is the pressure buildup from out-gassing of hydrogen from the uranium-zirconium hydride fuel-moderator alloy. TRIGA fuel with a hydrogen-to-zirconium ratio of 1.6 as used in the W.S.U. TRIGA reactor is single phase for temperatures in excess of 1150°C. The fuel-moderator alloy actually melts at about 1800°C. Furthermore, the higher hydride fuels do not undergo any significant thermal diffusion of hydrogen. These two facts and the intensive testing of the fuel-moderator alloy by the manufacturer plus extensive in-core experience clearly demonstrate that the fuel-moderator alloy characteristics would allow safe operating temperatures up to at least 1150°C.

The currently accepted limiting fuel temperatures for high hydride type TRIGA fuels are 1150°C for FLIP fuel and 1100°C for Standard fuel. It is customary to employ a 200°C safety margin to yield a limiting condition of operation of 950°C in FLIP fuel and 800°C in Standard fuel.

The cladding material for the W.S.U. TRIGA reactor fuel is type 304 stainless steel with a thickness of 20 mils. It is a well known and documented fact (see Page 57 of Appendix A) that the tensile and yield strength of this cladding material is not significantly reduced up to a temperature of 850°C. The analysis contained on Page 55 to 65 of Appendix A of this S.A.R. establishes the fact that the ultimate strength of the 304 stainless steel cladding for TRIGA (H-Zr 1.6) fuel is 940°C. This cladding temperature is the limiting condition for a Loss of Coolant accident.

6.3.4 Operating Power

The limitation on the maximum steady-state power level of a TRIGA-type reactor is determined by the ability of the cooling system to remove heat at a rate to assure that the fuel cladding temperature is held well below the safety limit during normal steady state operation. A limitation on the maximum power level is also imposed by the decay heat of fission products if an accident occurs in which all or part of the cooling water is lost. Sufficient cooling must be provided under this circumstance to insure integrity of the cladding. These considerations are analyzed in Appendix A of this section.

It is a well established fact that a TRIGA reactor can safely operate at a steady state power level of one megawatt with natural convection cooling if the pool cooling system is designed to remove the heat produced and to limit the

core cooling water outlet temperature to below 100°C. At power levels significantly above one megawatt, forced cooling systems are needed during steady state operation and an emergency spray cooling system for cooling in case of a loss of core cooling water. The W.S.U. TRIGA reactor utilizes natural convection cooling and is thus limited to a steady state power level of one megawatt.

6.3.5 Reactivity Addition During Pulsing

During a transient, the limiting factor, as with steady state operation, is the fuel-moderator alloy temperature and the corresponding hydrogen pressure beyond which a cladding rupture may occur. Thus the limiting temperatures are 1150°C for FLIP fuel and 1000°C for Standard fuel for pulsing. Applying the 200°C safety margin, the limiting conditions for pulsing operation become 950°C in the FLIP fuel and 800°C in the Standard fuel.

The peak fuel temperature in the core during a pulse is given by:

$$TP(max) = (T(ave) + \Delta TP) \times P/A \qquad (6.3.5\text{-}1)$$

where TP(max) = Peak Core Temperature, °C

T(ave) = Average Core Temperature before pulsing, °C

ΔTP = Average Core Temperature increase during pulse, °C

P/A = Peak to Average Temperature Ratio.

The average core temperature increase may be calculated using the Fuchs-Nordeim model equation given in Section 4.4 of Appendix A. Equation 6.3.5-1 and the Fuchs-Nordeim model

equation contain a number of parameters that are very core specific. Thus a universal pulsing limit for all TRIGA reactors can not be set. The pulsing response of a typical 110 rod TRIGA reactor is tabulated in Table 6.3.5-1 for the specified parameters.

Detailed calculations for the W.S.U. TRIGA reactor as fueled with a mixture of Standard and FLIP fuels are given in Appendix A. This analysis established a conservative pulsing limit of $2.50 for the W.S.U. modified TRIGA reactor. In addition, the S.A.R. for the conversion of the Texas A&M TRIGA reactor to TRIGA fuel established the fact that in a mixed core during pulsing for a given reactivity insertion, the average increase in core temperature decreases as the fraction of FLIP in the core increases.

TABLE 6.3.5-1

Typical 110-Rod TRIGA Core Pulsing Response

Reactivity $	Temp. Coeff. -$/°C	Lifetime Microseconds	ΔT, °C
1.5	.012	20	81
2.0	.012	20	160
2.5	.012	20	236
1.5	.014	34	70
2.0	.014	34	138
2.5	.014	34	203

6.3.6 TRIGA Fuel Rod Inspection

The rapid increase in power and the resultant increase in fuel temperature in a TRIGA reactor during pulsing subjects the fuel rod cladding to stress and to thermal cycling effects. In order to insure that the fuel rod cladding integrity has not been significantly deteriorated, it is customary to inspect the fuel rods periodically. This inspection at some specified interval of time involves checking the transverse bending and elongation of TRIGA fuel rods.

In order to inspect the fuel rods, they must be removed from the reactor core and placed in a jig or fixture in the reactor pool. This operation involves a considerable amount of manipulation of the fuel rods using underwater handling tools. During the manipulation there is a possibility that physical damage to the fuel rod may result from mishandling. A few fuel rods have even been dropped during such operations at some facilities. While it is important that adequate inspection frequency be maintained to guard against possible pulsing induced damage, it is also important to minimize the number of inspections in order to reduce the possibility of physical damage to the fuel rods.

The strain produced during the pulsing transient results from the stress of internal pressure in the heated rod and the differential expansion of the fuel-moderator rod and cladding. The increased pressure results from the increased temperature of the air in the cladding gap, the fission products released from the fuel, and the hydrogen released from the partial dissociation of the zirconium hydride. Actual measurements

made by General Atomic on specially instrumented fuel rods during pulsing reveal equilibrium pulsing pressure increase to be only about 20 psia (22).

A .25-inch gap is provided in a TRIGA fuel rod between the lateral end of the graphite reflector and the end piece welded onto the cladding. This gap reduces to about half this value (23) at a fuel rod temperature of 1200°C and a cladding temperature of 200°C. Because of this gap, differential expansion during pulsing will not produce a significant amount of lateral strain on the fuel rod cladding.

The predominant and most significant effect that pulsing has on the cladding is that of radial differential expansion in new, unpulsed rods. Near the middle region of the fuel rod the uranium-zirconium hydride is in close contact with the stainless steel cladding. The effects of differential expansion between the fuel rod and the cladding is greatest in the middle region. Assuming a temperature of 1200°C for the fuel-moderator rods and 200°C for the cladding, the amount of strain is equal to the fractional increase in the cladding circumference due to the fuel rod expansion and is calculated as follows:

1. Change in circumference of cladding due to increase in temperature above nominal 25°C

   ΔC_c = Circumference x Linear Coefficient of Expansion x Temperature Change = $1.41 \times \pi \times 17 \times 10^{-6} (200 - 25)$ = .0132 in.

2. Increased area of fuel rod due to increase in temperature above nominal 25°C

A_t = Area (1 + 2 x Linear Coefficient of Expansion x Temperature Change)

$$A_t = \left(\frac{1.36}{2}\right) \times \pi[(1 + 2 \times 10^{-6}) \times (1200 - 25)]$$

$$A_t = 1.452672 \times 1.01645 = 1.476569 \text{ in.}^2$$

3. Increase in circumference of fuel-moderator rod

$$\Delta C_r = \pi(D_r - D_c) = 2\pi(r_r - r_c) = 2\pi\left[\left(\frac{A_t}{\quad}\right)^{1/2} - \frac{1.36}{2}\right]$$

$$\Delta C_r = 2 \quad (.68577 - .6800) = .0350 \text{ in.}$$

4. Difference between circumference of heated cladding and heated fuel rod = strain

$$\Delta C_r - C_c = .0350 - .0132 = .0218 \text{ in.}$$

5. Radial strain on cladding due to differential radial thermal expansion

$$\text{Strain} = \text{Fractional Deformation} = \frac{\text{Increase in Cladding Circumference}}{\text{Cladding Circumference}}$$

Strain = .0218/1.41π = .0049 or about .5% strain.

The above amount of strain would cause some permanent deformation in the cladding but is well within the safety limit for the expansion of type 304 stainless steel. The fact that some permanent deformation is produced is substantiated by the fact that the heat transfer between the fuel-moderator rod and the cladding of a TRIGA fuel rod decreases in new fuel after pulsing. In other words, the time required for new instrumented TRIGA fuel rods to cool down from a given temperature to ambient increases

after pulsing. This factor is indicative of an increase in the space between the fuel rod and the cladding due to permanent stretching of the cladding by pulsing.

The amount of strain produced during extended pulsing will in actual fact be significantly lower than that calculated above. The permanent deformation of the cladding will obviously reduce the value of the strain. The actual fuel rod temperature will be below that assumed in the calculation and will not exceed 750°C. Furthermore, during pulsing, film boiling causes an increase in the fuel cladding temperature above the steady-state case. All of these factors will decrease the magnitude of the strain so that the value calculated above is very conservative.

Studies made for N.A.S.A. (24) on low-cycle fatigue indicate that the cladding could receive over 7,000 cycles of the postulated strain previous to the appearance of cracks that could allow fission product gases to escape. This value was obtained by the following consideration

$$N = (K/S_p)^2 = (.69/\frac{.0049}{2})^2 = 79,307$$

where N = number of cycles previous to fracture

S_p = the plastic strain (less than one-half of the total strain on the cladding)

K = a measured constant for a given material which is related to the fracture directly (for type 304 stainless steel, K has been measured to be .69).

Cracks may start to appear at about 10% of the cycles at which fracture occurs. Applying the 10% factor to the above calculation, a conservative estimate of 7,000 cycles of pulsing will occur before the onset of possible cracking that could cause a fission product leak.

The pulsing limit for the W.S.U. TRIGA reactor fueled with a mixed core is $2.50. If the core was pulsed 7,000 times with the maximum allowable pulse, this limit would amount to a total of $17,500 worth of pulses. As a prudent rule one could set an inspection frequency at 20% of the expected pulsing life or a total of $3,500 worth of $2.50 pulses. This inspection frequency limit is established for the W.S.U. TRIGA reactor.

In actual operation a variety of sizes of pulses up to the maximum allowable value are shot. Only those pulses above $1.50 will produce a fuel temperature higher than that attained during normal steady-state operation. Thus in making the tabulation for fuel rod inspection, only those pulses over $1.50 should be summed for inspection purposes.

6.4 Accident Analysis

6.4.1 Mixed Core Operation

A detailed analysis of the safety aspects of the W.S.U. Modified TRIGA reactor fueled with a mixture of Standard and FLIP fuels is given in Appendix A. This document establishes the following limiting conditions of operation:

(1) Maximum FLIP fuel temperature of 950°C

(2) Maximum Standard fuel temperature of 800°C

(3) Maximum reactivity insertion of $2.50

(4) LSSS of 500°C for fuel temperature scram

(5) Maximum allowable power density of 23.5 Kw/rod for FLIP and 22.3 Kw/rod for Standard fuels.

The analysis also demonstrates that no realistic hazard to the general public would result from the Design Base Accident, a Loss of Coolant Accident, the accidental addition of one 4-rod cluster, or the accidental ejection of the transient rod at full power.

6.4.2 Argon-41 Releases

Section 6.5 of the S.A.R. for the conversion of the W.S.U. TRIGA reactor to FLIP fuel as given in Appendix A of this report substantiates a 3×10^{-4} dilution factor for Argon-41 release due to the atmospheric wake effect in the lee of the building. A more thorough analysis of the distribution of Ar-41 in the atmosphere about the site may be obtained by the use of equation F-1 of Appendix F of Regulatory Guide 1.109, "Calculation Reactor Effluents for the Purposes of Compliance with 10 CFR Part 50, Appendix I."

The annual release of Ar-41 from the W.S.U. facility for the past five years has averaged 10 Ci/year. Thus the daily release is .027 Ci/day which is equivalent to a release rate of 3.17×10^{-7} Ci/sec. However, for the purposes of our calculations we shall assume a 100 Ci/year

release and a 3.17×10^{-6} Ci/sec release rate. Using a 100 Ci/year total release, the wind distribution data of Figure 2.4-2, and Equation (F-1), the Ar-41 concentration in the atmosphere about the site may be calculated. The results are shown in Figure 6.4-1 in terms of the % of the 10 CFR 20 limit of 4×10^{-8} $\mu Ci/cm^3$. The ground level Ar-41 concentration levels about the site for a 1000% normal release rate are significantly below the 10 CFR 20 limit as well as the ALARA criteria of 2% of the 10 CFR 20 limit. The closest occupied location to the site is 411 meters west and thus would be exposed to a 2.2×10^{-11} $\mu Ci/cm^3$ annual average Ar-41 concentration for the postulated release. Accordingly the Ar-41 released to the atmosphere by the operation of the W.S.U. TRIGA reactor does not endanger the health and safety of the general public.

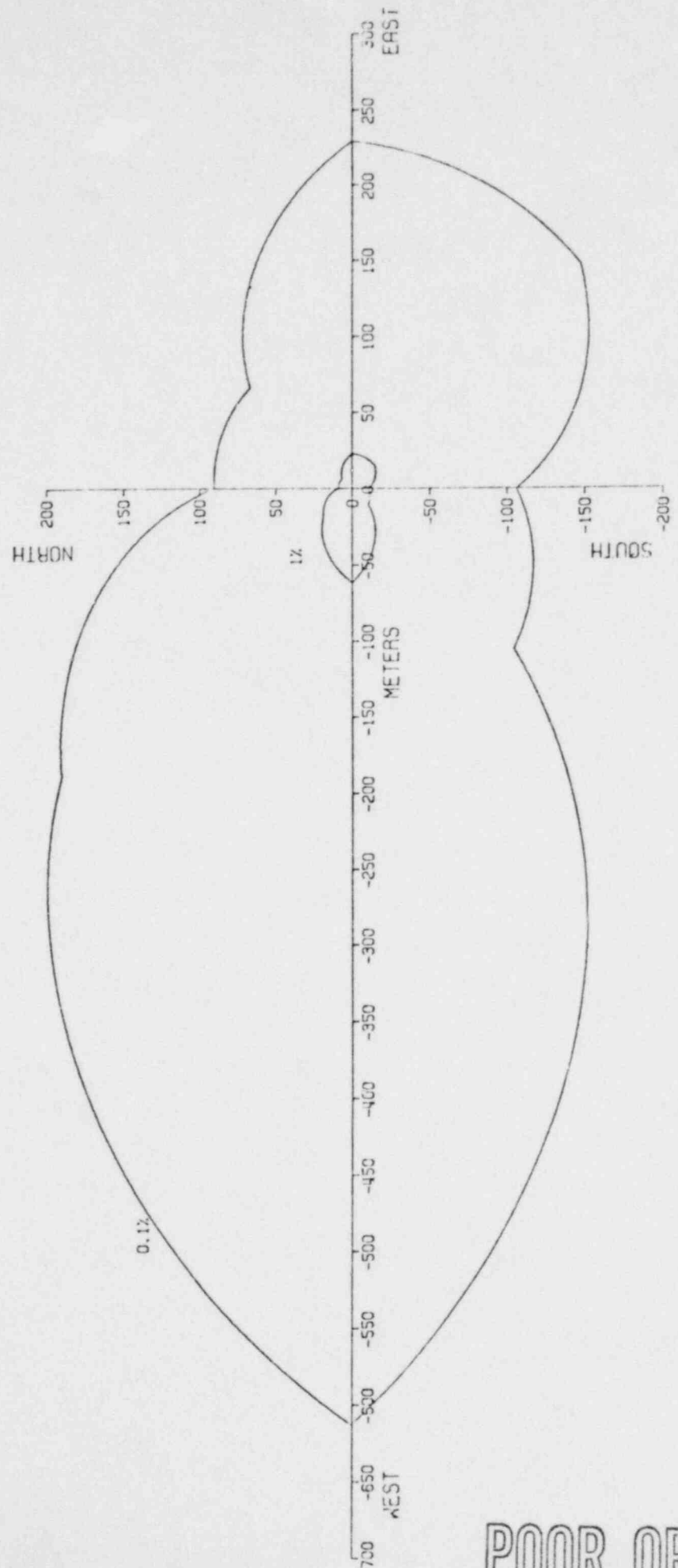

ANNUAL AVERAGE ARGON-41 CONCENTRATION DISTRIBUTION IN ATMOSPHERE ABOUT SITE IN % OF 10-CFR-20 LIMITS, ASSUMING A 100 CURIE/YEAR TOTAL RELEASE.

Figure 6.4-1

7.0 REFERENCES

1) E. G. Holzman, "Safeguard Report for Open Pool Reactor for State College of Washington," General Electric Company Report GEAP-3100, February 1959.

2) H. Stern and H. W. Dodgen, "Safety Analysis for the Washington State University Reactor Core Conversion and Power Increase," Washington State University, October 1966.

3) General Atomic Staff, "TRIGA MARK III Reactor Hazards Analysis," General Atomic Report GA-3886, February 1965.

4) Gulf General Atomic Staff, "Safety Analysis Report for the Torrey Pines TRIGA Mark III Reactor," Gulf General Atomic Report GA-9064, January 1970.

5) J. M. Batch, "Standard TRIGA 4-Rod Cluster Conversion Reactor Maintenance and Operating Manual for Washington State University," General Atomic Report GA-7677, February 1967.

6) R. J. Cashwell, "Safety Analysis Report for the University of Wisconsin Nuclear Reactor," University of Wisconsin, April 1973.

7) D. A. Swanson, "Geologic Map of the Columbia River Basalt in the Pullman and Walla Walla Quadrangles of Southwest Washington," U.S.G.S. Open File Report 77-100, 1977.

8) U.S.G.S. Staff, "The Channeled Scablands of Eastern Washington," U.S.G.S. Information booklet IF-72-2(R-1), 1972.

9) Bates McKee, Cascadia: The Geologic Evolution of the Pacific Northwest, McGraw-Hill Book Company, New York, 1972.

10) N. Rasmussen, "Washington State Earthquakes 1840 through 1965," Bull. Seism. Soc. Am., 57 (1967), pp. 463-476.

11) N. Rasmussen, Unpublished Additions to Washington State Earthquake List, June 1965 to 1979.

12) R. C. Newcomb, "Tectonic Structure of the Main Part of Basalt of the Columbia River Group, Washington, Oregon and Idaho," Miscellaneous Investigations Map I-587, 1:500,000, U.S. Geological Survey, 1970.

13) J. W. Crosly and R. M. Chatters, "Water Dating Techniques as Applied to the Pullman-Moscow Ground-Water Basin," W.S.U. Bulletin 296, 1965.

14) W. A. Goodwin and M. E. Wyman, "The Measurement of Radial Power Distributions in TRIGA Fuel Elements During Reactor Power Excursions," Nuc. App. & Tech., V. 18, March 1970.

15) W. E. Wilson and T. A. Lovas, "Washington State University Conversion to Mixed Core and Test Program," Report to N.R.C., April 1976.

7.0 REFERENCES (Cont.)

16) V. Ichimura, "Uranium Concentrations in Ground Waters of the Pullman-Moscow Basins," W.S.U. Dept. of Geology M.S. Thesis, 1979.

17) D. E. Feltz, "Amendment II to the Safety Analysis Report for the Texas A & M TRIGA Reactor," Texas A & M, Nov. 1972.

18) J. D. Randell, "Status Report on Damage to FLIP fuel During Operation of the NSCR at Texas A & M University," Report to the N.R.C., Nov. 1976.

19) W. E. Wilson, "Results of Inspection of W.S.U. TRIGA FLIP Fuel in Light of Texas A & M Fuel Damage," Report to N.R.C, Dec. 1976.

20) Gulf Atomic Staff, "Summary of TRIGA Fuel Fission Product Release Experiments," Gulf Atomic Report Gulf-EES-A10801, Sept. 1971.

21) W. E. Wilson, "Amendment I to Safety Analysis Report of October 1966 for the W.S.U. TRIGA Reactor," Report to the N.R.C., May 1974.

22) General Atomic Staff, " Safety Analysis Report for the Romania Annular Core Pulsing Reactor," General Atomic Report E-117-323, Vol. III.

23) G. Beck, "Safety Analysis Report for the Illinois Advanced TRIGA Reactor," University of Illinois, August 1967.

24) R. W. Smith, "Fatigue Behavior of Materials Under Strain Cycling in Low and Intermediate Life Range," NASA TN O-1574, April 1963.

WASHINGTON STATE UNIVERSITY
NUCLEAR RADIATION CENTER
Pullman, Washington 99164

SAFETY ANALYSIS FOR CONVERSION

TO FLIP FUEL

May 1979

TABLE OF CONTENTS

TABLE OF CONTENTS
(continued)

1.0 INTRODUCTION

This report considers the safety aspects of the operation of the W.S.U. modified TRIGA reactor with cores containing a mixture of standard and FLIP fuels. This document was orginally submitted in May of 1974 to the Commission as "Amendment I to the Safety Analysis Report of October 1966." The S.A.R. of 1966 is now replaced and superseded by the S.A.R. of May 1979 submitted to the Commission in application for the renewal of facility license R-76. This report now becomes "Appendix A" to the S.A.R. of May 1979 and constitutes the Safety Analysis for the use of FLIP fuel in the W.S.U. reactor.

2.0 CONTENT OF REPORT

This report only considers FLIP fuel related safety aspects of the operation of the W.S.U. TRIGA reactor. All other items are covered in the S.A.R. to which this report is an appendix. The specific items considered are:

1. Fuel Description and Safety Limits
2. Calculation Methods
3. General Safety Analysis
4. Design Base Accident
5. Reactivity Effect of Accidental Fuel Addition
6. Reactivity Effects of Transient Rod Ejection (Pulsing Limits)
7. Loss of Pool Water Accident

Each of these items will be considered in detail in the following sections of this report.

3.0 FUEL DESCRIPTION AND SAFETY LIMITS

The fuel in the mixed core will be both standard TRIGA and FLIP fuel elements. The two types of elements are identical in construction and differs

only in U-235 enrichment, burnable poison content, and hydrogen-to-zirconium ratio. The dimensional and physical description data on the fuel is contained in the revised SAR of May 1979. It is possible to visually distinguish the element types, however, by the markings on the upper tip of the FLIP fuel. Table I lists the principal design parameters of both FLIP and standard TRIGA elements.

The safety limitations on the fuel are those limiting values imposed to preclude a loss of fuel element integrity. During a reactivity excursion the limiting condition is fuel temperature and the corresponding hydrogen overpressures at which clad rupture may occur. Studies show that in FLIP fuel the hydrogen pressure which would result from a transient for which the peak fuel temperature is 1150°C* would not produce a stress in the clad in excess of the ultimate strength.(1) TRIGA fuel with a hydrogen-to-zirconium ratio of at least 1.65 has been pulsed to temperatures of about 1150° without any damage to the clad.(2) As a safety limit, the peak adiabatic fuel temperature to be allowed during transient conditions is set at 1150°C for FLIP fuel. Since standard TRIGA fuel nominally contains more hydrogen than FLIP fuel, its corresponding safety limit is reduced to 1000°C. For steady state operation (non-adiabatic case) fuel temperatures are dependent upon the heat transfer characteristics of the element and coolant; thus, an experimental limit on power density is selected to insure fuel integrity. This limit is well below the maximum allowable power density which corresponds to a heat flux value at which there is a departure from nucleat boiling. The maximum stady-state power density generated in the Torrey Pines TRIGA MARK III is 32 kw per element. (1,3) Since the WSU TRIGA pool depth is somewhat deeper than the Mark III, improved cooling characteristics are expected. Thus, for steady state operation at power densities of up to 32 kw

*See Appendix D

TABLE I

STANDARD AND FLIP FUEL PARAMETERS

Fuel Element Type	FLIP	STANDARD
Fuel-moderator material	$U\text{-}ZrH_{1.6}$	$U\text{-}ZrH_{1.7}$
Uranium content	8.5 wt%	8.5 wt%
U-235 enrichment	70%	20%
U-235 content (avg) per element	123 g	35 g
Burnable poison	natural erbium	none
Erbium content	1.5 wt%	--
Shape	cylindrical	cylindrical
Length of fuel meat	15 in.	15 in.
Diameter of fuel meat	1.371 in.	1.371 in.
Cladding material	Type 304 SS	Type 304 SS
Cladding thickness	0.020 in.	0.020 in.

per element, no cooling problems are expected. As will be seen later on, the loss of coolant accident imposes a more restrictive limitation on the maximum safe allowable power density per element.

4.0 CALCULATIONAL METHODS

4.1 Core Calculations

The calculations of the characteristics of the WSU TRIGA reactor core with standard fuel, and mixtures of FLIP and standard fuel were performed using the EXTERMINATOR-2 code[4] and temperature dependent cross section data obtained from Gulf General Atomic. The fast cross section data were generated with the GGC-4 code[5] and the thermal cross section data using the SUMMIT and THERMIDOR codes.[6,7] Seven energy groups were used in the core calculations as well as group dependent buckling for the FLIP fuel as listed below. This group structure and energy dependent buckling is identical to that conventionally used by Gulf General Atomic in their TRIGA reactor calculations including the Puerto Rico FLIP fueled reactor calculations.

TABLE II

Energy Groups and Group Dependent Buckling Use in WSU TRIGA Core Calculations

Group		Standard Fuel Buckling	FLIP Fuel Buckling
1	15.0 - .694 MeV	0.0041	0.00546
2	639 - 9.12 keV	"	0.00435
3	9.12 - 0.001125 keV	"	0.00347
4	1.125 - 0.414 eV	"	0.000324
5	.414 - .14 eV	"	0.00469
6	.14 - .05 eV	"	-0.0146
7	.05 - .0002 eV	"	-0.0614

The results of calculations made with the EXTERMINATOR-2 on the existing core of the WSU TRIGA reactor compare favorably with measured values. Furthermore, calculations on the Puerto Rico FLIP core at WSU with the code yield results comparable to those obtained by Gulf General Atomic. Thus the calculations performed on all standard and all FLIP fueled cores are known to be accurate and reliable. Consequently, the results obtained on mixed cores can be expected to be reasonably accurate and reliable. Furthermore, Texas A&M has had good success in using this code for calculating the characteristics of mixed cores.[8]

4.2 Fuel Element Temperature

The direct theoretical calculation of accurate fuel element temperatures for steady-state operation in a TRIGA core using natural convection cooling is very difficult. This is due to the fact that the contact coefficient between the fuel and the cladding is not known accurately, especially in fuel rods that have been pulsed. In other words, the fuel-cladding thermal contact coefficient is a function of the fuel temperature and the pulsing history and age of the fuel. In addition, the film coefficient of heat transfer between the cladding and the coolant under conditions of natural convection is uncertain. The film coefficient is a function of the coolant temperature, coolant velocity, and effective hydraulic diameter of the coolant channel.

In order to circumvent these uncertainties, we have chosen to utilize experimentally measured fuel temperature data obtained from the instrumented fuel rod coupled with calculated power distribution

data obtained with the EXTERMINATOR-2 code. A graph of the maximum fuel temperature of the instrumented fuel rod as a function of reactor power in WSU TRIGA core No. 28A during steady-state operation is shown in Figure 1. Calculations with the EXTERMINATOR-2 code indicate that the axial average power density in the instrumented fuel rod is .283 watts per kw of reactor power per cm of core height. Combining this result with the experimental power-temperature data yields a relationship between axial average fuel rod power density and fuel rod temperature. This relationship as determined by least squares fitting of the data to a polynominal is given in Appendix A.

The fuel temperatures calculated using the derived equation are shown in terms of power density in Figure 2. The maximum observed power density used in deriving the fuel temperature equation was 12 kw/rod and thus a linear extrapolation is used above this value. A comparison of the curve in Figure 2 with experimental measurements at Texas A&M and PRNC which are also displayed on the graph substantiate the validity of the relationship. That is, fuel rod temperatures calculated by the WSU equation are essentially identical or more conservative than measured values.

Due to the large number of calculations involved and the number of core configurations studied, a special program, PLDEQC[9], was written to calculate and display the neutron flux, power, and temperature distributions. This program utilized the output group flux and power generation matrixes from EXTERMINATOR-2 to make these calculations. The temperature and power density data given in Section 5.0 of this report were generated by this method.

Figure 1

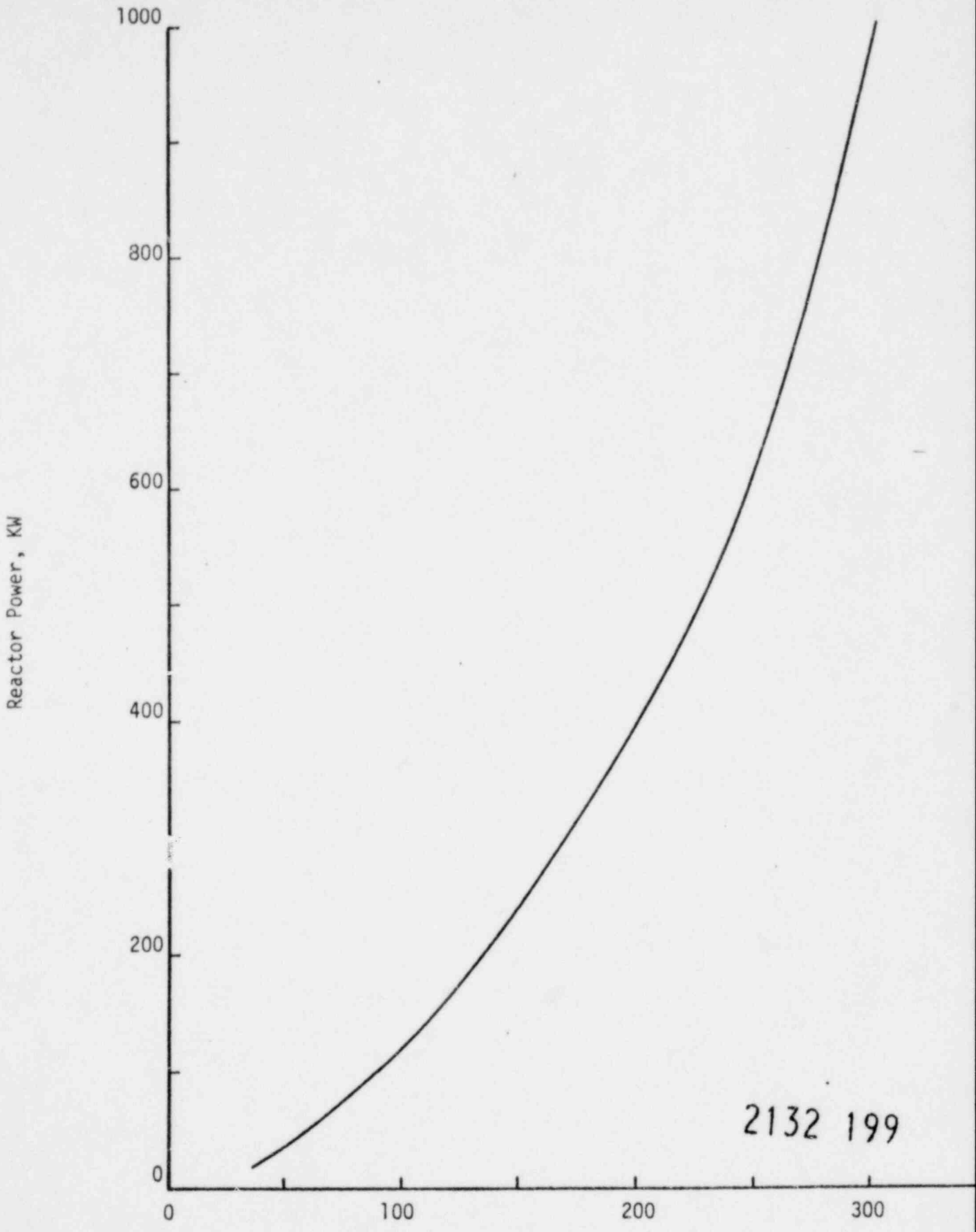

INSTRUMENTED FUEL ROD TEMPERATURE AS A FUNCTION OF REACTOR POWER

Figure 2

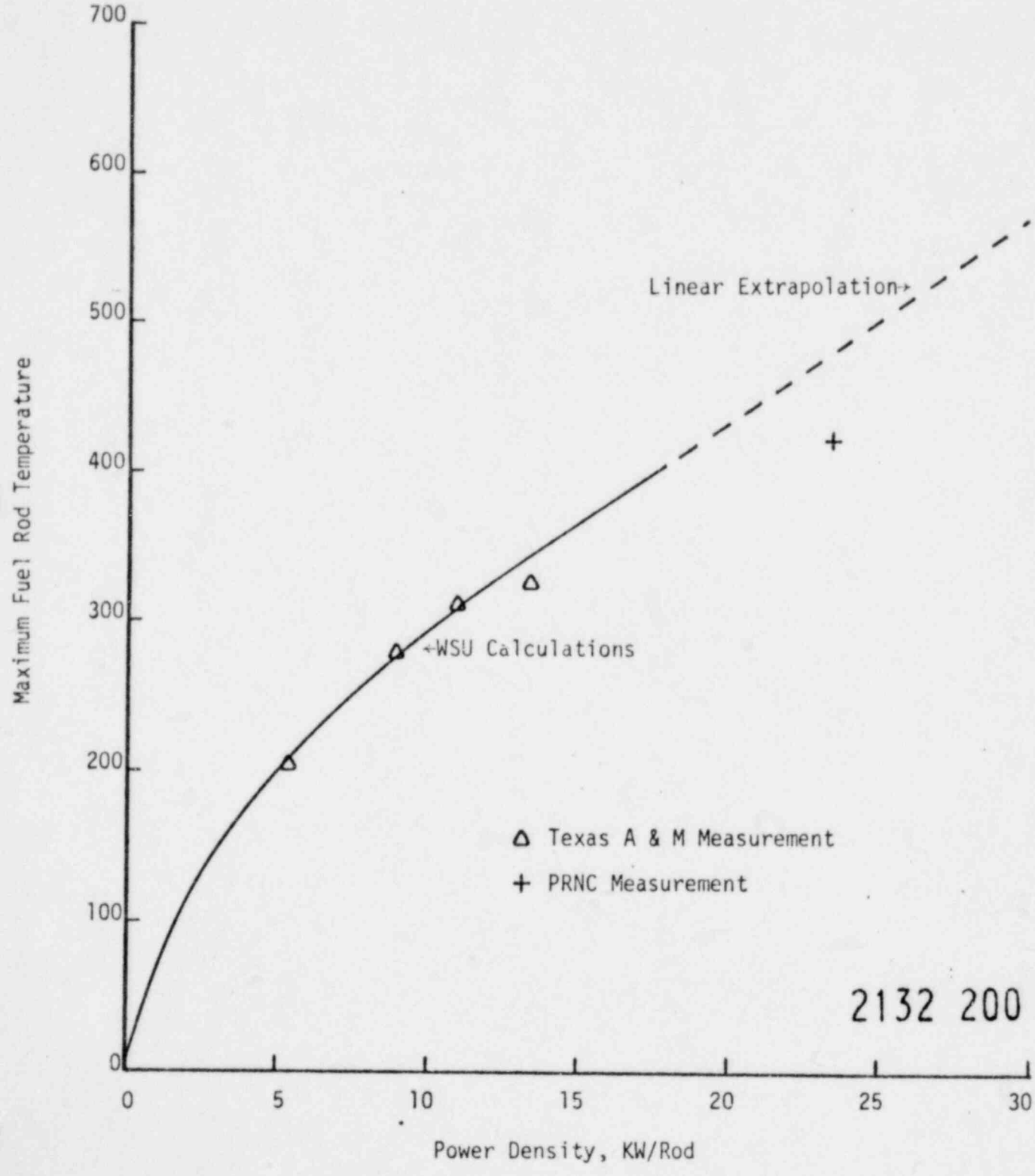

STEADY STATE FUEL ROD TEMPERATURE AS A FUNCTION OF POWER GENERATION

4.3 Prompt Negative Temperature Coefficient

Calculations of the prompt temperature coefficient of the WSU TRIGA reactor for all standard fueled cores were performed using the EXTERMINATOR-2 code and temperature dependent cross sections. The data thus obtained is plotted on the graph in Figure 3. The results thus obtained locally are essentially identical to those reported by Gulf General Atomic for similar type fuels. Experimental measurements of the overall temperature coefficient of WSU TRIGA core No. 28A at full power with all standard fuel yield a result of -$.014 per degree centigrade. The average fuel temperature for this core at 1 mw is 194°C which would give a theoretical value of -$.0147/°C for the temperature coefficient. Since it is a known fact that a TRIGA reactor has a slightly positive bath coefficient, the calculated and measured values agree as well as can be extected.

The direct calculation of a meaningful temperature coefficient for a mixed standard-FLIP fueled core with the EXTERMINATOR-2 code is not possible with the limited temperature dependent cross section data that was readily available. An alternate technique was adopted involving the summing of the appropriately weighted temperature coefficients of the standard and FLIP fueled regions of a mixed core (see Appendix B).

Accordingly, the mixed core prompt negative temperature coefficient is given by:

$$Tcm = Tcf(\overline{T}f) \times \frac{FF}{FT} + Tcs(\overline{T}s) \times \frac{FS}{FT}$$

where Tcm = Temperature coefficient of mixed core at mean core temperature

$Tcf(\overline{T}f)$ = Temperature coefficient of all FLIP core at temperature $\overline{T}f$

Figure 3

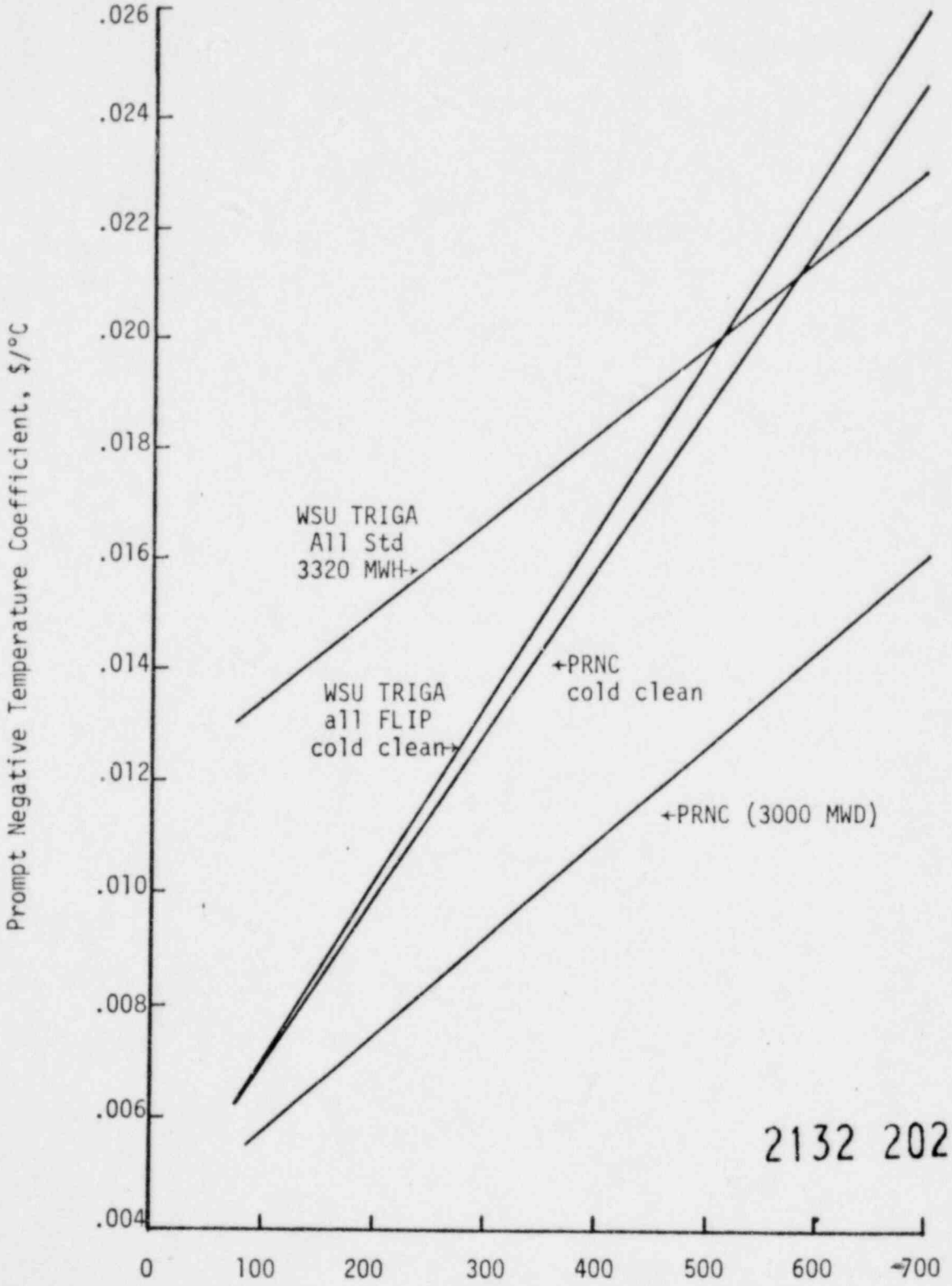

CALCULATED PROMPT NEGATIVE TEMPERATURE COEFFICIENT

$T_{cs}(\bar{T}_s)$ = Temperature coefficient of all-FLIP core at temperature $\bar{T}_s$

$\bar{T}_f$ = Mean temperature of FLIP fuel region

$\bar{T}_s$ = Mean temperature of standard fuel region

FF = Fissions in FLIP fuel region

FS = Fissions in standard fuel region

FT = Fissions in total core.

4.4. Pulsing Calculations

The peak power of a TRIGA reactor during a transient can be accurately described using a Fuchs-Nordheim model with variable heat capacity. Additional analysis of transient fuel rod temperatures by the group at the University of Illinois has shown that the values calculated by the model are conservative (high).[10] According to this model the peak reactor power during the transient, P(max), is given by

$$P(max) = P_o + \frac{C(\rho - 1)^2}{\alpha \ell} \left[\frac{1 + 3\sigma}{6\sigma}\right]$$

where $C = (C_o + \gamma T_o)N$ = Heat capacity of core at initiation of pulse

N = Number of rods in core

$\sigma = \alpha C / N(\rho - 1)$

C_o = Heat capacity of TRIGA fuel at 25°C = 769 wat-sec/°C/rod

T_o = Average initial temperature of the core above 25°C

ℓ = Prompt neutron lifetime of core

α = Prompt negative temperature coefficient

γ = Rate of change in heat capacity of TRIGA fuel = 1.47 wat-sec/°C/rod

ρ = Reactivity inserted.

In addition, the average peak core temperature, $\overline{T}_\infty$, is given by

$$\overline{T}_\infty = \frac{(\rho - 1)}{\alpha}\left[\frac{-3}{4}(\sigma - 1) + \frac{3}{4}\sqrt{(\sigma - 1)^2 + \frac{16\sigma}{3}}\right] + (To + 25).$$

The results of a series of calculations using the above two equations for a 100 rod and a 125 rod core and different values of the prompt negative temperature coefficient are given in Section 5.3 of this report.

5.0 GENERAL SAFETY ANALYSIS

5.1 Fuel Rod Temperature and Power Density

The limiting parameters which insure the safe operation of a TRIGA reactor are the maximum allowable fuel rod temperature and the maximum allowable fuel rod power density. These two parameters are interdependent and their limiting values were previously considered in Sections 3.0 and 4.2 of this report. The maximum allowable fuel rod temperature for FLIP fuel was found to be 1150°C and that for standard fuel found to be 1000°C. In order to provide a reasonable margin of safety during steady state operation, a safety margin of 200°C is established for the WSU TRIGA reactor. Thus, the limiting safety system settings would correspond to maximum temperatures of 950°C in the FLIP fuel and 800°C in the standard fuel. The limiting value of power density will be considered in Section 9.0.

A number of mixed cores were studied at WSU in order to establish their expected performance and characteristics. The current layout of the WSU TRIGA reactor core, core 29A, fueled with all standard fuel is shown in Figure 4. The maximum centerline fuel temperatures and rod power densities at a power level of one megawatt are shown in Figure 5 and Figure 6 respectively. A thermal neutron flux profile along the D row of this core is shown in Figure 7.

Starting with core 29A, six mixed cores of standard and FLIP fuel were studied by incremental replacement of standard fuel with FLIP fuel. The FLIP fuel was located in a contiguous block in the center region of the core. The maximum centerline fuel rod temperatures, rod power densities, and flux profiles along the indicated rows are shown in Figures

CORE ARRANGEMENT CORE NO. 29A : DATE AUGUST 13 , 1973

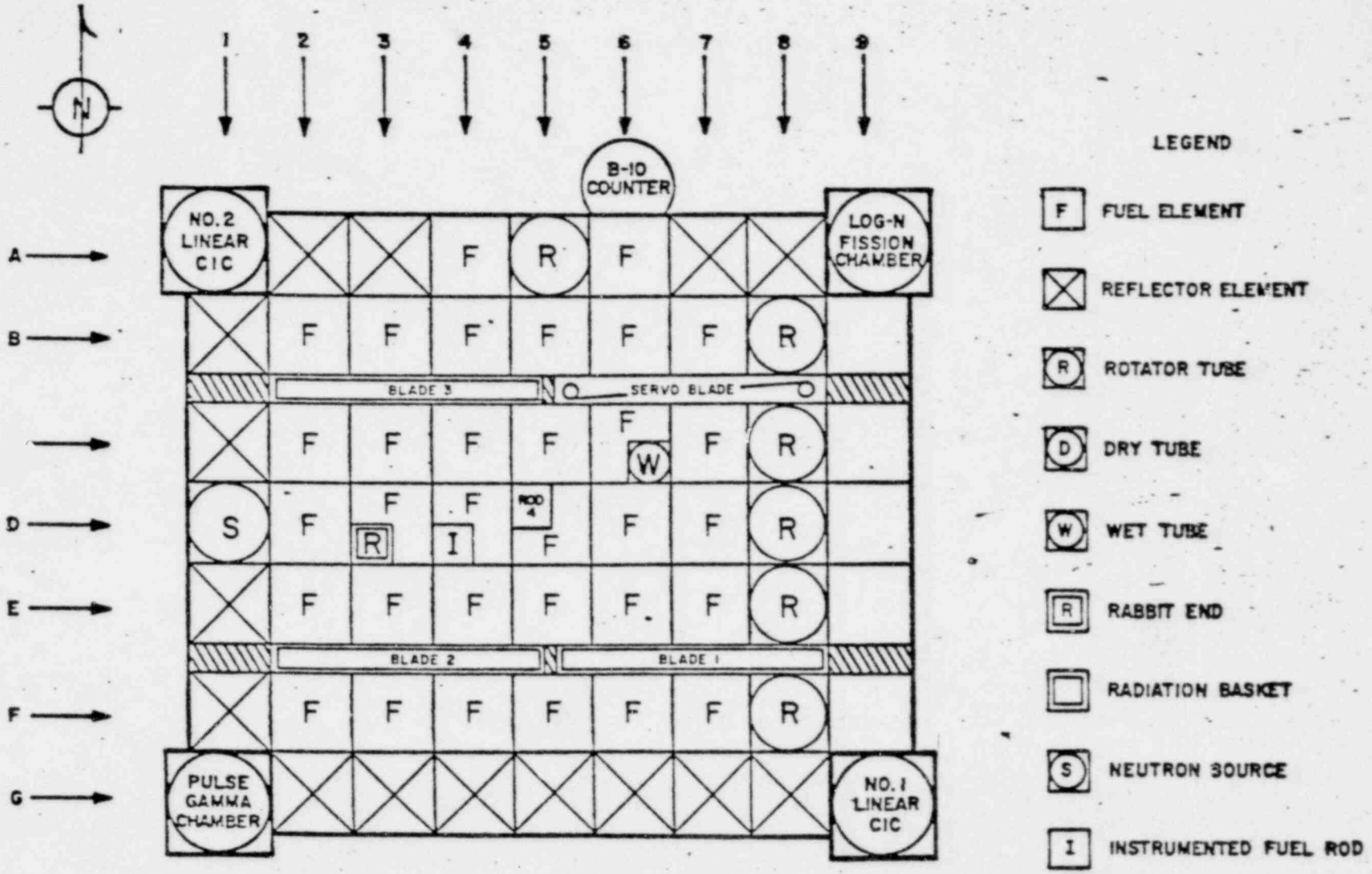

2132 206

Figure 4

CORE 29A
FUEL ROD MAXIMUM CENTERLINE TEMPERATURE, DEGREES C:

	2		3		4		5		6		7	
A	0	0	0	0	202	220	0	0	207	175	0	0
	0	0	0	0	210	234	0	0	220	183	0	0
B	188	197	215	229	240	252	256	262	240	216	193	187
	214	237	259	275	286	291	293	288	279	263	239	225
C	240	264	286	302	318	326	331	323	31[illegible]	302	272	252
	233	256	278	293	307	323	336	321	313	0	272	249
D	234	260	281	295	303	325	0	320	315	301	270	253
	234	262	0	294	302	317	327	313	306	289	263	253
E	231	256	276	289	306	315	317	311	298	282	257	247
	237	260	281	296	314	323	325	318	304	287	263	249
F	211	233	255	270	280	285	285	281	272	257	234	220
	184	192	210	225	234	239	239	235	226	211	191	182

PEAK/AVE = 1.27 MEAN = 264.6

Figure 5

CORE 29A
POWER DENSITY IN KW/ROD:

	2		3		4		5		6		7	
A	0.0	0.0	0.0	0.0	4.2	5.0	0.0	0.0	4.4	3.3	0.0	0.0
	0.0	0.0	0.0	0.0	4.6	5.7	0.0	0.0	5.0	3.6	0.0	0.0
B	3.8	4.1	4.8	5.4	6.0	6.7	7.7	7.4	6.0	4.8	3.9	3.7
	4.7	5.8	7.2	8.4	9.3	9.3	10.0	9.6	8.7	7.5	6.0	5.2
C	6.0	7.5	9.3	10.8	12.1	12.7	13.0	12.5	11.8	10.8	8.1	6.7
	5.6	7.0	8.6	10.0	11.2	12.4	13.3	12.3	11.7	0.0	8.1	6.5
D	5.7	7.3	8.9	10.1	10.9	12.6	0.0	12.3	11.8	10.7	8.0	6.8
	5.7	7.4	0.0	10.1	10.7	12.0	12.7	11.7	11.2	9.6	7.4	6.8
E	5.5	7.0	8.5	9.6	11.1	11.9	12.0	11.6	10.4	9.0	7.1	6.4
	5.9	7.3	8.9	10.3	11.8	12.4	12.6	12.1	10.9	9.5	7.4	6.6
F	4.6	5.6	6.9	8.0	8.8	9.2	9.3	8.9	8.2	7.0	5.7	5.0
	3.6	3.9	4.6	5.2	5.7	6.0	6.0	5.7	5.3	4.6	3.8	3.6

Figure 6

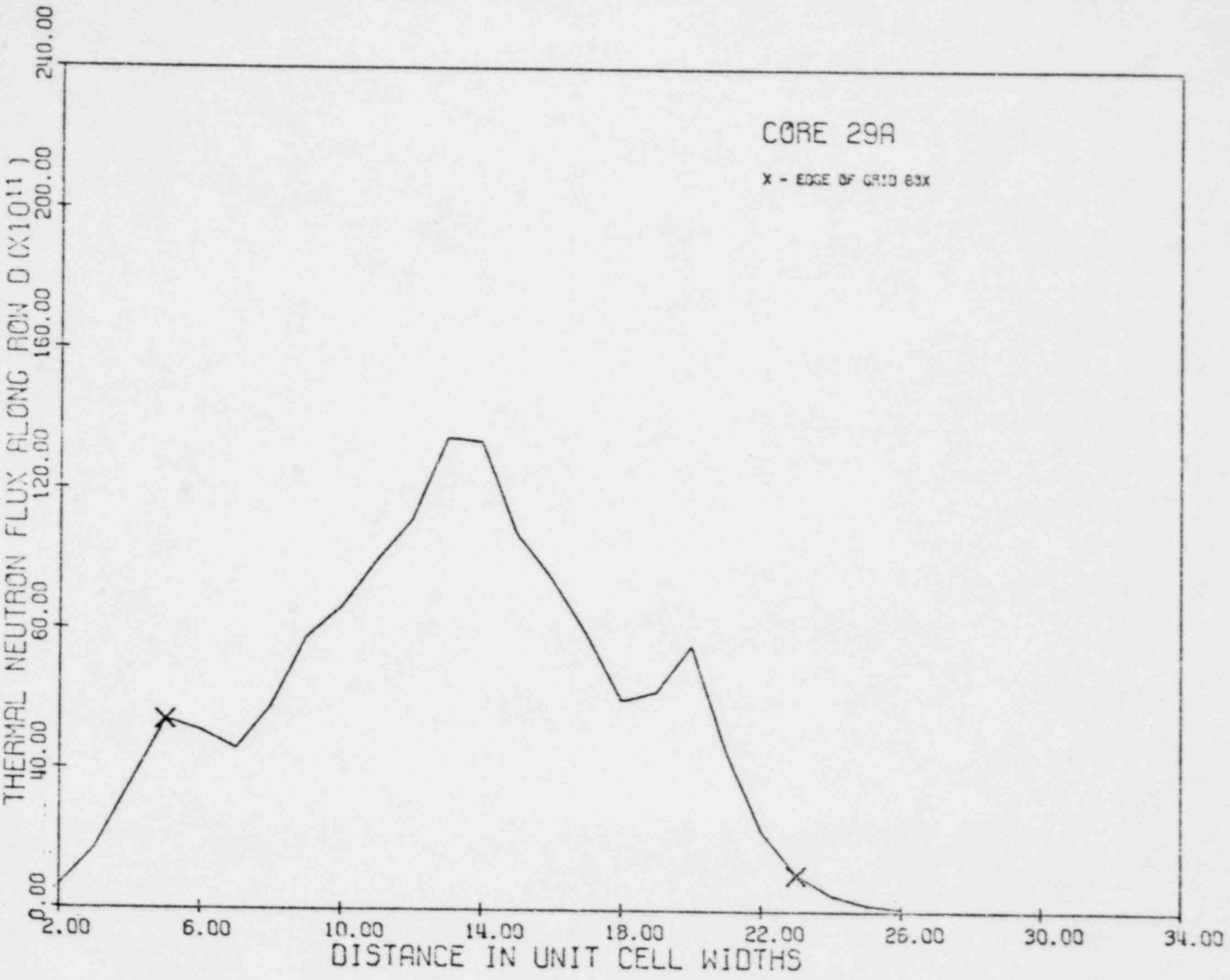

Figure 7

8 to 25. The FLIP region of each of these cores is outlined on each figure. Table III summarizes the results of the studies on these mixed cores.

TABLE III

Designation	No. FLIP Rods	Max Fuel Temp, °C	Peak/Ave Fuel Temp,°C	Mean Fuel Temp,°C	Max Power Density, kw/rod
30A	11	681	2.48	275	21.7
30B	23	501	1.86	269	18.8
30C	31	623	2.30	271	20.9
30D	31	559	2.07	271	19.9
30E	34	442	1.67	265	17.4
30F	45	403	1.54	262	16.3

The data on the six mixed cores studied indicates that these configurations, which all have a contiguous block of FLIP fuel surrounded by standard fuel, are safe to operate under steady state conditions. However, the temperature and power peaking effects in core 30A with only 11 FLIP rods and in cores 30C and 30D which have 4-rod water holes are rather severe. Furthermore, the large peaking factors in these cores would greatly limit the allowable reactivity addition under pulsing conditions. Thus, to provide a wider margin of safety and to permit a reasonable pulsing capability, the arrangement of a mixed core should be limited to configurations with moderate peaking effects.

The following configuration specification is established for the WSU TRIGA core. The FLIP-fueled region in a mixed core shall contain at least 22 FLIP fuel rods in a contiguous block of fuel in the central region of the reactor core. Water holes within the FLIP region shall be limited to single rod holes.

CORE 308
FUEL ROD MAXIMUM CENTERLINE TEMPERATURE, DEGREES C:

	2		3		4		5		6		7	
A	0	0	0	0	191	211	0	0	199	168	0	0
	0	0	0	0	200	226	0	0	214	177	0	0
B	174	183	202	218	231	247	262	258	236	211	188	191
	198	222	247	266	279	286	287	283	276	261	235	219
C	225	250	275	293	308	292	609	556	287	299	270	248
	217	243	267	285	300	291	629	470	284	0	270	245
D	219	248	271	287	297	296	0	562	284	299	268	250
	219	249	0	286	295	287	631	496	277	287	261	249
E	216	244	266	282	299	282	439	414	260	279	255	244
	222	247	270	288	305	290	557	520	273	285	260	245
F	196	219	243	261	274	280	280	277	270	285	231	215
	170	180	199	215	227	234	236	233	224	208	187	178

PEAK/AVE = 2.48 MEAN = 274.6

Figure 8

5.2 Operational Mixed Cores

The actual arrangement of the FLIP fuel that will be initially loaded into the WSU reactor is that of core 30E containing 34 FLIP rods. However, due to unforeseen needs and conditions that may arise in the future the mixed core configuration will not be limited to this arrangement. Any configuration that satisfies the requirement established in the previous section would be permissible. On the other hand, the arrangement of core 30E is not expected to be changed significantly and additional FLIP fuel will not in all probability be added to the core for a number of years. The standard fuel removed from the central portion of the core will be cycled into the standard region to maximize the fuel burnup per rod in that region.

It is anticipated that the operational mixed core will have a prompt negative temperature coefficient for pulsing of about -$.014/°C at the beginning of core life reducing to about -$.012 by the end of core life. Some of the other characteristics of this core are shown in Figures 20, 21 and 22.

5.3 Pulsing Characteristics of Operational Core

The exact pulsing characteristics of a mixed core are not as easily predicted as those for a core with a single type of fuel. The problem stems from the uncertainty in the exact magnitude of the prompt negative temperature coefficient and the temperature dependence of this parameter. The measured pulsing characteristics of the Texas A&M mixed core are shown in Figure 26. (11) This core contained 35 FLIP fuel rods and 64 standard fuel rods for a total of 98 fuel rods. The characteristics of a 100-rod TRIGA core with a temperature coefficient of -$.0145/°C and

CORE 30A
POWER DENSITY IN KW/ROD:

	2		3		4		5		6		7	
A	0.0	0.0	0.0	0.0	3.8	4.6	0.0	0.0	4.2	3.1	0.0	0.0
	0.0	0.0	0.0	0.0	4.2	5.3	0.0	0.0	4.7	3.4	0.0	0.0
B	3.3	3.6	4.3	4.9	5.6	6.4	7.4	7.1	5.8	4.6	3.7	3.5
	4.1	5..	6.4	7.7	8.7	9.3	9.4	9.1	8.5	7.3	5.8	5.0
C	5.2	6.6	8.4	9.9	11.3	9.9	20.7	19.9	9.4	10.5	8.0	6.5
	4.9	6.2	7.8	9.2	10.6	9.8	21.0	19.1	9.2	0.0	8.0	6.3
D	5.0	6.4	8.0	9.4	10.3	10.2	0.0	20.0	9.2	10.5	7.8	6.6
	5.0	6.6	0.0	9.4	10.2	9.4	21.7	18.7	8.5	9.4	7.3	6.5
E	4.8	6.2	7.7	8.9	10.5	8.9	17.3	16.6	7.9	8.8	6.9	6.2
	5.1	6.4	8.0	9.5	11.1	9.7	19.9	19.2	8.6	9.2	7.3	6.3
F	4.0	5.0	6.2	7.3	8.3	8.8	8.8	8.5	8.0	6.9	5.5	4.9
	3.2	3.5	4.1	4.8	5.4	5.7	5.8	5.6	5.2	4.5	3.7	3.4

Figure 9

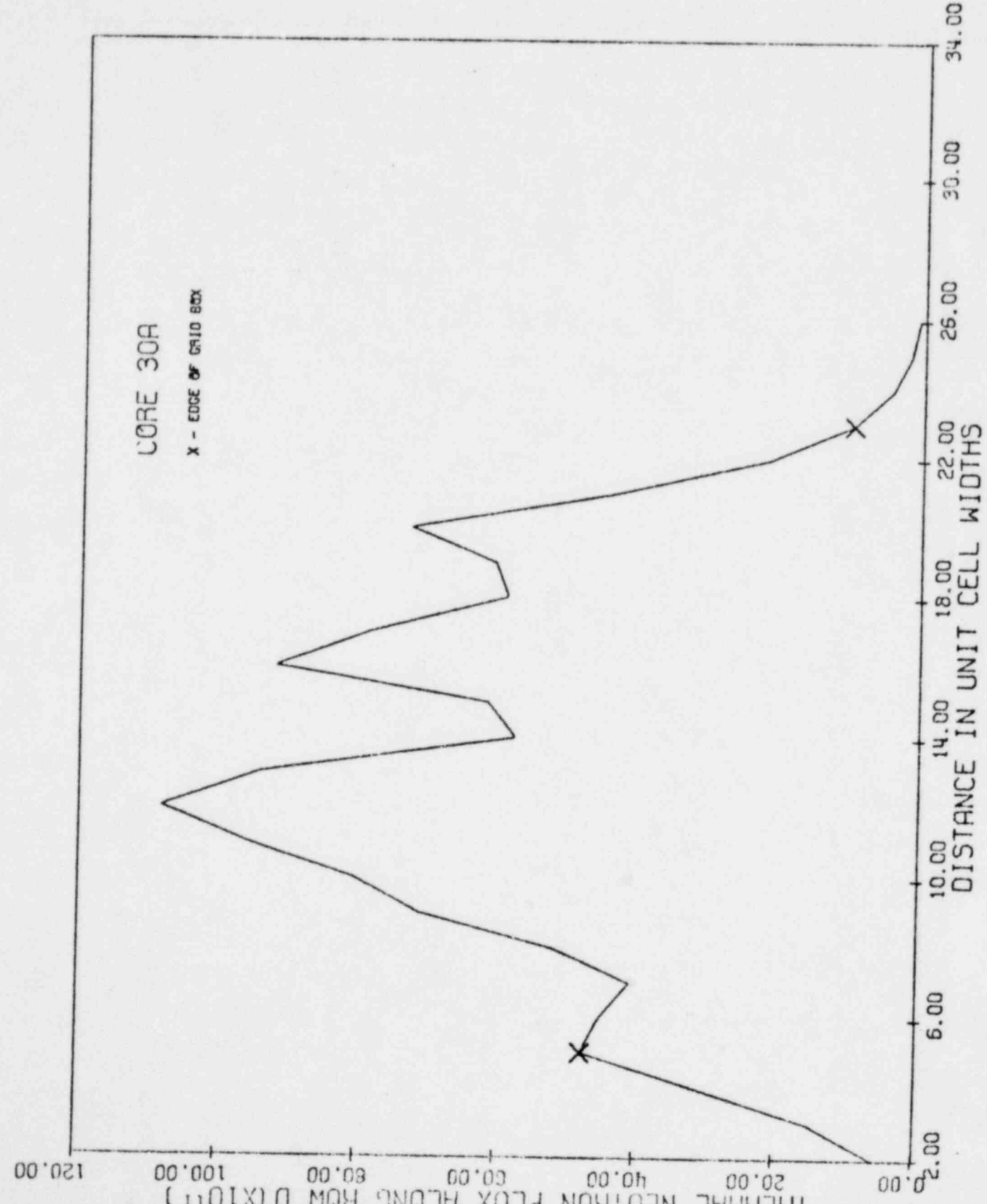
CORE 30A
X - EDGE OF GRID BOX
THERMAL NEUTRON FLUX ALONG ROW D (X10¹¹)
0.00
20.00
40.00
60.00
80.00
100.00
120.00
2.00
6.00
10.00
14.00
18.00
22.00
26.00
30.00
34.00
DISTANCE IN UNIT CELL WIDTHS

Figure 10

CORE 308
FUEL ROD MAXIMUM CENTERLINE TEMPERATURE, DEGREES C:

	2		3		4		5		6		7	
A	0	0	0	0	189	208	0	0	192	160	0	0
	0	0	0	0	199	223	0	0	207	169	0	0
B	174	184	204	219	232	245	258	253	229	203	179	171
	200	224	250	266	276	282	283	279	270	253	224	209
C	227	253	275	270	482	406	411	501	281	291	261	233
	219	245	268	258	382	357	385	430	277	0	261	235
D	221	250	271	259	394	394	0	499	277	291	259	239
	221	252	0	258	338	365	397	448	270	279	252	239
E	218	246	266	254	369	332	385	385	262	271	246	233
	224	249	271	264	448	335	388	467	271	277	251	235
F	196	220	245	261	270	275	276	272	258	247	221	205
	171	180	199	215	227	233	233	228	217	200	178	168

PEAK/AVE = 1.86 MEAN = 269.2

Figure 11

CORE 308
POWER DENSITY IN KW/ROD:

	2		3		4		5		6		7	
A	0.0	0.0	0.0	0.0	3.8	4.5	0.0	0.0	3.9	2.9	0.0	0.0
	0.0	0.0	0.0	0.0	4.1	5.2	0.0	0.0	4.4	3.1	0.0	0.0
B	3.3	3.6	4.3	5.0	5.6	6.3	7.1	6.8	5.5	4.3	3.4	3.2
	4.2	5.2	6.6	7.7	8.5	9.0	9.1	8.7	7.9	6.7	5.3	4.5
C	5.3	6.8	8.4	8.0	18.4	16.4	16.5	13.3	8.9	9.8	7.3	5.9
	5.0	6.3	7.8	7.1	15.5	14.5	15.6	17.1	8.6	9.0	7.3	5.7
D	5.1	6.6	8.0	7.2	16.0	16.0	0.0	18.8	8.6	9.7	7.2	6.0
	5.1	6.7	8.0	7.1	15.7	14.8	16.1	17.6	8.0	8.7	6.7	5.9
E	4.9	6.3	7.7	6.8	15.0	13.0	13.3	15.6	7.4	8.1	6.3	5.6
	5.2	6.5	8.0	7.6	17.6	15.6	15.8	13.1	8.1	8.5	6.6	5.7
F	4.1	5.0	6.3	7.3	8.0	8.4	8.4	8.1	7.5	6.4	5.0	4.4
	3.2	3.5	4.2	4.8	5.3	5.6	5.6	5.4	4.9	4.2	3.4	3.1

Figure 12

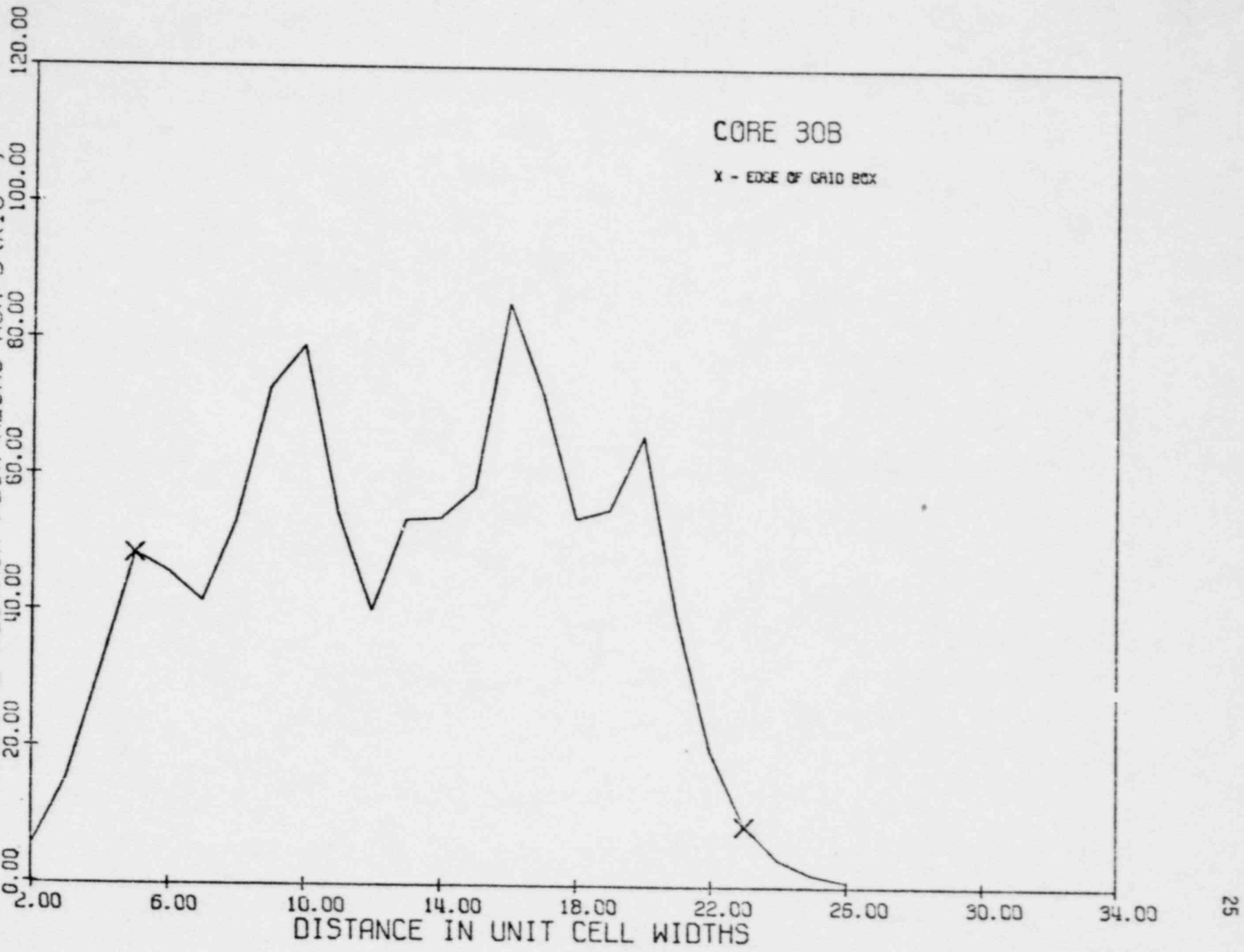

Figure 13

CORE 30C
FUEL ROD MAXIMUM CENTERLINE TEMPERATURE, DEGREES C:

	2		3		4		5		6		7	
A	0	0	0	0	185	202	0	0	182	149	0	0
	0	0	0	0	195	218	0	0	195	157	0	0
B	174	183	202	216	228	240	251	244	217	189	165	158
	199	224	249	264	273	277	277	270	262	245	213	194
C	228	253	275	269	468	391	389	623	0	0	273	228
	221	246	268	258	379	352	372	447	0	0	256	228
D	223	252	272	260	395	391	0	401	391	416	229	235
	223	254	0	260	393	367	393	353	317	322	219	239
E	221	248	268	256	377	336	338	328	312	317	217	235
	227	252	274	268	472	400	403	334	353	355	230	241
F	200	224	249	265	274	280	281	277	263	252	230	216
	175	184	204	221	232	238	239	235	226	210	188	179

PEAK/AVE = 2.30 MEAN = 270.9

Figure 14

CORE 30C
POWER DENSITY IN KW/ROD:

	2		3		4		5		6		7	
A	0.0	0.0	0.0	0.0	3.7	4.3	0.0	0.0	3.5	2.6	0.0	0.0
	0.0	0.0	0.0	0.0	4.0	4.9	0.0	0.0	4.0	2.8	0.0	0.0
B	3.3	3.6	4.3	4.9	5.4	6.0	6.7	6.2	4.9	3.8	3.0	2.8
	4.2	5.2	6.5	7.5	8.2	8.6	8.5	8.0	7.4	6.3	4.7	4.0
C	5.4	6.8	8.4	7.9	18.1	15.8	15.8	20.9	0.0	0.0	8.2	5.4
	5.0	6.4	7.8	7.1	15.4	14.2	15.1	17.6	0.0	0.0	6.9	5.4
D	5.1	6.7	8.1	7.2	16.0	15.9	0.0	16.2	15.9	16.7	5.4	5.7
	5.2	6.8	0.0	7.2	15.9	14.9	15.9	14.2	12.0	12.4	5.0	5.9
E	5.0	6.5	7.9	7.0	15.3	13.3	13.4	12.8	11.6	12.0	4.9	5.3
	5.3	6.7	8.3	7.8	18.2	16.2	16.3	15.6	14.3	14.4	6.5	6.1
F	4.2	5.2	6.5	7.6	8.3	8.8	8.9	8.6	7.8	6.7	5.5	4.8
	3.3	3.6	4.3	5.0	5.6	5.9	6.0	5.8	5.3	4.6	3.8	3.4

Figure 15

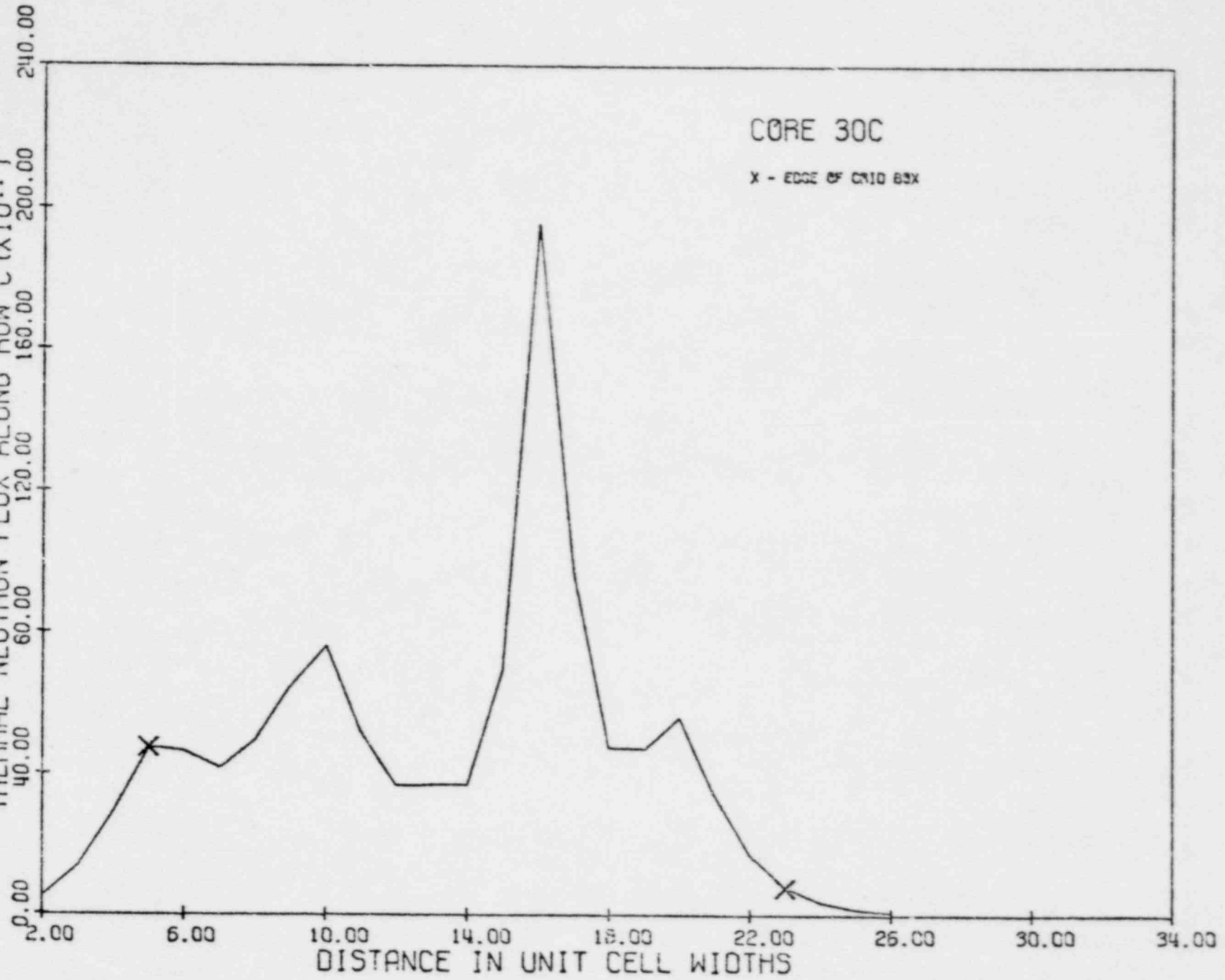

Figure 16

CORE 30D
FUEL ROD MAXIMUM CENTERLINE TEMPERATURE, DEGREES C:

	2		3		4		5		6		7	
A	0	0	0	0	187	207	0	0	194	164	0	0
	0	0	0	0	197	222	0	0	209	173	0	0
B	171	181	201	216	230	244	259	255	232	207	184	177
	196	221	246	263	274	280	283	279	269	253	239	215
C	223	249	272	267	462	397	400	382	352	355	229	240
	215	242	264	255	370	350	374	367	395	430	231	236
D	217	246	267	256	381	381	0	559	0	0	268	242
	217	248	0	254	375	355	384	493	0	0	268	241
E	214	242	262	250	358	326	328	339	384	418	229	233
	220	245	267	261	428	374	377	363	340	343	224	236
F	192	216	241	257	267	273	274	270	261	245	222	209
	167	177	196	212	224	231	232	228	218	202	181	172

PEAK/AVE = 2.07 MEAN = 270.7

Figure 17

CORE 30D
POWER DENSITY IN KW/ROD:

	2		3		4		5		6		7	
	0.0	0.0	0.0	0.0	3.7	4.5	0.0	0.0	4.0	3.0	0.0	0.0
A	0.0	0.0	0.0	0.0	4.1	5.1	0.0	0.0	4.6	3.3	0.0	0.0
	3.2	3.5	4.2	4.8	5.5	6.2	7.1	6.9	5.6	4.5	3.6	3.4
B	4.0	5.0	6.4	7.5	8.3	8.8	9.1	8.7	7.9	6.8	5.5	4.8
	5.1	6.5	8.2	7.7	17.9	16.1	16.2	15.5	14.2	14.3	5.4	6.0
C	4.8	6.1	7.5	6.9	15.1	14.1	15.2	14.0	16.0	17.1	5.5	5.8
	4.9	6.4	7.8	6.9	15.5	15.5	0.0	19.9	0.0	0.0	7.8	6.1
D	4.9	6.5	0.0	6.9	15.2	14.4	15.6	18.8	0.0	0.0	7.8	6.1
	4.7	6.1	7.4	6.6	14.5	12.7	13.8	13.5	15.6	16.8	5.4	5.7
E	5.0	6.3	7.8	7.3	17.1	15.	15.3	14.7	13.6	13.7	5.2	5.8
	3.9	4.8	6.1	7.1	7.8	8.2	8.3	8.0	7.3	6.3	5.1	4.5
F	3.1	3.4	4.0	4.7	5.2	5.5	5.6	5.4	4.9	4.3	3.5	3.2

Figure 18

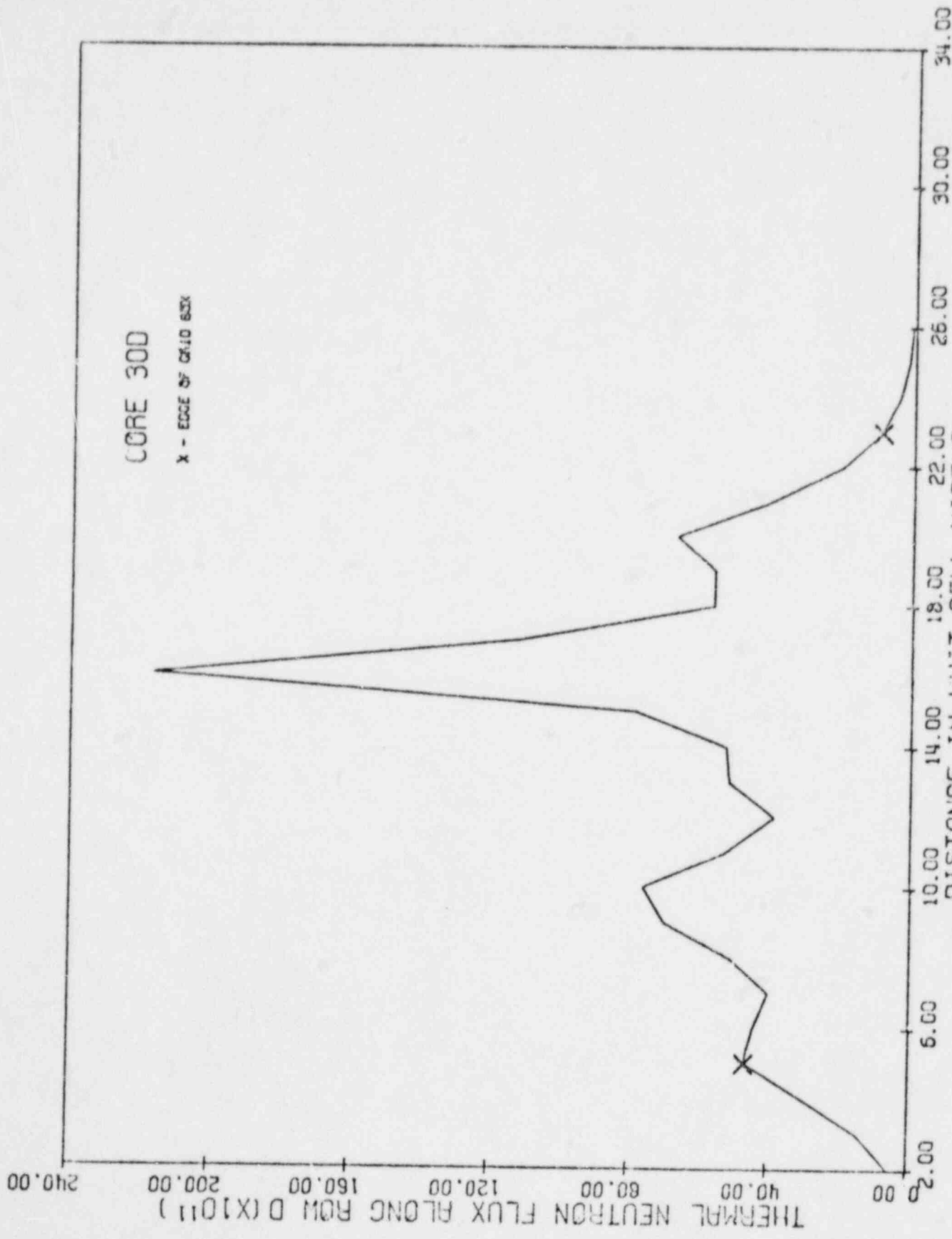
CORE 30D
X - EDGE OF CORE BOX
THERMAL NEUTRON FLUX ALONG ROW D (X10¹¹)
0.00
40.00
80.00
120.00
160.00
200.00
240.00
2.00
6.00
10.00
14.00
18.00
22.00
26.00
30.00
34.00
DISTANCE IN UNIT CELL WIDTHS

Figure 19

CORE 30E
FUEL ROD MAXIMUM CENTERLINE TEMPERATURE, DEGREES C:

	2		3		4		5		6		7	
A	0	0	0	0	184	204	0	0	193	163	0	0
	0	0	0	0	193	219	0	0	203	173	0	0
B	167	177	196	212	226	241	257	253	232	207	185	178
	191	216	242	260	271	278	231	278	269	254	232	218
C	218	245	268	263	442	388	396	393	378	.69	244	245
	210	237	260	251	362	346	371	344	344	0	244	242
D	212	242	263	252	371	376	0	374	335	361	237	245
	212	243	0	251	366	351	379	349	317	326	224	244
E	209	237	259	247	351	323	327	321	309	316	217	233
	215	241	263	257	412	367	373	363	341	346	227	239
F	188	212	237	254	264	271	273	269	261	245	224	211
	163	172	192	209	221	228	230	226	217	202	182	173

PEAK/AVE = 1.67 MEAN = 264.9

Figure 20

CORE 30E
POWER DENSITY IN KW/ROD:

	2		3		4		5		6		7	
A	0.0	0.0	0.0	0.0	3.6	4.3	0.0	0.0	3.9	3.0	0.0	0.0
	0.0	0.0	0.0	0.0	3.9	5.0	0.0	0.0	4.5	3.3	0.0	0.0
B	3.1	3.4	4.1	4.7	5.3	6.1	7.0	6.8	5.6	4.5	3.6	3.4
	3.9	4.3	6.1	7.2	8.1	8.6	8.9	8.7	7.9	6.8	5.6	4.9
C	4.9	6.3	7.8	7.5	17.4	15.8	16.0	15.6	15.4	17.4	6.2	6.3
	.6	5.8	7.3	6.6	14.7	13.9	15.1	13.8	13.4	0.0	6.2	6.1
D	4.7	6.1	7.5	6.7	15.1	15.3	0.0	15.2	13.2	15.5	5.9	6.3
	4.7	6.2	0.0	6.6	14.8	14.2	15.4	14.0	12.0	12.7	5.2	6.2
E	4.5	5.9	7.1	6.4	14.1	12.4	12.7	12.3	11.3	11.9	4.9	5.9
	4.8	6.0	7.5	7.1	16.6	14.9	15.2	14.7	13.6	13.9	5.3	6.0
F	3.7	4.7	5.8	6.8	7.6	8.0	8.2	7.9	7.3	6.3	5.2	4.6
	2.9	3.2	3.9	4.5	5.1	5.4	5.5	5.3	4.9	4.3	3.5	3.2

Figure 21

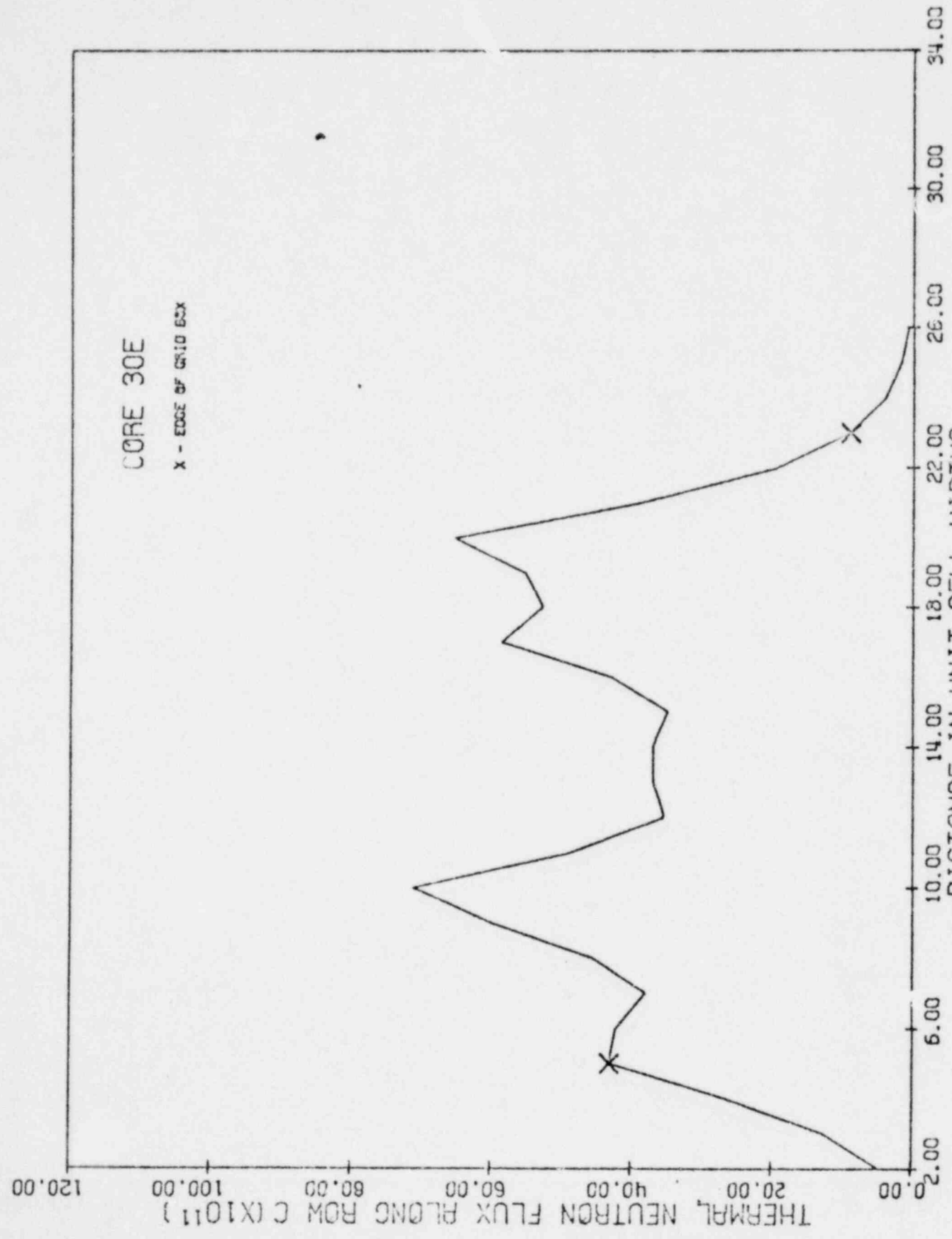
CORE 30E
X - EDGE OF QUAD BOX
THERMAL NEUTRON FLUX ALONG ROW C (X10¹¹)
0.00
20.00
40.00
60.00
80.00
100.00
120.00
2.00
6.00
10.00
14.00
18.00
22.00
26.00
30.00
34.00
DISTANCE IN UNIT CELL WIDTHS

Figure 22

CORE 30F
FUEL ROD MAXIMUM CENTERLINE TEMPERATURE, DEGREES C:

	2		3		4		5		6		7	
A	0	0	0	0	184	202	0	0	187	157	0	0
	0	0	0	0	194	217	0	0	202	167	0	0
B	173	182	201	215	226	239	253	249	226	200	178	171
	199	221	243	259	271	276	278	273	264	247	224	210
C	224	223	335	332	357	377	381	366	358	403	237	237
	216	210	305	299	313	338	359	333	331	0	237	234
D	218	218	319	304	318	365	0	358	323	358	230	237
	218	222	0	305	315	343	366	337	309	315	216	236
E	215	214	312	298	308	318	320	313	301	307	209	230
	221	219	328	324	344	359	382	349	329	331	220	232
F	196	217	238	254	264	269	270	265	255	239	217	203
	170	178	197	211	222	227	227	222	212	196	175	166

PEAK/AVE = 1.54 MEAN = 261.9

2132 227

Figure 23

CORE 30F
POWER DENSITY IN KW/ROD:

	2		3		4		5		6		7	
	0.0	0.0	0.0	0.0	3.6	4.2	0.0	0.0	3.7	2.8	0.0	0.0
A	0.0	0.0	0.0	0.0	3.9	4.9	0.0	0.0	4.3	3.1	0.0	0.0
	3.3	3.6	4.2	4.8	5.3	6.0	6.8	6.5	5.3	4.2	3.4	3.2
B	4.1	5.1	6.2	7.2	8.0	8.5	8.6	8.3	7.5	6.4	5.2	4.6
	5.2	5.1	13.2	13.1	14.4	15.3	15.5	14.8	14.5	16.3	5.8	5.9
C	4.8	4.6	11.1	10.5	11.7	13.5	14.5	13.1	13.0	0.0	5.8	5.7
	4.9	4.9	12.1	11.0	12.1	14.8	0.0	14.5	12.5	14.5	5.5	5.9
D	4.9	5.1	0.0	11.0	11.9	13.7	14.9	13.4	11.4	11.9	4.9	5.3
	4.8	4.7	11.6	10.4	11.3	12.1	12.3	11.7	10.7	11.2	4.6	5.5
E	5.1	5.0	12.8	12.5	13.8	14.6	14.7	14.1	12.9	13.0	5.0	5.6
	4.0	4.9	5.9	6.8	7.5	7.9	8.0	7.6	6.9	6.0	4.9	4.3
F	3.1	3.4	4.1	4.6	5.1	5.3	5.3	5.1	4.7	4.0	3.3	3.0

Figure 24

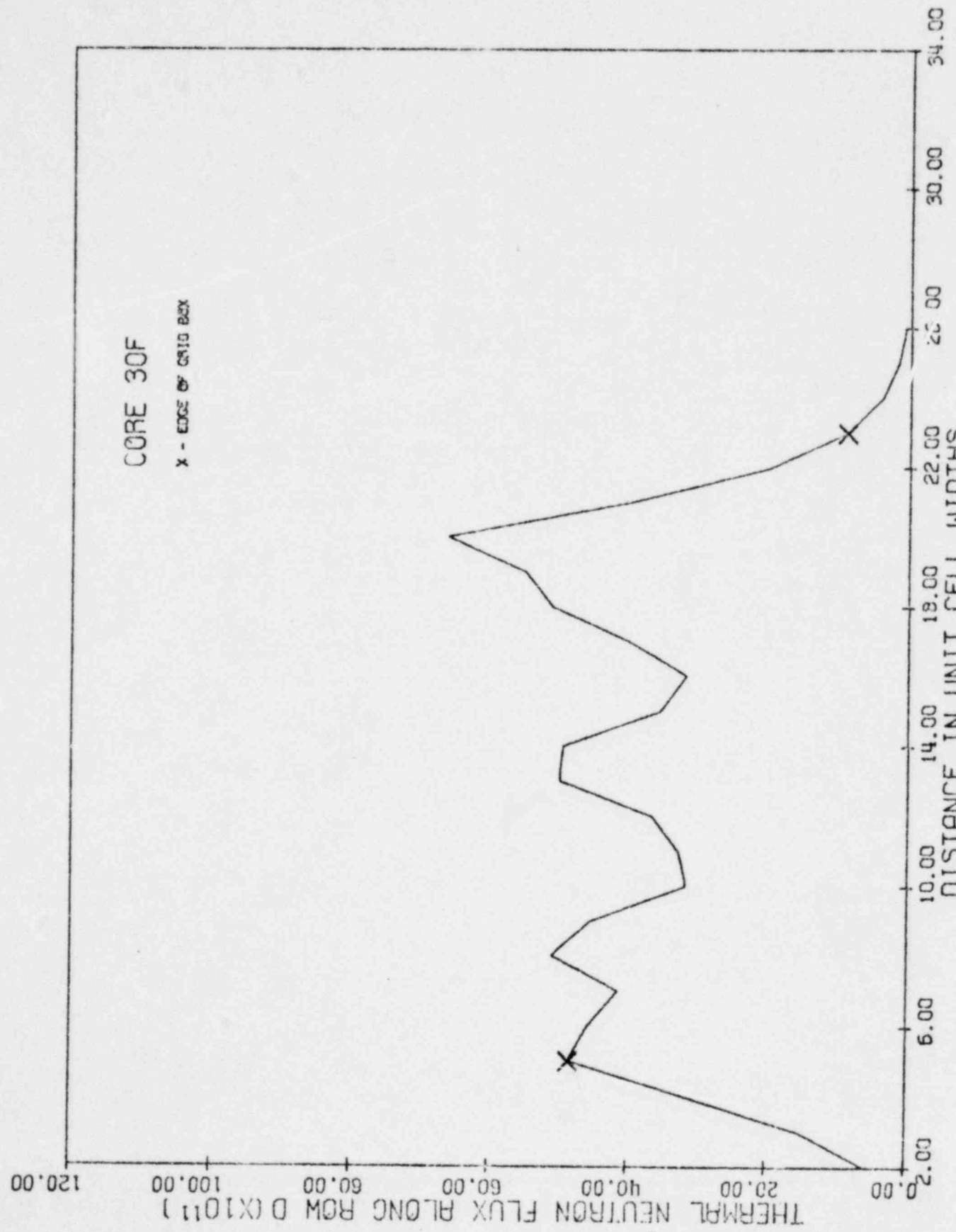
CORE 30F
X - EDGE OF CRID BOX
THERMAL NEUTRON FLUX ALONG ROW D (X10¹¹)
0.00
20.00
40.00
60.00
80.00
100.00
120.00
2.00
6.00
10.00
14.00
18.00
22.00
26.00
30.00
34.00
DISTANCE IN UNIT CELL WIDTHS

Figure 25

Figure 26

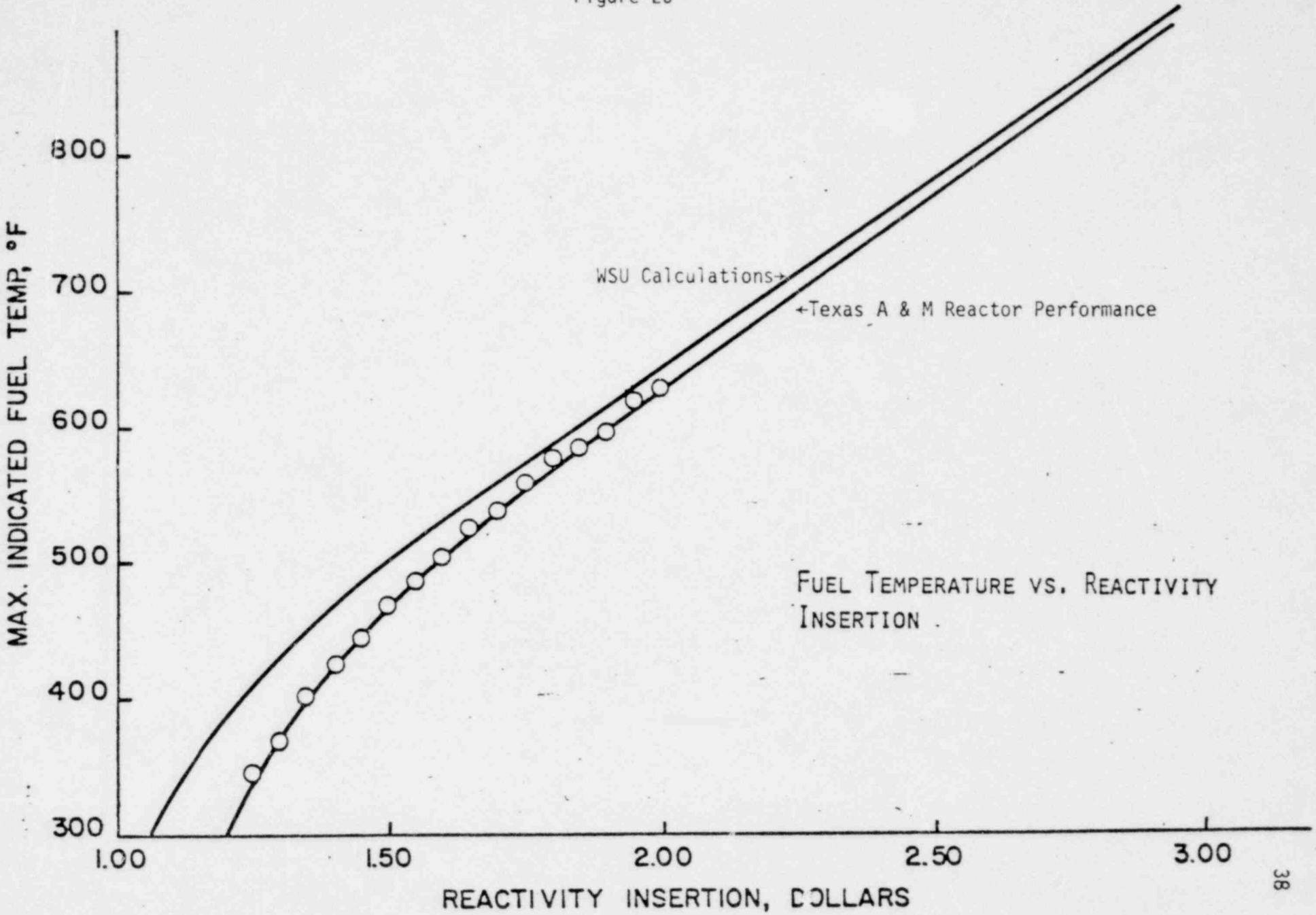

FUEL TEMPERATURE VS. REACTIVITY INSERTION.

with a prompt neutron lifetime of 32 microseconds as calculated by the equations in Section 4.4 is also plotted on this figure. The theoretical curve predicts a somewhat greater temperature than the measured values and assuming a 200°C core temperature before pulsing.

The FLIP fuel content of the initial WSU mixed core 30E will be comparable to that contained in the Texas A&M mixed core. We can thus expect the two cores to have comparable negative temperature coefficients and pulsing characteristics. If we assume a more conservative value of -$.014/°C for the temperature coefficient for the WSU mixed core along with a 32 microsecond prompt neutron lifetime, we obtain the results listed in Column A of Table IV. The expected performance at the end of core life is shown in Column B of Table IV.

TABLE IV

PULSING CHARACTERISTICS OF 125-ROD
MIXED TRIGA REACTOR CORE 30E

Reactivity in $	Peak Power in MW		Average Peak Fuel Temp Increase, °C	
	(A)	(B)	(A)	(B)
1.5	218	256	70	81
2.0	893	1048	139	161
2.5	2047	2411	204	237
3.0	3708	4380	269	312

(A) T_c = $.014/°C, (B) T_c = -$.012/°C

In order to provide at least a 200°C margin of safety during pulsing of mixed core 30E, pulsing should be limited to $2.50 so that the average core temperature increase is 250°C or less. Combining this 250°C limit

with the average core temperature of 265°C and a peaking factor of 1.67 yields a maximum possible fuel temperature of 861°C in this core. The peak fuel temperature obviously would be within the FLIP fuel region and the peak calculated value is below the established 950°C safety setting limit for FLIP fuel. In actual operation pulsing is not permitted above a power level of 1 kw and thus a wider safety margin actually exists than that calculated above.

5.4 Fuel Temperature Scram

In order to provide a further degree of safety for the WSU TRIGA reactor when operated with a mixed core, a fuel temperature channel with a scram capability shall be added to the control system. This channel shall scram the reactor if the instrumented fuel rod temperature exceeds the fuel temperature safety system setting. The instrumented fuel element for this channel shall be located in the FLIP fuel region.

The studies on mixed cores in Section 5.1 indicates that the core with the smallest allowable number of FLIP fuel rods has the highest FLIP region fuel temperatures. The cores with four (4)-rod water holes in the FLIP region are excluded as not being allowable configurations. Thus under the guidelines at the end of Section 5.1 core 30B is the core with the smallest allowable number of FLIP fuel rods. Figure 11 for this core indicates the following temperature characteristics for the FLIP region: maximum region temperature 501°C, minimum region temperature 332°C, and maximum-to-minimum fuel temperature ratio in the region 1.51. Taking this core as the worst case and applying the limiting safety system setting of 800°C for standard fuel to the FLIP region for an added margin of safety we obtain a value of 800/1.51 = 529°C for the

safety system setting. That is, if the instrumented fuel element is located in the FLIP fuel rod with the lowest power density in the FLIP region of core 30B and has an indicated temperature of 529°C, the temperature of the FLIP fuel rod with the highest power density would not exceed 800°C.

An examination of Figure 21 for core 30E indicates that this core has the following characteristics for the FLIP region: maximum region temperature 442°C, minimum region temperature 309°C, and maximum-to-minimum fuel temperature ratio in the region of 1.43. In core 30E the maximum possible fuel temperature for a 529°C indicated FLIP region temperature would be 758°C. Thus the 529°C safety system setting provides a wider margin of safety in this core.

A value of 500°C is established as the fuel temperature safety system setting for the WSU TRIGA reactor operating with a mixed core. This limit will provide an ample margin of safety as demonstrated above and will permit operation of all allowable mixed core configurations.

6.0 DESIGN BASIS ACCIDENT

The Design Basis Accident for a TRIGA reactor is defined as the loss of the integrity of the fuel cladding of one fuel rod in air. The hazard associated with this theoretical accident is thus the effects of the postulated fission product release within the facility and to the surrounding environment. For the purposes of the D.B.A it is assumed that all the fission products are released directly into the pool room air and that none are retained in the pool water.

The fission product release fraction for TRIGA-type reactor fuel has been measured experimentally (12) and documented before the AEC hearings on the Columbia reactor as being 1.5×10^{-5} at a fuel temperature of 300°C. The release fraction, FR, is, however, a function of the fuel temperature, T, in °C given by the relationship (12):

$$FR = 1.5 \times 10^{-5} + 3.6 \times 10^{3} \text{ EXP} - (1.34 \times 10^{4}/T + 273).$$

Assuming a fuel temperature of 500°C, the release fraction is calculated to be 1.2×10^{-4} by the above relationship. A release fraction of 1.2×10^{-4} will be used in the calculations for the D.B.A.

A power density of 30 kw per fuel rod and an infinite irradiation time will also be assumed for the D.B.A. Under these conditions the fission product inventory for one TRIGA fuel rod and the associated released fission products are tabulated in Tables V and VI. This tabulation was derived from the basic data of Perkins and King (13) along with the documented fact (12) that only the gaseous fission products escape when the cladding of a TRIGA fuel rod ruptures.

A summation of the fission product release data tabulated in Tables V and VI yields a total fission product release for the D.B.A. of 1.72 curies of gamma emitters and 2.25 curies of beta emitters. If this activity is uniformly

distributed in the pool room and control room which have a combined volume of 1×10^9 cm^3, the specific gamma activity would be 1.72×10^{-3} $\mu Ci/cm^3$ and the specific beta activity would be 2.25×10^{-3} $\mu Ci/cm^3$.

TABLE V

SOLUBLE GASEOUS FISSION PRODUCTS

CONTAINED IN AND RELEASABLE FROM A SINGLE TRIGA FUEL ROD*

Isotope	Saturated Inventory Ci	Released Activity mCi	Half-Life
Br-82	40	4.8	35.3 hr
83	137	16.4	2.3 hr
84	253	30.4	31.8 min
85	330	39.6	3.0 min
87	780	93.6	55 sec
Total Br	1540	184.8	
I-130m	260	31.2	9.2 min
131	734	88.1	8.1 days
132	1115	133.8	2.3 hr
133	1672	200.6	21 hr
134	2027	243.2	54 min
135	1546	185.5	6.8 hr
136	785	94.2	86 sec
Total I	8139	976.6	

Total Released Soluble Gaseous Fission Products = 1.16 Ci

Total Gamma Emitters = 1.03 Ci

Total Beta Emitters = 1.16 Ci

*Power Density = 30 kw/rod, fuel temperature = 500°C, release fraction = 1.2×10^{-4}

TABLE VI

INSOLUBLE GASEOUS FISSION PRODUCTS

CONTAINED IN AND RELEASABLE FROM A SINGLE TRIGA FUEL ROD*

Isotope	Saturated Inventory Ci	Released Activity mCi	Half-Life
Kr-83m	137	16.4	1.9 hr
85m	330	39.6	4.4 hr
85	67	8.0	10.7 yr
87	634	76.1	78 min
88	912	109.4	2.8 hr
89	1115	133.8	3.2 min
Total Kr	3195	383.3	
Xe-131m	7	0.8	12 days
133m	40	4.8	2.3 days
133	1672	200.6	5.3 days
135m	457	54.8	15 min
135	1621	194.5	9 hr
137	1545	185.4	3.9 min
138	1166	139.9	17 min
Total Xe	6508	780.8	

Total Released Insoluble Gaseous Fission Products = 1.16 Ci

Total Gamma Emitters = 0.69 Ci

Total Beta Emitters = 1.08 Ci

2132 237

*Power Density = 30 kw/rod, fuel temperature = 500°C, release fraction = 1.2×10^{-4}

6.1 Whole Body Dose in Pool Room

In the calculation of the whole body dose from the gamma emitters we may approximate the pool room by a hemisphere with a radius of 808 cm. The dose at the center of the hemisphere may then be calculated from the equation

$$D = \frac{S_v(1 - e^{-\Sigma R})}{2\Sigma C}$$

where D = dose rate, mr/min

S_v = photons/sec cm^3 of air

Σ = attenuation coefficient for air

R = outer radius of hemisphere (808 cm)

C = flux to dose rate conversion.

In the case of fission products, the average energy of the gamma emitters is .7 MeV which gives a value 3.5×10^{-5} cm^{-1} for Σ and 4.2×10^4 γ/cm^2 sec per mr/min for the conversion factor C. The specific photon activity of the pool room air is 63.6 photons/sec cm^3. Substituting these values in the above equation yields a maximum dose rate of .6 mr/min or 36 mr/hr. Using a quality factor of 1 for gamma rays, the maximum whole body exposure rate for operating personnel in the pool room as a result of the D.B.A. would be 36 mrem/hr.

6.2 Lung Dose in Pool Room

The primary hazard to operating personnel in the pool room, however, would be from the inhalation of gaseous fission products rather than the whole body dose. In this case the critical organs are the lungs and the thyroid and the beta emitters are the source of the internal exposure. The "standard man" has a lung capacity of 3×10^3

cm^3 and breathes 1.25 m^3 of air per hour. After a few breaths the lungs of a person in the pool room would contain 2.25×10^{-3} Ci/cm^3 x 3×10^{10} cm^3 = 6.8 Ci of beta emitters. The lung dose from this inhaled beta activity may be calculated from

$$D = \frac{ACR}{m} \sum_{i}^{8} \frac{f_i E_1}{\lambda_1} (1 - e^{-\lambda_i t}) \text{ rads (beta)} ,$$

where A = activity in the lungs on leaving the reactor room, μCi

C = conversion factor $\frac{(3.7 \times 10^4 \text{ β/sec μCi})(1.6 \times 10^{-6} \text{ erg/MeV})}{100 \text{ ergs/g-rad}}$

R = retention factor (0.125)

m = mass of lungs (1000 grams)

f_i = fraction of total activity

E_i = energy of beta from nuclide i, MeV

λ_i = radioactive decay constant + biological release rate*

t = time of exposure (assumed to be infinite).

The weighted average energy of the beta particles emitted by the gaseous fission products is .78 MeV. Substituting this and the other values in the above equation and assuming an infinite exposure time yields a lung exposure of 8 mrads. This is significantly below the limiting biological exposure of 50 rads for the lungs.

6.3 Thyroid Dose in Pool Room

The thyroid dose to a person in the pool room was calculated using the conventional assumptions that the individual remains in the room for 10 min after the fission product release. All of the iodine is assumed to be absorbed into the bloodstream and carried immediately

*$(6.7 \times 10^{-8} \text{ sec}^{-1})$

to the thyroid which is assumed to have a retention factor of 25%. The thyroid dose resulting from the inhaled activity may be calculated from the equation

$$D_{thyroid} = Bt \sum_i (Q_i E_i)$$

where $D_{thyroid}$ = thyroid dose in rem

B = inhalation rate = 200 cm^3/sec

t = time = 600 sec

Q_i = concentration of the i^{th} isotope in Ci/cm^3

E_i = effectivity of the i^{th} isotope in rem/Ci inhaled.

The results of the calculations are shown in Table VII. The 29.7 rem thyroid dose does not exceed the yearly maximum permissible thyroid dose of 30 rem. It is to be noted that the thyroid dose would be reduced by about a factor of 10 if the water remained in the pool as 90% of the iodine would remain in the pool water.

TABLE VII

Ten-Minute Thyroid Dose to Persons
in the Pool Room Following as a Result of the D.B.A.

Isotope	Curies Released	Q_i $\mu c/cm^3$	E_i rem/μCi inhaled	$D_{thyroid}$ rem
I-131	.088	8.8×10^{-5}	1.48	15.6
I-132	.134	13.4×10^{-5}	.0535	.9
I-133	.201	20.1×10^{-5}	.40	9.7
I-134	.243	24.3×10^{-6}	.025	.7
I-135	.186	18.6×10^{-6}	.125	2.8
			TOTAL	29.7 rem

6.4 Discharge of the Fission Products into the Environment

The rate at which the fission products from the D.B.A. are released into the environment is primarily dependent upon the effects of the pool room ventilation system. If the ventilation system is in operation, air is exhausted from the pool room at the rate of 2000 cfm or 9.44×10^5 cm^3/sec. If the ventilation system is off, the release to environment would only be by leakage from a sealed building which is estimated to be of the order of 100 cfm or 4.81×10^4 cm^3/sec.

The time integrated activity exhausted from the facility is given by the equation

$$A_i = A_i \, q/(\lambda_i + q/V), \ \mu Ci.$$

where A_i = the concentration of the i^{th} isotope in the room at t = 0 in Ci/cm^3

q = the building exhaust rate in cm^3/sec

V = the volume of room in cm^3

λ_i = the decay constant of the i^{th} isotope in sec^{-1}.

The activity discharged into the atmosphere as a result of the D.B.A. with the ventilation system on and off as well as the relevant MPC values are tabulated in Table VIII. Column D is the released activity with the ventilation system on divided by the annual volume of the ventilation system. Column E is the released activity with the ventilation system off divided by the annual volume of the ventilation system. Column G is the ratio of the annual average released specific activity with the ventilation system on (Column D) divided by the MPC for unrestricted areas for that isotope.

An examination of Column D of Table VIII indicates that the only

TABLE VIII

FISSION PRODUCT RELEASE CONCENTRATIONS AS A RESULT OF THE D.B.A.

A	B	C	D	E	F	G
Isotope	Activity Released in mCi Ventilation System ON	OFF	Release Concentration in $\mu Ci/cm^3$ Averaged Over One Year * ON	OFF	MPC Unrestricted Areas	Ratio D/F
Br-82	4.8	4.3	1.6×10^{-10}	1.4×10^{-10}	4×10^{-8}	4×10^{-3}
83	15.1	5.9	5.0×10^{-10}	2.0×10^{-10}	2×10^{-6}	2.5×10^{-4}
84	22.0	3.6	7.4×10^{-10}	1.2×10^{-10}	2×10^{-6}	3.7×10^{-4}
85	7.7	.49	2.6×10^{-10}	1.6×10^{-11}	3×10^{-5}	8.7×10^{-6}
87	6.5	.36	2.2×10^{-10}	1.2×10^{-11}	4×10^{-5}	5.5×10^{-6}
I-130m	13.8	1.1	4.6×10^{-10}	3.7×10^{-11}	-----	-----
131	88	88	3.0×10^{-9}	3.0×10^{-9}	1×10^{-10}	30
132	123	49	4.1×10^{-9}	1.6×10^{-9}	3×10^{-9}	1.4
133	201	169	6.7×10^{-9}	5.7×10^{-9}	4×10^{-10}	17
134	198	45	6.6×10^{-9}	1.6×10^{-9}	6×10^{-9}	1.1
135	180	117	6.0×10^{-9}	3.9×10^{-9}	1×10^{-9}	6
136	9.4	.6	3.2×10^{-10}	2.0×10^{-11}	1×10^{-7}	3.2×10^{-3}

*Annual Volume of Ventilation System = $2.98 \times 10^{13} cm^3$

TABLE VIII Continued:

A Isotope	B Activity Released in mCi Ventilation System ON	C OFF	D Release Concentration in $\mu Ci/cm^3$ Averaged Over One Year* ON	E OFF	F MPC Unrestricted Areas	G Ratio D/F
Kr-83m	14.8	5.2	5.0×10^{-10}	1.7×10^{-10}	2×10^{-6}	2.5×10^{-4}
85m	38	21	1.3×10^{-9}	7.0×10^{-10}	1×10^{-7}	1.3×10^{-2}
85	8	8	2.7×10^{-10}	2.7×10^{-10}	3×10^{-7}	9×10^{-1}
87	66	18.6	2.2×10^{-9}	6.2×10^{-10}	2×10^{-8}	1.1×10^{-1}
88	103	45	3.5×10^{-9}	1.5×10^{-9}	2×10^{-8}	1.8×10^{-1}
89	28	1.8	9.3×10^{-10}	6.0×10^{-11}	2×10^{-8}	4.7×10^{-2}
Xe-131m	.8	.8	2.7×10^{-11}	2.7×10^{-11}	4×10^{-7}	6.8×10^{-5}
133m	4.8	4.8	1.6×10^{-10}	1.6×10^{-10}	3×10^{-7}	5.3×10^{-4}
133	201	201	6.7×10^{-9}	6.7×10^{-9}	3×10^{-7}	2.2×10^{-2}
135m	31	3.3	1.0×10^{-9}	1.1×10^{-10}	2×10^{-7}	5×10^{-3}
135	190	135	6.4×10^{-9}	4.5×10^{-9}	1×10^{-7}	6.4×10^{-2}
137	45	3.0	1.5×10^{-10}	1.0×10^{-10}	3×10^{-8}	5×10^{-2}
138	81	9.2	2.7×10^{-9}	3.1×10^{-10}	4×10^{-8}	6.8×10^{-4}

*Annual Volume of Ventilation System = $2.98 \times 10^{13} cm^3$

isotopes released that exceed the MPC values are Iodine 131, 132, 133, 134, and 135. Due to the long half-life of these iodine isotopes, shutting off of the ventilation system will have very little effect on the quantity of these isotopes that escape to the environment under the postulated leakage rate of 100 cfm (see Column F). On the other hand, however, the ventilation system of the pool room is provided with a dilution mode of operation in which 1700 cfm of outside air is mixed with 300 cfm of air from the pool room and discharged from the facility. The 300 cfm of air from the pool room in this mode of operation is passed through an absolute filter system which would remove sufficient iodine from the pool room air so that the quantity of iodine discharged when averaged over one year would be below the MPC values.

6.5 Dilution of Discharge in the Lee of the Building

The gaseous radioactive material discharged from the facility ventilation system will be diluted by atmospheric air in the lee of the building due to turbulent wake effects. The dilution is proportional to the product of the cross sectional area of the building times the wind speed. That is,

ϕ = dilution factor = $1/cAu$ (sec/cm^3)

C = constant (2 to .5), select 1 (cm^3/m^3)

where A = building cross-sectional area in square meters

U = wind speed in meters/sec.

Thus for a nominal 2/msec wind velocity (4.4 mph)* and a 56 x 28 ft building, the dilution factor is $\phi = 3.4 \times 10^{-3}$.

*Average annual wind speed is in excess of 5 mph (14)

6.6 Whole Body Dose Outside Facility

A simple and conservative estimate of the maximum whole body dose to an individual outside the facility may be obtained by assuming that the individual is at the center of a large hemispherical cloud of fission products. The concentration of the fission products in the cloud is assumed to be equal to the concentration in the pool room divided by the turbulent wake dilution factor at a wind speed of 2 m/sec. The size of the cloud is assumed to be infinite and the exposure time to the individual is assumed to be equal to twice the time for one change of air in the pool room (20 min).

On the basis of these assumptions and using the equation in Section 6.1 we find that

Diluted release = 5.9×10^{-5} $\mu Ci/cm^3$ total gamma emitters

Sv = .22 photons/sec cm^3 of air

D = .075 mr/min.

For an exposure time of 40 minutes and a quality factor of 1, the maximum whole body dose from a cloud of fission products discharged from the facility as a result of the D.B.A. is 1.5 mrem.

6.7 Thyroid Dose Outside the Facility

The maximum thyroid dose to an individual outside the facility may be calculated using the equation in Section 6.3 and the assumption of Section 6.5. On this basis the maximum possible thyroid dose to an individual outside the facility is found to be .26 rem. If the water remained in the pool this value would be reduced by a factor of

10 and if the ventilation system were in the dilution mode this dose would be reduced by another factor of about 100.*

6.8 Summary of Results of D.B.A.

The preceding calculations on the consequences of the D.B.A. indicate that the only significant radiation exposure is the thyroid dose to a person in the pool room. The conditions necessary to produce this exposure are the failure of the cladding of one fuel rod along with a complete loss of pool water. The maximum possible radiation exposure to an individual outside the facility under the postulated conditions is minimal. Thus, no realistic hazard to the general public would result from the Design Base Accident.

*A 1" activated charcoal filter has a removal efficiency of 99.9% for elemental iodine

7.0 REACTIVITY EFFECTS OF ACCIDENTAL FUEL ADDITION

The conditions for this postulated accident are the accidental addition of a FLIP four(4)-rod fuel bundle to the central region of the core with the reactor operating at full power. In actual practice the Technical Specifications prohibit operation of the reactor with a vacant grid position. The maximum worth of a FLIP four(4)-rod cluster in the central region of the WSU TRIGA core is calculated to be less than $3.75. Thus the maximum possible reactivity insertion for an accidental fuel addition would be less than $3.75.

A step increase of $3.75 in core 30E at the end of core life would produce an average core temperature increase of 422°C. Adding this average core temperature increase to the average full power core temperature of 265°C and multiplying by a 1.67 peaking factor yields a maximum possible peak fuel temperature of 1142°C. This is below the 1150°C safety limit for FLIP fuel. The high temperature scram would in this accident limit the maximum fuel temperature to below the value calculated above and thus increase the margin of safety. Thus no additional hazard is caused by the addition of a four(4)-rod FLIP fuel cluster to the core during full power operation.

8.0 REACTIVITY EFFECT OF TRANSIENT ROD EJECTION

The conditions for this postulated accident are the accidental ejection of the full worth of the transient rod with the reactor operating at full power. During normal operation, pulsing will be administratively limited to the maximum value established in Section 5.3. However, for the purposes of this accident it will be assumed that the operator deliberately violates the established limit and also bypasses the interlock that inhibits pulsing

above 1 kw. Thus the total maximum worth of the pulse rod of $3.75 would be added to the core at full power.

The effects of a $3.75 reactivity addition at full power were shown not to exceed the safety limit in Section 7.0. Thus no additional hazard is caused by the ejection of the pulse rod at full power.

9.0 LOSS OF COOLANT ACCIDENT

The conditions for this postulated accident are that the reactor has been operating at 1 Mw for essentially an infinite length of time and then a sudden complete loss of coolant (pool water) occurs. The loss of water will shut down the reactor; however, the decay heat from the fission products will continue to produce heat in the fuel elements. In order to insure the safety of the reactor in the event of this postulated accident, the fuel cladding temperature in air must be maintained below the point where a cladding failure could occur.

The strength of the fuel element cladding is a function of its temperature which is a function of the fuel element temperature. The conservative assumption is made for purposes of this analysis that the fuel and cladding are at the same temperature. The stress imposed on the cladding by hydrogen disassociation within the fuel is a function of the fuel temperature, the fuel burnup, and the free gas volume with the fuel rod. Figure 27 (1,3) shows the stress imposed upon the cladding by TRIGA reactor fuels with H-Zr ratios of 1.6 and 1.7 as a function of fuel temperature. This figure also shows the yield and ultimate strength of the cladding as a function of temperature.

An examination of Figure 27 indicates that the maximum temperature that standard fuel (H-Zr 1.7) can tolerate in air without damage to the cladding

and subsequent release of fission products is 900°C; that is, the point at which the hydrogen pressure equals the yield strength of the cladding. This point for FLIP fuel (H-Zr 1.6) is 940°C. Thus the operating conditions of the reactor must be limited such that in the event of a loss of water accident, the fuel cladding temperature does not exceed the above limiting values.

The maximum fuel cladding temperature after a loss of pool water as a function of fuel rod power density is shown in Figure 28. This curve was generates from data calculated with a two-dimensional transient transport computer code TAC developed by Gulf General Atomic. It was assumed that the fuel has been operated for 7700 Mw-days, and that the reactor is shut down 15 minutes prior to the loss of coolant. The 15-minute delay was selected because it would take approximately 15 minutes for the pool to drain down from a point where a low level alarm would occur to the point where the core was uncovered from the catastrophic failure of a 10-inch beam port.

The results of the TAC code calculations summarized in Figure 28 indicate that Standard and FLIP fuel rods operated at power densities up to 22.3 and 23.5 Kw/rod respectively would not fail in the event of a loss of coolant accident. That is, the loss of coolant immediately after shutdown from 21 continuous years of operation at full power would not produce a fuel cladding failure and subsequent release of fission products.

An examination of the power density data given in Section 5.0 of this report indicates that all the analyzed core configurations have fuel rod power densities below the above-mentioned limiting values. Thus a loss of coolant accident would not precipitate a fuel cladding failure and the fission product decay heat would be removed primarily by natural convection of air.

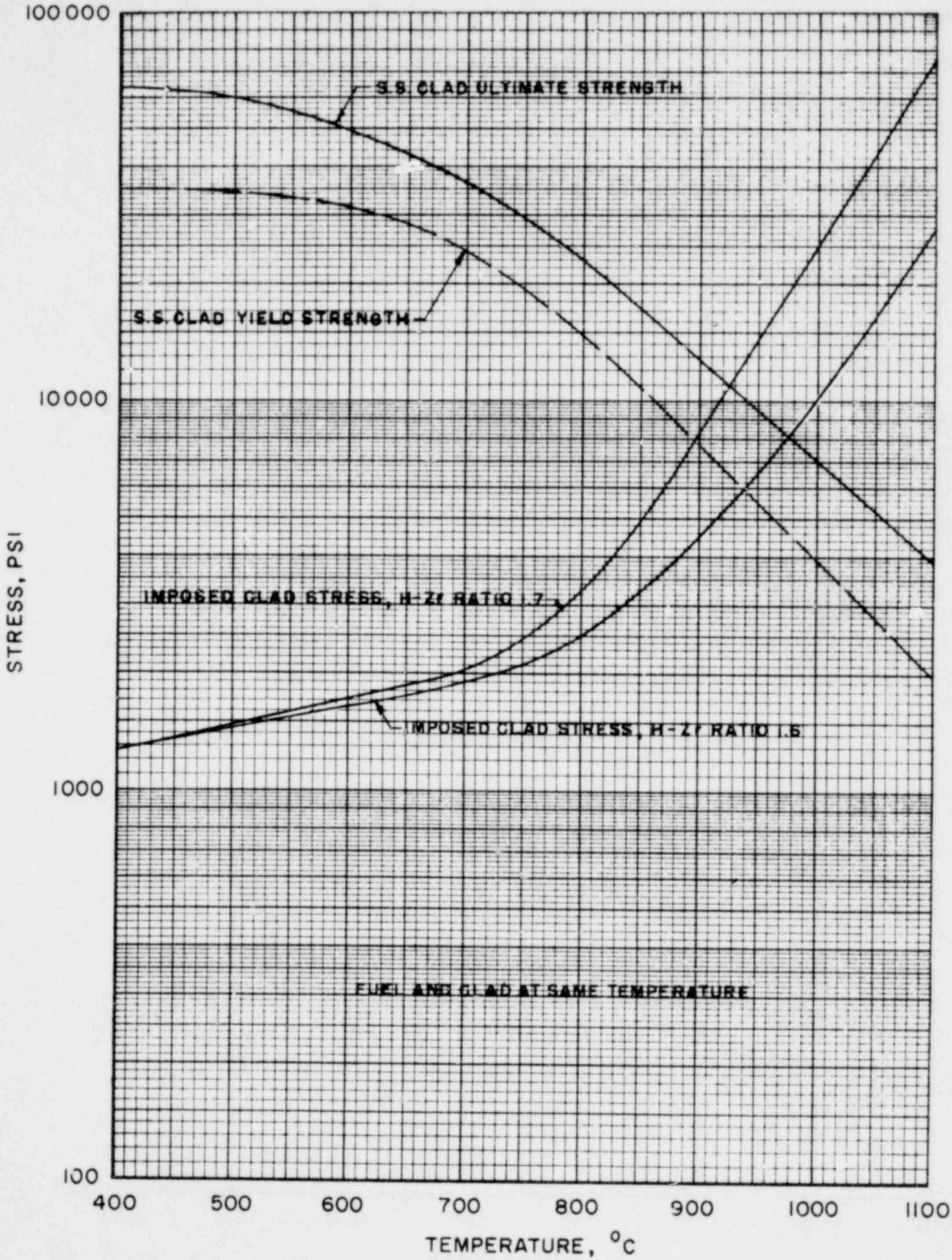

FIGURE 27 STRENGTH AND APPLIED STRESS AS A FUNCTION OF TEMPERATURE FOR 1.7 AND 1.6 H-Zr TRIGA FUEL

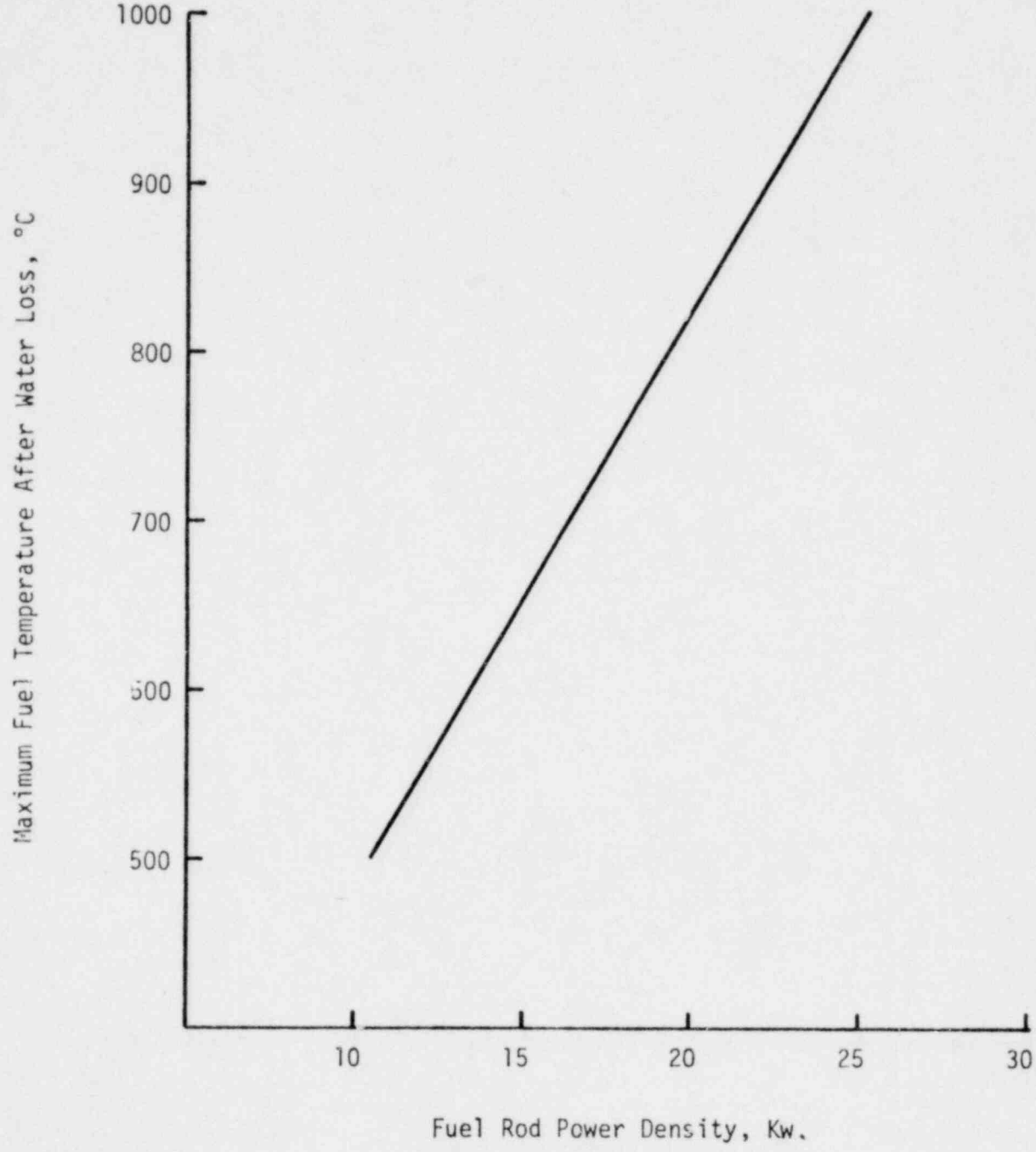

Figure 28: Maximum Fuel Rod Temperature as a Function of Fuel Rod Power Density for a Loss of Coolant 15 Minutes After Shut Down from 7700 MW-Days of Operation.

10.0 FLIP FUEL LOADING AND MIXED CORE PERFORMANCE TESTS

The addition of FLIP fuel into the Washington State University TRIGA reactor will be performed as a normal fuel loading in accordance with the standard procedure for such operations. The excess reactivity of the new core, control element worths, and shutdown margin will be measured at low power. The loading of the full operational core will be approached in a stepwise fashion to insure that the operating limits set forth in the technical specifications are not exceeded.

The power level of the full operational core will be increased in a stepwise fashion with checks of power indication and fuel temperature at each step. The first step will be at 100 Kw, the second at 200 Kw, and then in 200 Kw increments or less up to the licensed power limit. The power level of the reactor will then be measured by the calirometric method and the power level indication adjusted accordingly.

The pulsing characteristics of the W.S.U. TRIGA reactor will be measured after completion of the power calibration. At least two pulses of each reactivity input up to the licensed limit will be performed to assure repeatibility of the data. The reactor will then be placed in routine operation.

APPENDIX A

Fuel Rod Temperature Calculations

The experimental instrumented fuel rod temperature data shown in figure 1 was fit to a polynomial expression by the method of least squares and the following equation was obtained:

$$T = 31.77 + 0.6148\ (Pw) - (5.396 \times 10^{-4})\ (Pw)^2 + (1.958 \times 10^{-7})\ (Pw)^3$$

where T = Instrumented fuel rod temperature in °C

Pw = Reactor power in KW.

Calculations with the EXTERMINATOR-2 code for this core indicated that the axial averaged power density in the instrumented fuel element is 283 watts per centimeter of fuel rod heighth at 1 MW. If we assume that the power density in the instrumented fuel rod as well as all fuel rods is a linear function of reactor power and that all rods behave identically to the instrumented fuel rod, then we can calculate the temperature of any rod from the data on the instrumented fuel rod. That is, axial averaged fuel rod power densities calculated with the EXTERMINATOR-2 code may be used with the experimental data on the instrumented fuel rod to calculate the centerline fuel rod temperature of any rod.

The power density, Pd, in the instrumented fuel rod at any power, Pw, is Pd = .283 x Pw, where Pd = axial averaged power density in watts per cm of core height and Pw is the reactor power in KW. Thus Pw = Pd/.283. This may be combined with the instrumented fuel rod temperature equation to yield a relationship between fuel rod power density and fuel rod temperature. This equation is:

$$T = 31.77 + 2.172\ (Pd) - (6.738 \times 10^{-3})\ (Pd)^2 + (8.639 \times 10^{-6})\ (Pd)^3.$$

APPENDIX B

Temperature Coefficient Weighting Factor for a Mixed Core

The multiplication factor, k, of a reactor according to modified one group reactor theory is given by:

$$k = \frac{\eta p f \varepsilon e^{-B^2\tau}}{1+B^2L^2} = \frac{p e^{-B^2\tau}}{\Sigma a + DB^2} \cdot \varepsilon\nu\Sigma f(\text{fuel})$$

$$= \frac{p e^{-B^2\tau}}{\Sigma a + DB^2} \cdot \text{Fast Neutron Production.}$$

$$\text{Thus } Tc = \frac{dk}{dT} = \frac{d}{dT}\left[\frac{p e^{-B^2\tau}}{\Sigma a + DB^2} \cdot \text{Fast Neutron Production}\right]$$

for a TRIGA reactor

$$Tc \approx \frac{d}{dT}\left[\frac{p e^{-B^2\tau}}{\Sigma a + DB^2}\right] \cdot \text{Fast Neutron Production}$$

APPENDIX C

Calculation of Temperature Coefficient of Core 30E at Full Power

$\overline{Tm}$ = 265°C

$\overline{Ts}$ = 229°C

$\overline{Tf}$ = 360°C

FS/FT = .5105

FF/FT = .4895

Tcs(229°C) = .0155

Tcf(360°C) = .0152

Tcm = .0155 x .5105 + .0152 x .4895 = $.0154/°C ←

APPENDIX D

Fuel Temperature Limitation for TRIGA FLIP Fuel

The determining factor that sets the temperature safety limit for FLIP U-$ZrH_{1.6}$ fuel is the disassociation pressure of the hydrogen in the fuel. As the fuel temperature increases the hydrogen pressure increases and imposes a stress on the fuel cladding material. If the fuel temperature were to increase without limit, some point would be reached at which the internal pressure could cause the cladding to yield and eventually rupture. The purpose of the fuel temperature safety limit is to limit the hydrogen pressure to preclude a cladding failure.

The hoop stress exerted on the cladding by the hydrogen pressure is given by the equation

$$\delta = P_h \frac{r_c}{t_c} = P_h \cdot 35.25 \quad (t_c = .02,\ r_c = .705)$$

where δ is the hoop stress in psi, P_h is the hydrogen pressure in psi, r_c is the radius of the cladding, and t_c is the thickness of the cladding. Under normal steady state operating conditions at full power the temperature of the type 304 stainless steel cladding will not exceed 140°C. At 140°C the yield strength of type 304 stainless steel is 38,000* psi and the ultimate strength is 68,000 psi (16). Thus at a 140°C cladding temperature a 1078 psi hydrogen pressure would produce a .2% deformation in the cladding and the maximum allowable hydrogen pressure would be 1929 psi.

The hydrogen-to-zirconium ratio in FLIP fuel has a nominal value of 1.6 and a maximum value of 1.65. A detailed analysis performed by G.A. (17)

*Stress to produce a .2% deformation

indicates that the equilibrium hydrogen pressure in a U-$ZrH_{1.65}$ fuel rod which is constant temperature over the entire volume of the fuel is given by

$$P_e = 2.59 \times 10^9 \text{ EXP}[-1.997 \times 10^4/(T = 273)]$$

where P_e is the equilibrium hydrogen pressure in psi and T is the fuel temperature in degrees centigrade. Solving this equation for the maximum allowable hydrogen pressure of 1929 psi produces a maximum allowable uniform fuel and temperature of 1142°C.

The equilibrium condition pressure defined above never occurs, however, in the real case because a fuel rod is not at constant temperature over the whole volume of the rod. Consequently, the hydrogen pressure will be much lower than the equilibrium value calculated from the maximum fuel rod temperature. The axial power distribution along a typical TRIGA fuel rod varies from P max in the center to about .63 P max at the end of the fuel region (1). If we make the conservative assumptions that the fuel rod temperature does not vary in the radial direction and that the axial fuel rod temperature distribution follows the fuel rod power distribution, then the average fuel temperature equals the maximum fuel temperature divided by 1.2. Under these conservative conditions the maximum allowable fuel temperature under steady state conditions that does not exceed the yield strength of the cladding is 1370°C.

In addition to the steady state case, the effects of the transient fuel temperature increase during pulsing must be considered. A detailed analysis performed by G.A. (17) has shown that the hydrogen pressure during pulsing increases to a maximum value of 22% of the equilibrium value in about .3 seconds and then falls off. Under pulsing conditions some film boiling

occurs and the peak cladding temperature is greater than under steady state full power operation. A conservative value of 500°C is selected as the maximum cladding temperature under conditions of film boiling.

The ultimate strength of type 304 stainless steel at 500°C is 57,000 psi. At this temperature the maximum allowable hydrogen pressure is 1617 psi. A peak transient fuel temperature of 1290°C would be required to produce this pressure during pulsing. As a safety limit the peak adiabatic fuel temperature occurring during the pulse mode of operation for U-$Zr_{1.65}$ is selected to be 1150°C. The peak hydrogen pressure that would result at this temperature is approximately 460 psi. This would produce a stress of 16,000 psi which would not exceed the ultimate strength of the cladding at a temperature of 700°C.

Actual measurements of the peak hydrogen pressure during pulsing have been made at G.A. Five special instrumented fuel rods were tested in the ATPR during these experiments that involved a total of 426 pulses. The maximum peak fuel temperature during these tests was 1175°C and the maximum observed peak transient hydrogen pressure was 41 psia. The peak pressure transient occurred during the first pulse and decreased to about 20 psia by the 220th pulse. These experiments clearly indicate that the actual peak hydrogen pressure during pulsing is at least a factor of ten below the calculated values.

The 1150°C fuel temperature safety limit for TRIGA Reactor FLIP U-$ZrH_{1.65}$ fuel is seen to be a conservative limit. This limit will preclude a fuel cladding failure due to the internal hydrogen pressure in both the pulsed and steady state modes of operations. Furthermore, TRIGA fuel with a hydrogen-to-zirconium ratio of 1.65 has been pulsed to a temperature above 1150°C without damage to the cladding.

References

1. "Safety Analysis Report for the Torrey Pines TRIGA Mark IV Reactor," GA-9064, Gulf General Atomic, January 5, 1970.
2. "Annular Core Pulse Reactor," General Dynamics, General Atomic Division Report GACD 6977, Supplement 2, 9/30/66.
3. "Amendment II to the Safety Analysis Report - Texas A&M University Nuclear Science Center," November 1, 1972.
4. "EXTERMINATOR-2: A FORTRAN IV Code for Solving Multigroup Neutron Diffusion Equations in Two Dimensions," ORNL-4078, Oak Ridge National Laboratory, T. B. Fowler, M. L. Tobias, and D. R. Vondy, April 1967.
5. "Theory of Methods used in GGC-Y Multigroup Cross Section Code, Gulf General Atomic Report GA-9021, October 1968.
6. "SUMMIT: An IBM-7090 Program for the Calculation of Crystalline Scattering Kernels," General Atomic Report GA-2492, February 1, 1962.
7. "THERMIDOR: A FORTRAN II Code for Calculating the Nelkim Scattering Kernel for Bound Hydrogen," General Atomic Report GAMD-2622, November 10, 1961.
8. Private Communication with D. E. Feltz, Assistant Director, Texas A&M University, Nuclear Science Center.
9. "PLDEQC: A FORTRAN Code for Calculating Power Density, Fuel Temperature, and Plotting Neutron Flux Profiles for the W.S.U. TRIGA Core," unpublished report by T. R. Evans and W. E. Wilson, Nuclear Radiation Center, Washington State University, 1973.
10. "Safety Analysis Report for the Illinois Advanced TRIGA," University of Illinois, August 1967.

11. "Results of Critical Test Program for Loading Number III, Nuclear Science Center, Texas A&M University," November 1973.

12. "Summary of TRIGA Fuel Fission Product Release Experiments," Gulf-EES-A10801, September 1971.

13. "Energy Release from the Decay of Fission Products," Nuclear Science and Engineering, 3, 726 (1968), J. F. Pecking and R. W. King.

14. "Safeguards Report, Washington State College Research Reactor," March 1955.

15. "Safeguards Summary Report for the TRIGA-FLIP Reactor at the Puerto Rico Nuclear Center," PRNC-123, Revision C, November 11, 1969.

16. Reactor Handbook, Vol. 1, p. 569.

17. "Safety Analysis Report for the Romanian Annular Core Pulsing Reactor", G.A. Report No. E-117-323, Vol. III.